

1971

# Neutron activation analysis for osmium and ruthenium in platinum

Gerald James Payton  
*Iowa State University*

Follow this and additional works at: <https://lib.dr.iastate.edu/rtd>

 Part of the [Inorganic Chemistry Commons](#)

---

## Recommended Citation

Payton, Gerald James, "Neutron activation analysis for osmium and ruthenium in platinum " (1971). *Retrospective Theses and Dissertations*. 4497.  
<https://lib.dr.iastate.edu/rtd/4497>

This Dissertation is brought to you for free and open access by the Iowa State University Capstones, Theses and Dissertations at Iowa State University Digital Repository. It has been accepted for inclusion in Retrospective Theses and Dissertations by an authorized administrator of Iowa State University Digital Repository. For more information, please contact [digirep@iastate.edu](mailto:digirep@iastate.edu).

72-5245

PAYTON, Gerald James, 1939-  
NEUTRON ACTIVATION ANALYSIS FOR OSMIUM AND  
RUTHENIUM IN PLATINUM.

Iowa State University, Ph.D., 1971  
Chemistry, inorganic

University Microfilms, A XEROX Company, Ann Arbor, Michigan

Neutron activation analysis for  
osmium and ruthenium in platinum

by

Gerald James Payton

A Dissertation Submitted to the  
Graduate Faculty in Partial Fulfillment of  
The Requirements for the Degree of  
DOCTOR OF PHILOSOPHY

Major Subject: Inorganic Chemistry

Approved:

Signature was redacted for privacy.

In Charge of Major Work

Signature was redacted for privacy.

Head of Major Department

Signature was redacted for privacy.

Dean of Graduate College

Iowa State University  
Ames, Iowa

1971

**PLEASE NOTE:**

Some Pages have indistinct  
print. Filmed as received.

**UNIVERSITY MICROFILMS**

## TABLE OF CONTENTS

	Page
NATURE AND PURPOSE OF THIS INVESTIGATION	1
NEUTRON ACTIVATION ANALYSIS	5
Neutron Activation Analysis for Osmium and Ruthenium in Platinum	24
Review of Neutron Activation Methods and Related Radiochemical Techniques for Osmium and Ruthenium	41
EXPERIMENTAL	56
Materials	59
Reagents	60
Preparation and Standardization of Carrier Solutions	61
Irradiation Procedure	65
Chemical Separations	67
Radiochemical Analyses of the Irradiation Standards	85
Gamma-ray Spectra	86
RESULTS AND DISCUSSION	91
Irradiation Conditions	91
Analysis for Osmium in Platinum	91
Analysis for Ruthenium in Platinum	102
Analysis for Iridium in Osmium	108
Analysis for Iridium in Ruthenium	120
Error Considerations	120
Implications	127
SUMMARY	129
BIBLIOGRAPHY	132
ACKNOWLEDGMENTS	141

## NATURE AND PURPOSE OF THIS INVESTIGATION

The chemical behavior of platinum in its compounds may be influenced by trace impurities. Determination of the identity and quantity of possible impurities in platinum furnished the motivation for this investigation. Platinum is commonly found in the native form associated with the other noble metals; osmium, ruthenium, rhodium, iridium, palladium, silver and gold. The first five with platinum constitute the heavier group VIII members, usually called the platinum group. Due to their closely similar chemical behavior, the other noble metals often remain as trace impurities in refined platinum. Even in carefully purified laboratory platinum stock, three of the noble metals have been found (1). The thermal-neutron activation analysis procedure indicated the following impurity levels;  $15 \pm 2$  ppb Ir,  $28 \pm 4$  ppb Pd and  $2.4 \pm .3$  ppm Ag. This investigation extends the above work to include osmium and ruthenium, which were expected to occur at similar or even lower levels. Such concentrations exclude the use of most conventional methods of quantitative analysis. Both osmium and ruthenium have potential (n, $\gamma$ ) produced isotopes (2) amenable to multichannel gamma-ray scintillation spectrometry. The sensitivity and selectivity of neutron

activation analysis made it the method of choice. Ruthenium-102 with a 31.3% natural isotopic abundance has a thermal neutron activation cross section of 1.23 barns (1 barn =  $1 \times 10^{-24} \text{ cm}^2$ ) to form ruthenium-103 with a half-life of 40 days while osmium-190 with 26.4% natural isotopic abundance has a thermal neutron activation cross section of 3.9 barns to form osmium-191 with a half-life of 15 days. Both the product radionuclides decay with distinctive gamma-ray energies to stable daughter isotopes. Both of the elements have other (n, $\gamma$ ) produced isotopes of consequential amounts, but they have both shorter half-lives and smaller neutron activation cross sections. Therefore, after a suitable decay period, the gamma-ray spectra of each element characterizes essentially one isotope. The platinum matrix activity produced in the ruthenium and osmium trace neutron activation analysis precluded a nondestructive technique. Thus with the available NaI(Tl) crystal detector coupled to a 400-channel pulse height analyzer, a destructive separation scheme was dictated for the removal of "masking" platinum activity.

The extensive industrial utilization of the catalytic properties of platinum metals strongly indicated the potential for significant influence of trace impurities on the chemical

behavior of platinum in its compounds. Metallic platinum is known to catalyze over seventy oxidation-reduction and decomposition reactions. All of the platinum metals have two or more stable oxidation states. The readily reversible one electron oxidation-reduction couple of iridium(III-IV) is known to have a catalytic effect on the reaction of platinum compounds. Iridium impurities have been shown to inhibit the photo-induced exchange of chloride between  $(\text{PtCl}_6)^{2-}$  and  $(\text{PtCl}_4)^{2-}$  plus the exchange between  $\text{Cl}^-$  and  $(\text{PtCl}_6)^{2-}$  (3). Much earlier Klason (4) noted that the oxalate reduction of  $(\text{PtCl}_6)^{2-}$  to  $(\text{PtCl}_6)^{4-}$  required the presence of at least a trace of iridium. Traces of osmium and ruthenium, each having five oxidation states, could likewise catalyze platinum-(IV) reactions. An indirect catalytic effect could be produced by extraneous metal ions acting as reducing agents to form platinum(II) which in turn is known to catalyze platinum(IV) substitution reactions (5,6) and exchange reactions (7-11).

The continuing exchange and kinetic studies conducted at this laboratory on systems involving platinum(II) and (IV) complexes suggested the need for a quantitative determination of trace impurities that may occur in the platinum stock



material. The earlier investigation (1) determined three of the noble metals as trace impurities. Therefore this investigation was conducted in order to: (1) establish the amount of osmium and ruthenium impurities in the purified platinum stock, (2) determine similar impurities in commercial platinum wire and (3) develop an effective, sensitive separation technique for the simultaneous neutron activation analysis of these two elements in a platinum matrix.

---

## NEUTRON ACTIVATION ANALYSIS

Activation analysis is a method of elemental analysis utilizing induced radioactivity of the nucleus. When a material is bombarded by certain projectiles, usually neutrons, photons or charged particles, some of the atoms present in the material will interact with the bombarding particles and be converted into radioactive isotopes of the same element or of different elements depending on the type of impinging particle. The identity of the radioactive isotope thus formed can be characterized by its half-life, type of radiation, and energy of radiation. The quantitative measure of the emitted radiation can then be used as a measure of the quantity of the parent isotope present in the irradiated material.

Activation analysis as a quantitative technique had its genesis in 1936 through the work of von Hevesy and Levi (12), two years after the discovery of artificial radioactivity by Curie and Joliet (13) who found that radioactivity could be induced in a number of light elements by bombardment with alpha particles. The work reported by Fermi et al. (14) greatly increased the number of elements that could be activated artificially. They used neutrons from a Ra-Be source, moderated by passage through water or paraffin wax, as projec-

tiles. von Hevesy and Levi (12) used a 300-millicurie radium-beryllium neutron source to determine 0.1% (1,000 ppm) dysprosium in rare earth mixtures. The 2.3-hr half-life induced activity due to  $^{165}\text{Dy}$  was compared with that induced in mixtures of known dysprosium content. They used a similar method to determine europium in gadolinium. In 1938 Seaborg and Livingood (15) bombarded iron samples with deuterium produced by the Berkeley cyclotron to determine gallium at the 6 ppm level. They also determined copper in iron by the non-destructive activation analysis technique. But it was the development of nuclear reactors that first advanced activation analysis beyond the stage of a laboratory demonstrated possibility. The easily accessible high neutron fluxes of reactors, which followed the first critical experiment of December 2, 1942, (16) were almost immediately used for analysis. As soon as late 1943, certain determinations of trace constituents were being carried out routinely at reactors (17). The proliferation of reactors and accelerators in the postwar years has resulted in an exponential growth of activation analysis as evidenced by a bibliography of literature contributions (18) and expanding scope of applications (19). By far the largest number of investigations have utilized the

thermal neutrons of nuclear reactors, but activations by portable neutrons sources, photons, deuterons, helium-3 and alpha particles have become increasingly numerous. The use of photon activation analysis has been quite useful for light elements and is being extended to heavier elements (20). The simplicity and maintenance-free operation offered by isotopic neutron sources has recently received increased interest with the availability of mg amounts of  $^{252}\text{Cf}$  (21).

Regardless of the nature of the activating particle, the number of radioactive atoms produced for a given isotope is governed by the following considerations. When a sample is placed in a homogeneous flux of bombarding particles, some atom nuclei will become activated. The newly formed nuclides have a definite probability of decay and will disintegrate at a specific rate during the bombardment. As a result, concentration of the radioactive species will increase until it is such that the rate of formation is equal to the rate of decay.

$$\text{rate of formation} = f\sigma N \quad (1)$$

$$\text{rate of decay} = \lambda N_t \quad (2)$$

$f$  = activating flux, particles, in  $\text{cm}^{-2}\text{sec}^{-1}$

$\sigma$  = activation cross section of reaction, in  $\text{cm}^2$

$N$  = number of target nuclei of isotope

$\lambda$  = decay constant of radioactive produce =  $\ln 2 \cdot T_{\frac{1}{2}}^{-1}$

$T_{\frac{1}{2}}$  = half-life of radioactive product

$N_t$  = number of radioactive atoms present

Therefore the overall rate of growth is given by:

$$\frac{dN_t}{dt} = f\sigma N - \lambda N_t \quad (3)$$

Integration over the irradiation period  $t$  gives:

$$N_t = \frac{f\sigma N}{\lambda} (1 - e^{-\lambda t}) \quad (4)$$

At the end of the irradiation the activity,  $A$ , in disintegrations per second from the  $N_t$  unstable atoms present is  $\lambda N_t$ , thus:

$$A = f\sigma N(1 - e^{-\lambda t}) \quad (5)$$

The expression within parentheses is termed the saturation factor and reaches a maximum value of unity for an infinitely long irradiation period  $t$ . For an integral number,  $n$ , of half-lives, the saturation factor SF is

$$SF = 1 - \frac{1}{2^n} \quad (6)$$

It is evident that the increase in activity rapidly decreases for irradiations of four or more half-lives. Except in the case of very short-lived isotopes, it is seldom worthwhile to irradiate for periods longer than one half-life

since extraneous impurities with  $T_{1/2}$  greater than the desired isotope are then activated at a relatively greater rate.

The activity can be expressed in terms of the weight  $W$  of the element present for any time after irradiation as follows:

$$A = \frac{W\phi\sigma fN_0}{M} (1-e^{-\lambda t})(e^{-\lambda t'}) \quad (7)$$

$N_0$  = Avagadro's number

$M$  = chemical atomic weight

$\phi$  = abundance of the isotope activated

$t'$  = time elapsed after irradiation

$W$  = weight of element

It is evident from the above equation that the weight  $W$  of the element can be determined from the measured absolute disintegration rate  $A$  once the flux  $f$  and cross section  $\sigma$  are known since the other terms are fixed or easily measured quantities.

Neutron activation analysis seldom uses the above absolute method because of several experimental difficulties. One, the absolute method requires accurate knowledge of the true disintegration rate  $A$  which necessitates knowing the decay scheme, detector efficiency, and counting geometry. Second, the neutron flux  $f$  is rather difficult to measure.

Furthermore, the flux may not be uniform throughout the sample matrix or the irradiation period  $t$ . This is particularly true for a matrix containing nuclides with high thermal neutron absorption cross sections or capture resonances. The extent of this flux attenuation, self-shielding effect, has been estimated (22-26) by means of the following equation for specific sample matrices.

$$f = f_0 e^{-N\sigma r} \quad (8)$$

$f_0$  = initial flux  $\text{cm}^{-2}\text{sec}^{-1}$

$f$  = attenuated flux  $\text{cm}^{-2}\text{sec}^{-1}$

$\sigma$  = total neutron absorption cross for the complete  
neutron energy spectrum

$r$  = radius of a spherical sample

$N$  = number of absorbing nuclei per cubic centimeter

Obviously such a correction introduces additional hard to measure values in the absolute method. To some extent the self-shielding effect can be eliminated by using small samples and diluting the samples with material of low cross section. Also, the use of internal standards (27,28) in some cases may correct for neutron flux variations. Third, the activation cross sections ( $\sigma$ ) for most nuclides are not accurately known. This is further complicated by the fact that the

activation cross section is a function of neutron energy which is usually heterogeneous within a reactor. This produces a significant error in thermal neutron activation  $\sigma$  values if the cadmium ratio is less than 50 (29,30). Girardi et al. (31,32) have shown that the nuclear constants involved are usually sufficiently well known to allow many elements to be determined absolutely with an accuracy of less than 10 percent.

However the comparator method is much more widely used than the absolute method. The comparator method has the sample irradiated simultaneously with known amounts of a pure material. The radioactivity induced in the element to be determined in the sample is then compared with the radioactivity induced in the standard. When the two activities are counted under identical conditions the ratio of weights are directly proportional to the measured decay corrected activity A of Equation 7.

$$\frac{W_S}{W_C} = \frac{R_S}{R_C} \quad (9)$$

$W_S$  = weight of element in sample

$W_C$  = weight of element in standard

$R_S$  = measured activity of sample

$R_C$  = measured activity of standard



The measured activity  $R$  is related to the absolute activity  $A$  through a constant which compensates for a branching decay system, counter efficiency and counting geometry. But since this constant plus the other terms of Equation 7 are ideally the same for both the sample and standard, Equation 9 can be used. The most likely source of error in the comparator method is inhomogeneities in the neutron flux producing an unequal degree of activation in the sample and standard. The predominate flux effect usually is due to the flux gradient within the reactor. Such effects are minimized by irradiating sample and standard close together in identical containers. The use of flux monitors permits the calculation of a normalized flux dose. Another flux normalization technique uses a rotary specimen rack which ideally insures that simultaneously irradiated samples receive the same integrated flux. Self-shielding may also produce a flux inhomogeneity between the sample and standard in the comparator method. Speecke and Maes (33) have shown that the standard should have a matrix of the same size and composition as the sample to obtain uniform self-shielding. The comparator method self-shielding problem can also be minimized by the same techniques as described for the absolute method.

A nondestructive activation analysis can be used if the radioactivity produced in other components of the sample does not interfere with the measurement of the activity of the element to be determined. Such a technique requires no pre-counting radiochemistry, hence it is rapid, easy and free of several steps of possible experimental error. Numerous examples of non-destructive activation have been described (19) along with an extensive review of the methods used through 1965 (34). However for trace analysis when a highly active matrix is produced or when maximum sensitivity is required, some post-irradiation technique of radiochemical separation is often employed to remove the interfering radionuclides. Such chemical separations are usually devised to isolate the elements to be determined, either in a radiochemically pure form that can be counted by simple counting equipment, or into groups which can then be further resolved by gamma-ray spectrometry. Leinihan and Thomson (29) have emphasized the importance of considering the number of atoms involved when chemical methods are used. Normal chemical procedures involve milligram ( $10^{-3}$  g) quantities of material which represents  $10^{19}$ - $10^{20}$  atoms. In trace activation analysis, the amount of radioactive atoms to be radiochemically

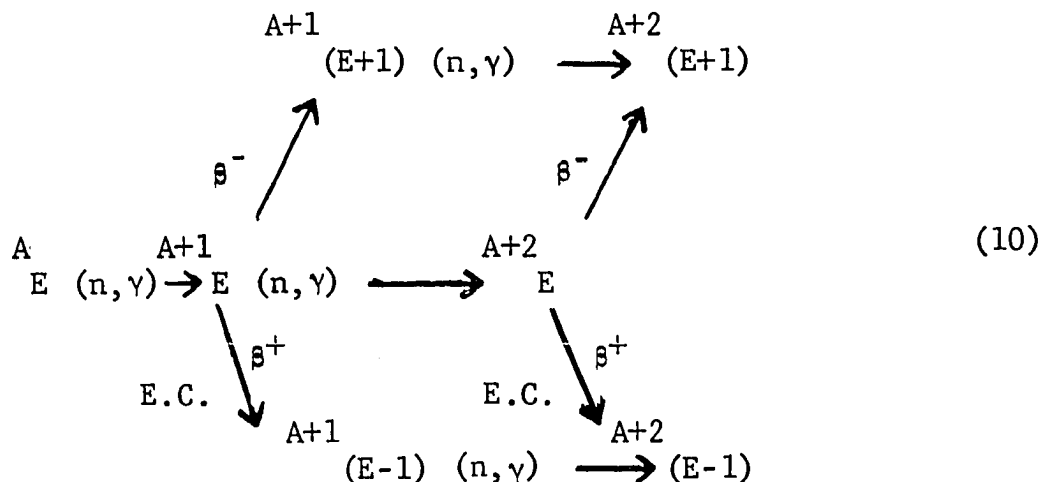
separated could be  $10^{-10}$  g which represents  $10^{12}$ - $10^{13}$  atoms. In a glass container with  $10^{15}$  adsorption sites  $\cdot\text{cm}^{-2}$ , it would be possible to lose a significant portion of the radioactive atoms to these sites. To eliminate such consequences, a carrier which is a weighable amount of nonradioactive component, chemically identical to the radioactive component being analyzed, is added to the radioactive matrix. If the carrier contains about  $10^{19}$  atoms, then the loss of component atoms on  $10^{15}$  adsorption sites is less than 0.01 percent. Furthermore, since the radioisotope and the inert carrier should not appreciably separate during chemical manipulations, all losses of the radioisotope are directly proportional to measurable losses of carrier. Since the steps used in the separations need not be 100 percent quantitative, considerable flexibility is available in their selection. If the radiochemical separation is not fully conservative of carrier added, a chemical yield factor  $Y$  has to be incorporated into Equation 9. The radiochemistry of most elements is summarized in a series of monographs issued by the U.S. National Academy of Sciences, Nuclear Science Series NAS-NS, where most of the references utilized carrier methods.

Chemical treatment of the sample before irradiation has

been used in a limited number of activation schemes when losses were expected to be small (35). More recently a rather novel technique has employed nonthermal neutron produced radioactive tracers added in pre-irradiation chemistry to monitor concentration yields, which are analogous to carrier yields. Green et al. (36) used cyclotron produced  $^{195}\text{Au}$  to monitor the preconcentration steps for gold from various sample matrices. The separated gold was then neutron activation analyzed by counting  $^{198}\text{Au}$ . Park et al. (37) used this same technique for the trace determination of some platinum metals in lead foam.

Examination of Equation 7 reveals that the ultimate sensitivity, production of the largest activity for a given weight of an element, depends on the flux  $f$ . Neutron fluxes in the range of  $10^{11}$ - $10^{14}$   $\text{n}\cdot\text{cm}^{-2}\cdot\text{sec}^{-1}$  are commonly available with most research reactors. However in the TRIGA reactor it is possible to obtain neutron pulses of about 30-millisecond duration with peak fluxes of  $5\times 10^{16}$   $\text{n}\cdot\text{cm}^{-2}\cdot\text{sec}^{-1}$  (38). But this has been shown to be advantageous only for elements with half-lives of less than 50 seconds (39). Potential interfering reactions can occur which are unique to high fluxes. Under high neutron flux conditions second order nuclear

reactions can lead to significant interferences. The following equation illustrates how successive nuclear reactions can lead to second-order effects.



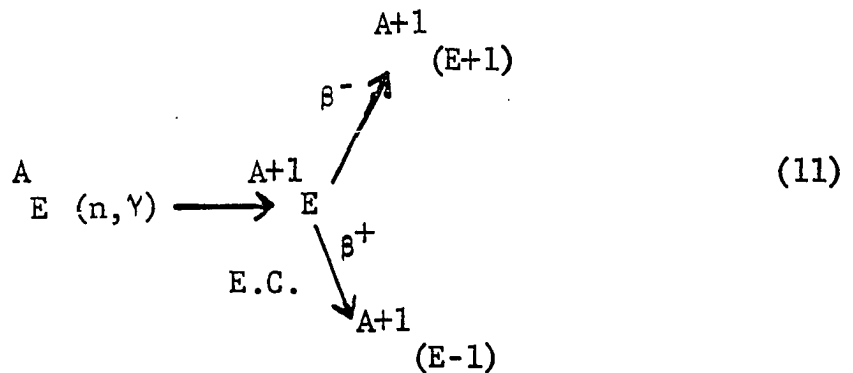
NUCLIDE 1 (n,  $\gamma$ ) NUCLIDE 2 (decay) NUCLIDE 3 (n,  $\gamma$ ) NUCLIDE 4

Although NUCLIDE 3 is usually stable, NUCLIDE 4 is nearly always radioactive. Hence if an element  $A+1(E+1)$  or  $A+1(E-1)$  is to be determined in a sample matrix containing large amounts of  $A E$ , the above second-order effect can be significant. The extent of this interference can be calculated (40). The magnitude of the interference for any specific case is a function of eleven independent terms. But the most significant fact is that it increases directly with irradiation time and directly with the square of the flux. By careful choice of irradiation time, flux intensity and radionuclide that will represent the

element to be determined, the second-order effect can be minimized or essentially eliminated.

Errors may also arise in thermal neutron activation through the occurrence of alternative neutron-induced reactions. These alternatives are:  $(n,2n)$ ,  $(n,n')$ ,  $(n,p)$  and  $(n,\alpha)$  reactions. Only the last two reactions lead to new elements, but this can be significant with transition elements, where the atomic number of the impurity usually differs by one or two units from that of the matrix. The cross sections for  $(n,p)$ ,  $(n,2n)$  and  $(n,\alpha)$  reactions for fission-spectrum neutrons are tabulated by Roy and Hawton (41) and others (42, 43). The cross section for the  $(n,\gamma)$  reactions are generally much larger than the above alternate reactions. Since the flux of thermal neutrons is usually equal to or greater than fission-spectrum neutrons, the interference of the alternate reactions is usually minimal. Possible interferences to be encountered with such threshold reactions have been reviewed by Durham et al. (44) and Maslov (45). When the epithermal and fast neutron fluxes are known, the extent of the threshold reaction interference can be calculated. The extent of the interference can be experimentally determined by irradiation with and without cadmium shielding, which is essentially

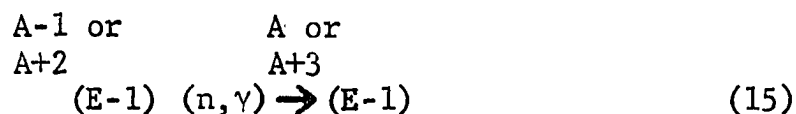
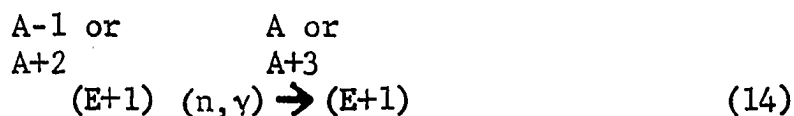
opaque to thermal neutrons. Conversely, reactor fast neutron fluxes have been utilized in specific cases where threshold reaction provides better sensitivities, or fewer interferences, than thermal neutron activation (46,47). Another source of error may develop for  $(n,\gamma)$  reactions on elements which decay to an active daughter.



If the element being determined is monitored through activity produced by the following reactions when element  ${}^A_E$  is also present,



it is obvious that serious interference can occur. Less obvious is the case where the following reactions are used.



The interference develops when the decay energies of the daughter of Equation 11 are quite similar to the decay energy of Equation 14 or 15 radionuclides. Such matrix produced interferences have been examined by Rudelli et al. (48). Thus it is usually necessary to check the probable concentrations of all neighboring isotopes for consideration of what effect they may produce.

Neutron activation predominately produces radioisotopes which emit only beta particles and photons. Without chemical separation, little specificity can be obtained by measuring beta particles, because of their broad energy spectra. In favorable cases, tedious absorber and decay work can drastically enhance heterogeneous beta spectra resolution. Even though gamma-rays have discrete energies, characteristic of the individual radioisotopes from which they are emitted, Geiger-Muller (GM) tubes are not capable of discriminating between different gamma energies plus having a low detection



efficiency for gamma-rays. Thus the majority of early activation analysis work involved tedious radiochemical separations necessary to prepare counting samples free of extraneous activity. Qualitative identification of the individual radioisotope was difficult, requiring careful decay and absorption measurements to improve the specificity of the analysis. The instrumental discrimination and improved detection efficiency of individual gamma-rays became available with the application by Kahn and Lyon (49) of NaI(Tl) crystal single channel gamma-ray scintillation detectors. The early single channel systems were soon developed into multi-channel analyzers (50) which greatly extended the scope of activation analysis. It was then possible to measure specifically different radionuclides in a mixture of activities. This reduced or often eliminated the necessity of complete chemical separations since most radionuclides have characteristic gamma-rays emitted as part of the decay scheme. Despite its relatively low resolution and interference arising from Compton "tails", gamma-ray spectrometry with NaI(Tl) scintillation counters has been effectively used to analyze activities from quite complex matrices. Background information on techniques of NaI(Tl) gamma-spectrometry is contained in a book edited by Crouthamel

(51) while several compilations of gamma-ray spectra of individual radionuclides in graphical and digital form have been published (52-54).

A relatively new instrumental development in gamma-ray spectrometry involves the use of lithium-drifted germanium Ge(Li) detectors. Such detectors have an energy resolution on the order of four-six KeV, which is 10-20 times better than the NaI(Tl) detector. Consequently complete separation can be obtained for many photopeaks which remain unresolved by NaI(Tl) detectors. The application of Ge(Li) detectors to activation analysis was first reported in 1965 by Girardi et al. (55) for analyzing hafnium in zirconium oxide and Prussin et al. (56) for the nondestructive analysis of aluminum. Despite the much lower detection efficiency of Ge(Li) vs. NaI(Tl) crystals, plus the necessity of operating the germanium semiconductor in a vacuum at 77°C, their application has rapidly expanded. Procedures have been developed which are capable of determining over 25 elements within a single sample (57) and Ge(Li) detectors were in prominent use for measurements on lunar samples (58).

The above gamma-ray detection systems yield multicomponent spectra consisting of several photopeaks of various sizes and

energies which may overlap. For the evaluation of a simple spectrum containing a few well resolved peaks, the method of Covell (59) or modifications thereof (60,61) are quite satisfactory. The imposing problem of resolving a complex spectrum into individual components has been attacked rather effectively by the development of computer programs, such as those pioneered by Salmon (62) and by Anders and Beamer (63). Their approach utilized a successive spectrum stripping method. Another computer approach involves the solution of a set of simultaneous equations, where the number of equations is determined by the number of identified peaks in the data (64). The method of least squares has been applied with considerable success to resolve complex gamma-ray spectra (65-69). This method, along with the equivalent vector analysis method (70), decay curve analysis (71,72) plus spectrum smoothing and differentiation (73) have made computers an integral part of most activation analyses. An excellent review of activation analysis computation methods has been presented by Yule (74). Automated radiochemical separations (75) plus automated data collection and analysis (76) allows the processing of monumental amounts of data. The use of special counting techniques like coincidence (77) and sum-coincidence (78) detec-

tion has also been used to increase the sensitivity by suppressing the detection of undesired activities.

From the foregoing discussion, it is obvious there are several parameters which may be varied in neutron activation analysis. Specifically, these are the energy and intensity of the neutron flux, length of irradiation, period of decay (cooling), method of counting, and in some cases the radionuclide that will represent a certain element. It is by optimizing these conditions for a given situation that the maximum sensitivity may be obtained. The inherent sensitivity of the neutron activation technique has resulted in considerable use for the determination of very low concentrations. Lukens (79) has experimentally determined the limits of detection for some 76 elements using a flux of  $10^{12} \text{ n} \cdot \text{cm}^{-2} \cdot \text{sec}^{-1}$  for a one hour irradiation. With no interference from other activities, the limits of detection ranged from  $10^{-4}$  g down to  $10^{-11}$  g ( $10^{-5}$   $\mu\text{g}$ ). The latter value corresponds to a 10 ppb level in a one mg sample. When the indicator activity is long-lived and higher fluxes are available, somewhat lower limits have been obtained. Numerous other calculated and experimental sensitivities have been reported for the neutron activation analysis of various elements (80-83). An analogous tabulation

of sensitivities was recently reported in a review of photon activation analysis (84).

### Neutron Activation Analysis for Osmium and Ruthenium in Platinum

Several nuclear and chemical properties have to be considered when formulating a destructive method for the simultaneous neutron activation analysis for osmium and ruthenium in platinum. The possible (n, $\gamma$ ) produced radionuclides (2) are tabulated in Table 1. The platinum matrix yields relatively short half-life nuclides when compared to  $^{191}\text{Os}$  and  $^{103}\text{Ru}$  half-lives. The use of the short-lived radionuclides of osmium and ruthenium was essentially precluded because of the anticipated time necessary for radiochemical separations. Another primary consideration in selecting the longer-lived isotopes for analysis was to allow a decay reduction of the radiation hazard during radiochemical manipulation of the platinum matrix. This presented  $^{103}\text{Ru}$  and  $^{191}\text{Os}$  as the radiochemically safer radionuclides to select for representation of the elements to be determined.

For irradiation periods less than one half-life, Equation 5 shows that the increase in total activity is essentially linear with time of irradiation. Therefore, the product of

Table 1. Nuclear properties of (n, $\gamma$ ) products of naturally occurring Ru, Os, and Pt isotopes

Naturally occurring isotope	Natural abundance (%)	Cross section $\sigma$ (barns)	Product radio-nuclide	Product half-life	Product radiation (MeV)
$^{96}\text{Ru}$	5.5	0.2	$^{97}\text{Ru}$	2.88d	E.C. $\gamma$ : 0.216
$^{102}\text{Ru}$	31.6	1.4	$^{103}\text{Ru}$	39.5d	$\beta^-$ : 0.22, 0.10, 0.71 $\gamma$ : (0.040), 0.50, 0.61
$^{104}\text{Ru}$	18.9	.48	$^{105}\text{Ru}$	4.44h	$\beta^-$ : 1.15, 1.08, 1.087 $\gamma$ : 0.72, 0.21-1.7
$^{184}\text{Os}$	.018	<200.	$^{185}\text{Os}$	93.6d	E.C. $\gamma$ : 0.646
$^{189}\text{Os}$	16.1	.008	$^{190\text{m}}\text{Os}$	9.9m	$\gamma$ : 0.50, 0.62, 0.36
$^{190}\text{Os}$	26.4	8.6	$^{191\text{m}}\text{Os}$	13.0h	I.T.: 0.014
		3.9	$^{191}\text{Os}$	15.0d	$\beta^-$ : 0.142 $\gamma$ : 0.064, 0.129
$^{192}\text{Os}$	41.0	1.6	$^{193}\text{Os}$	31.5h	$\beta^-$ : 0.677-1.136 $\gamma$ : 0.139, 0.073, 0.107-0.56

Table 1. (Continued)

Naturally occurring isotope	Natural abundance (%)	Cross section $\sigma$ (barns)	Product radio-nuclide	Product half-life	Product radiation (MeV)
$^{190}\text{Pt}$	.0127	~150.	$^{191}\text{Pt}$	3.0d	E.C. $\gamma$ : 0.54,0.36,0.41
$^{192}\text{Pt}$	.78	2	$^{193\text{m}}\text{Pt}$	4.3d	I.T.: 0.136 $\gamma$ : 0.013
		<14	$^{193}\text{Pt}$	<500y	E.C.
$^{194}\text{Pt}$	32.9	.09	$^{195\text{m}}\text{Pt}$	4.1d	I.T. 0.030 $\gamma$ : 0.099
$^{196}\text{Pt}$	25.3	.05	$^{197\text{m}}\text{Pt}$	78m	I.T. 0.346, $\gamma$ : 0.05 $\beta^-$ : 0.73, $\gamma$ : 0.28,.13
		.9	$^{197}\text{Pt}$	18h	$\beta^-$ : 0.67,0.48 $\gamma$ : 0.077,0.19,0.27
$^{198}\text{Pt}$	7.21	.03	$^{199\text{m}}\text{Pt}$	14.1s	I.T.: 39 $\gamma$ : 0.032
		4	$^{199}\text{Pt}$	31m	$\beta^-$ : 1.7,0.7-1.6 $\gamma$ : 0.54,0.075-0.96

the percent natural abundance with the cross section values of Table 1 reveals that  $^{103}\text{Ru}$  and  $^{191}\text{Os}$  would also yield the highest sensitivity, if all other variables remain constant. Although  $^{105}\text{Ru}$  and  $^{193}\text{Os}$  radionuclides could be used, they do not have any intense gamma-rays which are not subject to interference from the  $^{103}\text{Ru}$  and  $^{191}\text{Os}$  gamma-rays. To use the shorter lived isotopes for radioactivity measurements of osmium and ruthenium would require a simultaneous determination for both the sample being analyzed and the corresponding irradiated standard in order to normalize the effect of the time-varying activity ratio. This clearly inconvenient technique is eliminated by using the longer lived isotopes while allowing the shorter-lived ones to decay.

The decay scheme of  $^{103}\text{Ru}$  and  $^{191}\text{Os}$  (2) are shown in Figure 1. Both of these radionuclides decay with the emission of characteristic gamma-rays which can be measured via scintillation techniques. The radionuclide  $^{103}\text{Ru}$  decays by beta (negatron) emission to stable  $^{103}\text{Rh}$ . The predominate gamma-ray produced is 0.497 MeV arising from 89 percent of the beta decay going to the 0.5370 level which immediately de-excites to the 0.0400 level. A considerably less intense 0.611 MeV gamma-ray results from seven percent of the beta



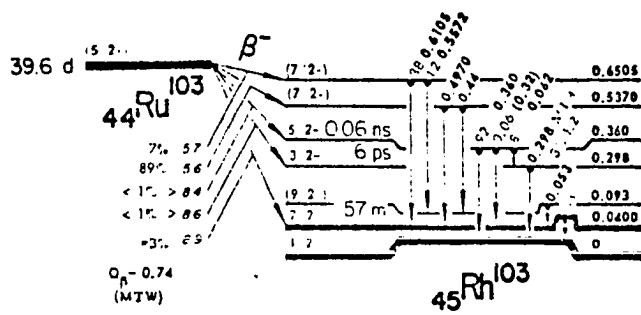
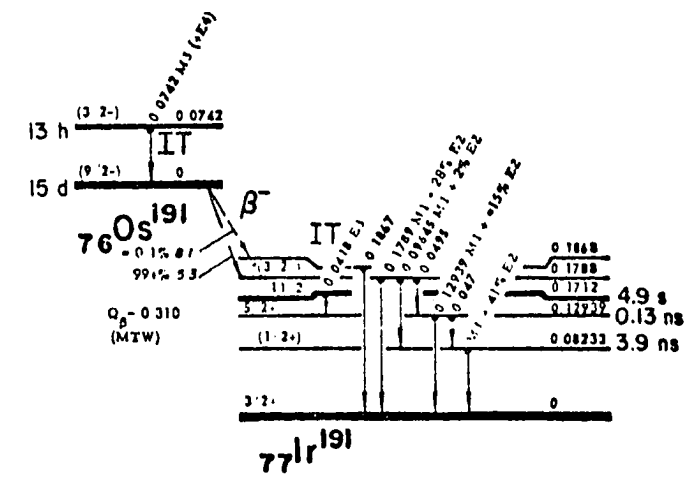


Figure 1. Decay schemes of  $^{191}\text{Os}$  and  $^{103}\text{Ru}$

decay going to the 0.6505 level which also immediately de-excites to the 0.0400 level. The radionuclide  $^{191}\text{Os}$  decays by negatron emission to stable  $^{191}\text{Ir}$ . A principal 0.129 KeV gamma-ray arises from 99+ percent of the negatron decay going to the 0.1788 level which then predominately cascades to the ground level via the 0.12939 level. Another principal 0.064 MeV photon arises from the K x-ray emitted by the  $^{191}\text{Ir}$  decay daughter.

The experimental gamma-ray spectra of  $^{103}\text{Ru}$  and  $^{191}\text{Os}$  are shown in Figures 2 and 3. These spectra were obtained using a NaI(Tl) crystal detector coupled to a 400-channel pulse height analyzer. The 0.497 MeV peak is the predominate feature of the  $^{103}\text{Ru}$  spectra. After one half-life period, the  $^{191}\text{Os}$  spectra displays three detectable peaks of 0.042, 0.064 and 0.129 MeV. The minor 0.646 MeV peak is attributed to the 94d  $^{185}\text{Os}$  radionuclide whose decay scheme is shown in Figure 4 along with the decay schemes of  $^{193}\text{Os}$  and  $^{105}\text{Ru}$ . The 0.646 MeV peak becomes much more pronounced after two or more half-life decay periods for 15d  $^{191}\text{Os}$ .

Obviously the eight (n, $\gamma$ ) produced platinum isotopes described in Table 1 would also yield considerable activity at the termination of irradiation. Although a "cooling"

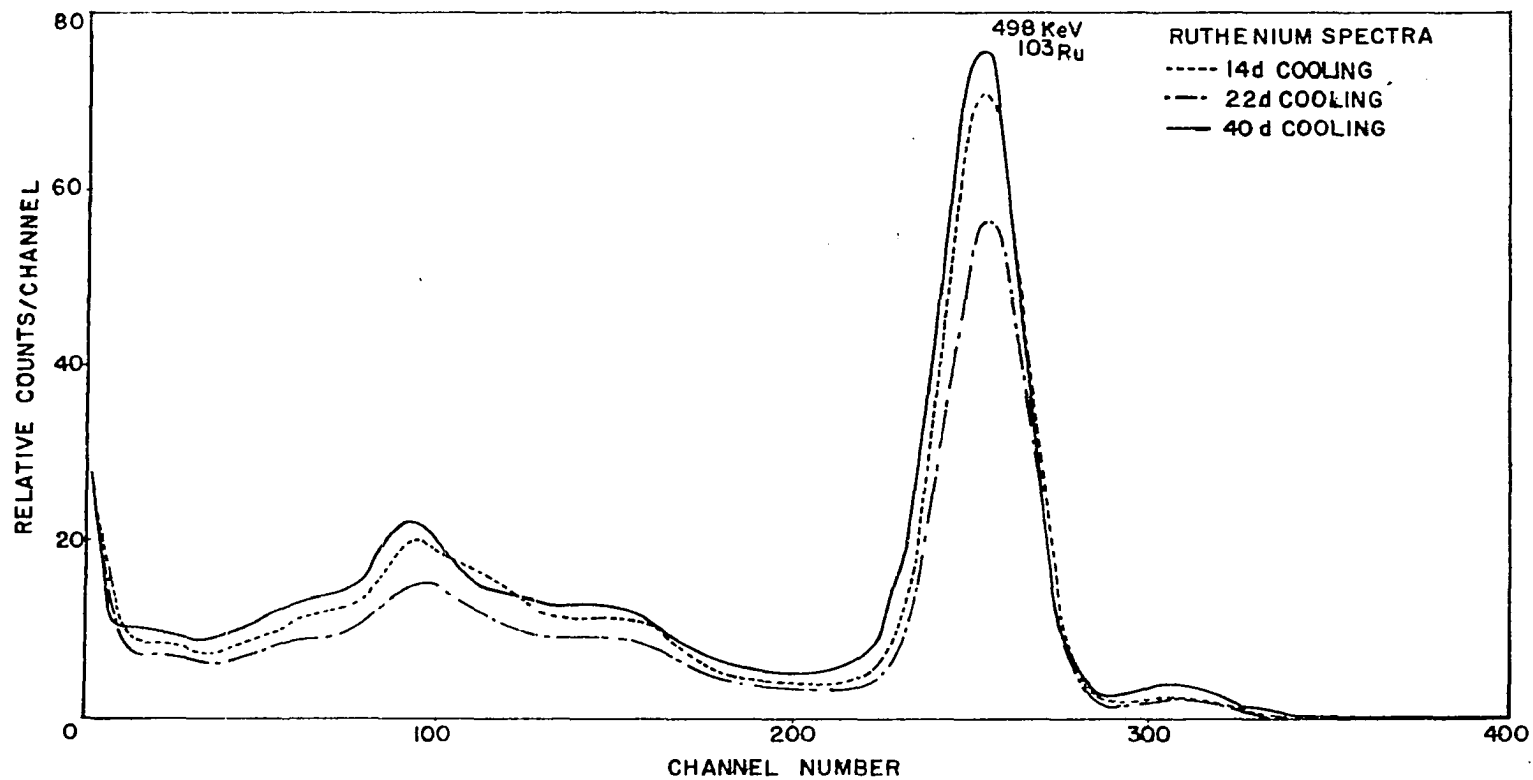


Figure 2. Gamma-ray energy spectra of distilled ruthenium

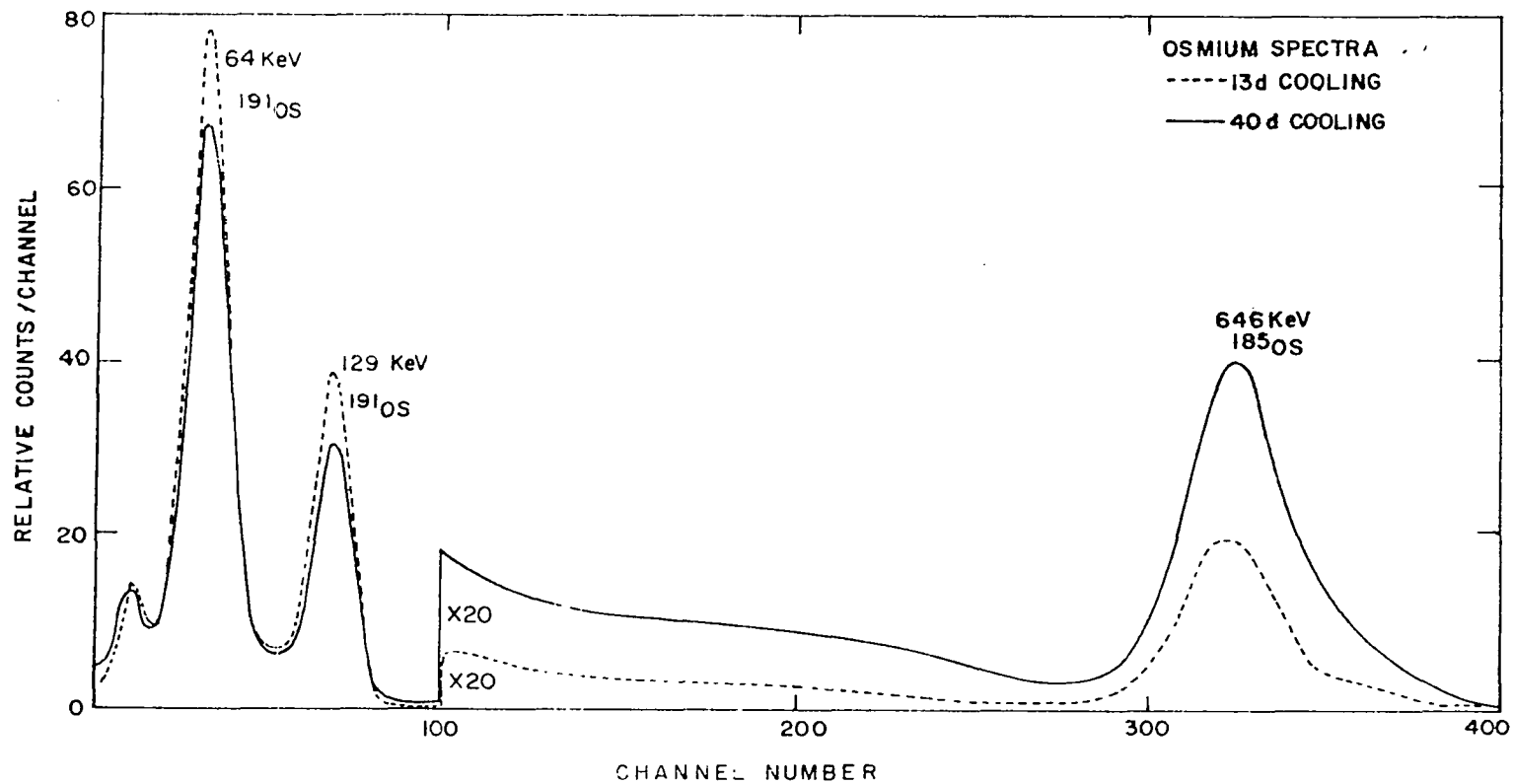


Figure 3. Gamma-ray energy spectra of distilled osmium

Figure 4. Decay schemes of  $^{105}\text{Ru}$ ,  $^{185}\text{Os}$ , and  $^{193}\text{Os}$



period of three or more days would eliminate a major portion of platinum radiation, the 3.15d  $^{199}\text{Au}$  daughter of 31m  $^{199}\text{Pt}$  and 4.1d  $^{195\text{m}}\text{Pt}$  would still be present. Using relevant data from Table 1, Table 2 shows some theoretically calculated platinum radionuclide activities expected immediately after irradiation of 100-mg of platinum at  $3 \times 10^{13} \text{ n}\cdot\text{cm}^{-2}\cdot\text{sec}^{-1}$  flux, plus activities remaining after cooling periods of one day and one week.

Table 2. Millicurie activity levels produced in 100 mg of platinum

Cooling period	One day irradiation			One week irradiation		
	0	1d	1 wk	0	1d	1 wk
$^{191\text{m}}\text{Pt}$	3.45	0.96	--	4.77	1.33	--
$^{193\text{m}}\text{Pt}$	0.58	0.49	0.19	2.64	2.25	0.85
$^{193}\text{Pt}$	--	--	--	--	--	--
$^{195\text{m}}\text{Pt}$	1.15	0.97	0.35	5.14	4.34	1.57
$^{197\text{m}}\text{Pt}$	3.17	--	--	3.17	--	--
$^{197}\text{Pt}$	34.37	13.64	0.05	56.89	22.58	0.09
$^{199\text{m}}\text{Pt}$	0.54	--	--	0.54	--	--
$^{199}\text{Pt}$	72.16	--	--	72.16	--	--
$^{199}\text{Au}$	13.85	11.14	2.10	77.47	62.60	16.71
Totals	129.27	27.20	2.69	222.78	93.10	19.22

Even a one week cooling period following a one day irradiation leaves a significance activity of ca. 2.69 mc. Since for trace analysis, the matrix represents from  $10^4$ - $10^8$  times larger number of atoms than of the trace elements, the above longer lived platinum isotopes would still constitute the major portion of the activity after a one week decay. The decay schemes for the expected platinum radionuclides are shown in Figure 5. The experimental gamma-ray spectra of platinum, obtained in the same manner as for Figure 3, are shown in Figure 6. The three curves represent four, 23 and 40 day decay periods for the same sample. The 0.070 MeV and 0.158 MeV gamma-rays of  $^{195m}\text{Pt}$  and  $^{199}\text{Au}$  would seriously mask the 0.064 and 0.129 MeV gamma-rays of  $^{191}\text{Os}$ , thus providing additional impetus for a destructive analysis. Additionally, the NaI(Tl) detector coupled to a multichannel analyzer can not respond accurately for dead-time levels above ca. 85-90 percent. Thus high levels of matrix activities seriously raise the sensitivity limits which can be obtained for any impurity element, even if there is no serious overlap of the gamma-ray peaks for the matrix and impurity activities.

If the dead-time instrumental difficulties could be eliminated, the overlapping of platinum gamma-rays with those



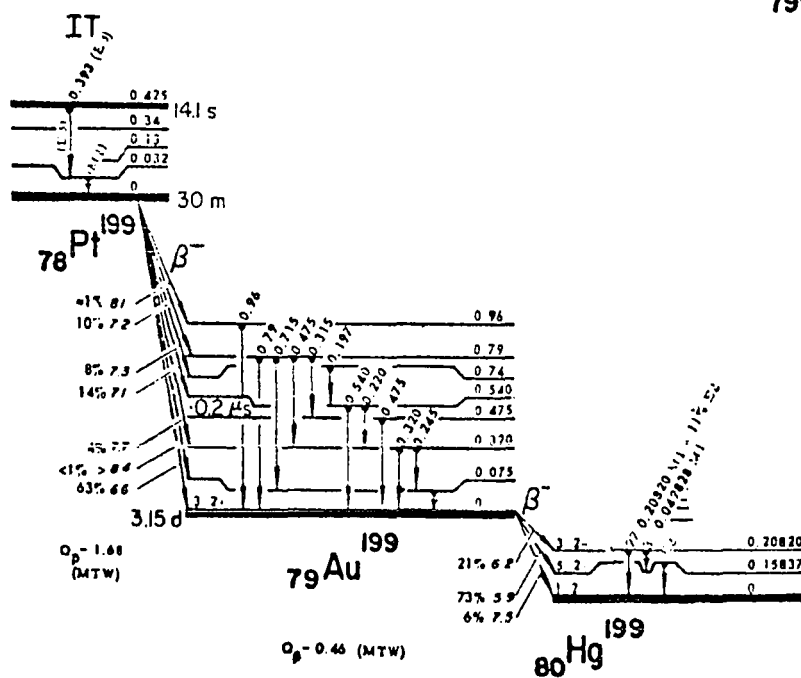
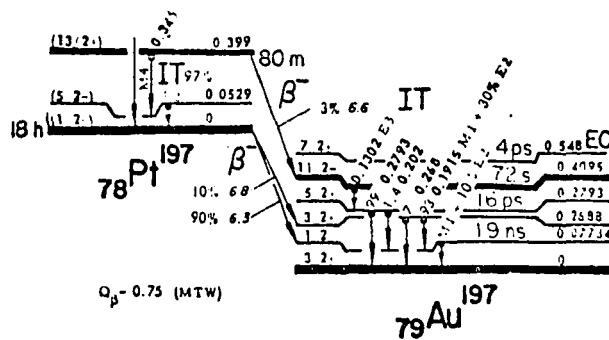
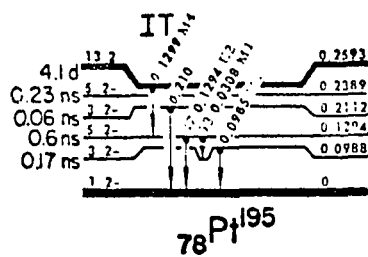


Figure 5. Decay schemes of the Pt radionuclides

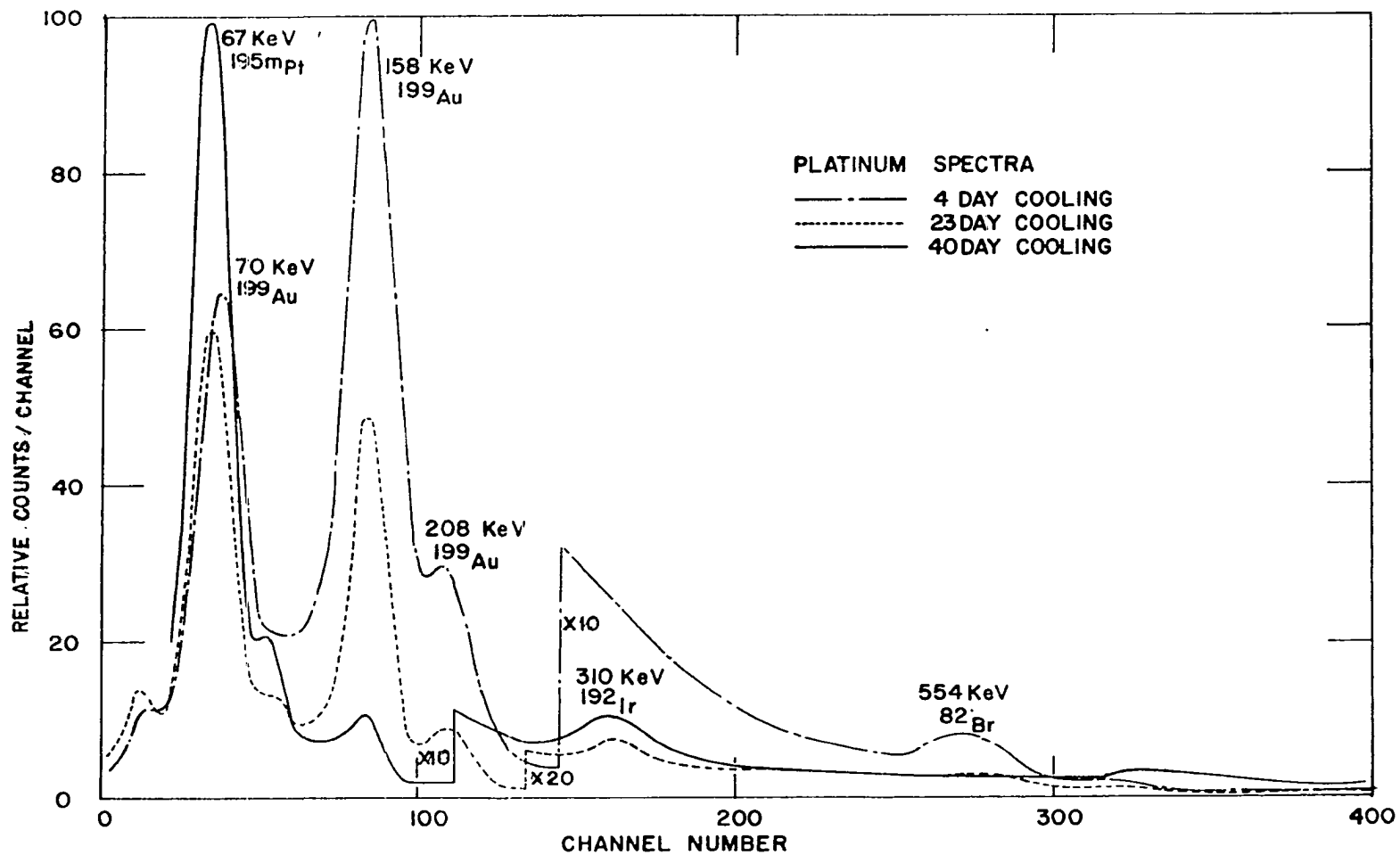


Figure 6. Gamma-ray spectra of platinum radionuclides

of  $^{191}\text{Os}$  could be avoided by monitoring the amount of osmium with the 0.646 MeV peak of 93.6d  $^{185}\text{Os}$ . But Table 1 values indicate that for irradiation periods under 15 days, the sensitivity using  $^{185}\text{Os}$  would be approximately 0.10 that obtainable by using  $^{191}\text{Os}$ . Since the  $^{184}\text{Os}$  cross section value is not accurately known and may be considerably less than 200, the relative sensitivity could be much less than the 0.10 value. Thus  $^{191}\text{Os}$  appears to be the best radio-nuclide to use. The potentially interfering platinum activities will have to be eliminated by suitable radiochemical purification methods coupled with decay data evaluation techniques.

Examination of Equation 7 reveals that several parameters may be varied in order to obtain sufficient activity for accurate measurement. However for a specific experimental facility the usual parameters adjusted are time of irradiation ( $t$ ), time of "cooling" ( $t'$ ) and weight ( $W$ ) in order to obtain a measureable activity ( $A$ ). The sample weight and irradiation time selected is usually a compromise necessitated by the need to keep the matrix activity low enough for safe handling in a conventional radiochemical laboratory while still producing sufficient activity of the element to be measured. This is

the case with a platinum matrix as Table 2 indicates. Routti (80) has calculated some saturation activities for 1 mg amounts of elements of natural composition subjected to a flux of  $10^{12} \text{ n}\cdot\text{cm}^{-2}\cdot\text{sec}^{-1}$ . Although  $^{191}\text{Os}$  and  $^{103}\text{Ru}$  saturation activities of  $1 \times 10^7$  and  $1.1 \times 10^6$  dps respectively could be expected, irradiation periods of 60-160 days would be required. While such irradiation periods would yield the highest sensitivity, very long cooling periods on the order of one to three weeks would also be required to reduce the matrix radiation hazard. In order to determine if sufficient  $^{191}\text{Os}$  and  $^{103}\text{Ru}$  activity could be expected for irradiation periods of one week or less, Table 3 values were calculated using Table 1 data. The maximum expected  $^{185}\text{Os}$  activity was also determined. The calculated values are for a 100-mg quantity of platinum containing 0.1  $\mu\text{g}$  (1 ppm) of each elemental impurity subjected to a constant flux of  $3 \times 10^{13} \text{ n}\cdot\text{cm}^{-2}\cdot\text{sec}^{-1}$  for a specified time. These theoretical values are merely indicative of the relative detection limits possible. The actual experimental sensitivities depend mainly on the chemical separation achieved and type of activity measurement used. Even with a conservatively estimated counting efficiency of 10 percent, a value which is easily obtained in NaI(Tl) gamma-

Table 3. Activity in dps of radionuclide produced in 0.1  $\mu\text{g}$  of natural occurring element

Length of irr.	S.F.	0d	Cooling time		
			1d	7d	28d
$^{185}\text{Os}$					
1d	.007	2.52	2.51	2.40	2.06
7d	.05	17.3	17.2	16.4	14.1
sat.	1.0	342	340	325	279
$^{191}\text{Os}$					
1d	.045	442	422	320	121
7d	.28	2704	2582	1957	741
sat.	1.0	9784	9345	6820	2580
$^{103}\text{Ru}$					
1d	.017	135	133	120	83.1
7d	.11	898	883	795	489
sat.	1.0	7863	7730	6847	4215

ray spectrometry, the above calculations indicate ruthenium and osmium can be detected at levels below one ppm. Although  $^{191}\text{Os}$  produces a larger activity than ruthenium for any irradiation condition, its shorter half-life and lower energy gamma-rays make it subject to more interferences. The values calculated for  $^{185}\text{Os}$  indicate that its relative sensitivity would be ca. 0.01 that of  $^{191}\text{Os}$  for a one week irradiation followed by a one week decay. This assumes that counting efficiencies for the respective activities would be equal.

Even after a four week decay following a one week irradiation, the  $^{191}\text{Os}$  provides ca. 50 times greater theoretical sensitivity. Lukens (79) has reported experimental sensitivities obtained for a one hour irradiation at a flux of  $4.3 \times 10^{12} \text{ n}\cdot\text{cm}^{-2}\cdot\text{sec}^{-1}$  in the absence of interfering activities. The  $10^{-7}$ - $10^{-8}$  g osmium and ruthenium detection limits correspond to 0.1-1 ppm levels in 100 mg of platinum, provided all interfering activities could be removed. Although a longer irradiation period would lower the experimental detection limits, the radiation hazard of the platinum matrix has to be considered as shown by Table 2. In view of the considerations cited in the preceding discussion, the main aspect of this investigation was the development of a destructive activation analysis emphasizing chemical separations with high decontamination factors.

Under high flux conditions and long irradiation times, the effect of possible secondary interference from (n,2p) and (n, $\alpha$ ) nuclear reactions must be considered. Platinum can not affect the ruthenium analysis since the ruthenium atomic number is 34 units below that of platinum. The (n, $\alpha$ ) threshold reaction on  $^{194}\text{Pt}$  and  $^{196}\text{Pt}$  producing  $^{191}\text{Os}$  and  $^{193}\text{Os}$  respectively could conceivably be produced by the fission neutrons,

but the  $^{193}\text{Os}$  possibility is of no consequence since it is allowed to decay. Fission neutrons normally have an energy range of a few ev to 25 MeV although the average energy is ca. 1.5 MeV. However, it is only with neutron energies of 10-50 MeV that  $(n,\alpha)$  and  $(n,2p)$  reactions become possible for nuclei of  $A \geq 80$  (47). Even then they are the least probable reactions of several that may occur. For the  $^{194}\text{Pt} (n,\alpha) ^{191}\text{Os}$  reaction, the threshold energy required for the incident neutron is 6.99 MeV while the potential coulomb barrier for alpha emission is ca. 30 MeV. For  $^{192}\text{Pt} (n,2p) ^{191}\text{Os}$  reaction, a threshold energy of 6.37 MeV coupled with a potential coulomb barrier of ca. 25-30 MeV for double proton emission makes both reactions extremely improbable for producing significant interference. Since the estimated cross sections for  $(n,p)$  reactions of Group VIII heavy elements is less than one millibarn (85), the cross section for  $(n,2p)$  and  $(n,\alpha)$  would be expected to be even smaller. In order to obtain a rough approximation, an estimated 40 MeV fission neutron flux of 0.0001 the thermal flux was coupled with an estimated cross section of 0.01 millibarn to calculate possible  $^{191}\text{Os}$  produced activities by the method used for Table 3. The following calculated activity values are for a 100-mg platinum sample

of natural isotopic composition.

Table 4. Activity after one week at a thermal flux of  $3 \times 10^{13} \text{ n} \cdot \text{cm}^{-2} \cdot \text{sec}$

---

$^{194}\text{Pt}(\text{n}, \alpha)^{191}\text{Os}$	8.5 dps
$^{192}\text{Pt}(\text{n}, 2\text{p})^{191}\text{Os}$	0.01 dps

---

For a one ppm level of osmium in platinum, the interference would be less than one percent. But for a one ppb level of osmium, the secondary  $^{191}\text{Os}$  activity would be ca. three times that produced by the osmium impurity. These calculations are highly speculative but such an interference would be serious. If the combined cross section and flux estimated are 100-1000 times too large, then such an interference would be negligible at one ppb levels. This is assumed to be the case by analogy to the experimental results found by Jowanovitz et al. (86). No  $^{192}\text{Pt}(\text{n}, \text{p})^{192}\text{Ir}$  reaction interference was observed in 24-hour irradiations with an epithermal neutron flux of  $1.6 \times 10^{13} \text{ n} \cdot \text{cm}^{-2} \cdot \text{sec}^{-1}$  in the neutron activation analysis for iridium in platinum.



## Review of Neutron Activation Methods and Related Radiochemical Techniques for Osmium and Ruthenium

Neutron activation analysis has been used for trace noble metal analysis of several types of matrix materials, ranging from pure metals or alloys to meteorites, sea water, minerals and organic matter. Although reactor neutron activation analysis techniques were being applied in 1943 (16), their use was not reported for osmium or ruthenium until 1959 (87). A chronological review of neutron activation methods used for osmium begins with the work of Leddicotte et al. (87). Osmium levels of 10-100 ppm were reported for iron and palladium. The samples and standards were irradiated for 16 hours at a flux of  $6.5 \times 10^{11} \text{ n} \cdot \text{cm}^{-2} \cdot \text{sec}^{-1}$ . The irradiated materials were dissolved in aqua regia from which the osmium was distilled as  $\text{OsO}_4$  into 6N NaOH. The osmium was precipitated as  $\text{OsS}_2$ , dissolved in  $\text{HNO}_3$  and distilled a second time into 6N NaOH. The catch solution was acidified and the osmium precipitated by powdered magnesium for a gravimetric carrier yield. The osmium activity was determined by beta and gamma-ray scintillation.

Miller's (85) studies of the neutron-activation of the elements of Group VIII produced considerable information on

the nuclear reactions of osmium and the assay of the resulting radionuclides.

Merz and Herr (88) used neutron-activation to study the isotopic abundance of osmium isotopes. Herr et al. (89) subsequently used a destructive comparator method for osmium determination. One to two gram samples of iron meteorites were irradiated for three days at a flux of  $10^{12} \text{ n} \cdot \text{cm}^{-2} \cdot \text{sec}^{-1}$ . The irradiated samples were dissolved in a  $\text{HNO}_3\text{-H}_2\text{SO}_4$  acid mixture from which the osmium was distilled as  $\text{OsO}_4$  into 6NHC1-thiourea catch solution. The carrier yields of 60-70 percent were obtained spectrophotometrically. Gamma-ray counting yielded osmium levels of 0.6 to 3.2 ppm in 10 samples.

Morris and Killick (90) determined 0.08-1.0 ppm levels of osmium and 0.1-11 ppm levels of iridium in 100 mg samples of palladium and platinum. The samples and standards were irradiated for one week at a flux of  $10^{12} \text{ n} \cdot \text{cm}^{-2} \cdot \text{sec}^{-1}$ . The irradiated samples were dissolved in HCl and distilled with  $\text{HNO}_3$  into a solution of NaOH and methanol. The osmium was precipitated hydrolytically as  $\text{OsO}_2$  which was then converted into the metal by reduction with hydrogen, and then weighed as the metal for chemical yield although no experimental values were reported. The osmium activity was measured via the beta decay

of  $^{191}\text{Os}$  and  $^{193}\text{Os}$ . It was reported that the 6.2:1 thermal to fast neutron flux ratio of the BEPO reactor produced a spurious osmium content of ca. 0.03 ppm osmium and ca. 0.16 ppm iridium from (n, $\alpha$ ) and (n,p) reaction of platinum.

Gijbels and Hoste (91) reported levels of osmium down to 1.7 ppm in ruthenium sponge. Ten mg samples were irradiated for three to five days at a flux of  $8 \times 10^{11} \text{ n} \cdot \text{cm}^{-2} \cdot \text{sec}^{-1}$ . After sodium peroxide fusion, the osmium was quantitatively separated from the ruthenium by a 30 minute  $\text{H}_2\text{SO}_4\text{-H}_2\text{O}_2$  distillation with less than 0.01 percent of ruthenium co-distillation. Tracer experiments indicated that Pt, Ir, Pd and Rh did not distill under the above conditions. The distilled  $\text{OsO}_4$  was collected in 9N NaOH and gamma-ray counted using both a 3 in. x 3 in. NaI(Tl) crystal and a 3 in. x 1 mm. NaI(Tl) wafer. The wafer suppressed detection of interfering  $^{103}\text{Ru}$  activity by a factor of three over the lower energy  $^{191}\text{Os}$  gamma-rays. The osmium content was obtained by a spiking method where the osmium activity of successively more dilute samples was plotted against the added amount of osmium. The slope of the straight line and its intercept with the ordinate allowed the calculation of the original osmium content of the unspiked ruthenium sponge.

Bate and Huizenga (92) reported osmium and ruthenium concentrations of 0.89 and 0.91 ppm respectively in chondrites. The samples and standards were irradiated for periods of one day to two weeks at a nominal slow neutron flux of  $3 \times 10^{13} \text{ n} \cdot \text{cm}^{-2} \cdot \text{sec}^{-1}$ . The irradiated samples were fused with sodium peroxide, dissolved in dilute NaOH, and the ruthenium was precipitated with ethyl alcohol. The osmium remaining in solution was subsequently precipitated with hydrogen sulfide. The ruthenium fraction was purified by distillation with  $\text{NaBiO}_3$  followed by solvent extraction of the octavalent oxide by  $\text{CCl}_4$ , back-extraction of NaOH, precipitation by ethanol, scavenging and precipitation of gold with hydrazine hydrochloride, plus further scavenging with lead iodide and cadmium sulfide. A final precipitation was made of ruthenium oxide plus treatment of the supernatant liquid with hydrogen sulfide to recover the residue ruthenium. The combined ruthenium precipitates were again subjected to a bismuthate distillation after which the ruthenium was finally precipitated as cesium hexachlororuthenate(IV). This was mounted on a weighed filter paper for counting. The initial osmium precipitate was purified by distillation, solvent extraction, scavenging and precipitation as for ruthenium. The final precipitate as cesium

hexachloroosmate(IV) was mounted and gamma-ray counted, as was the ruthenium, with a 256-channel pulse height analyzer. The chemical yields were 50-60 percent.

In 1965, Morgan (93) reported osmium levels from 800 down to  $0.65 \pm 0.39$  ppb in 0.1-0.2 g rock samples irradiated for one week at a thermal flux of  $9 \times 10^{12} \text{ n} \cdot \text{cm}^{-2} \cdot \text{sec}^{-1}$ . The irradiated samples were dissolved in sodium peroxide and then the osmium was isolated by anion-exchange elution with 0.8M  $\text{HNO}_3$ . After several solvent extraction steps, the osmium was precipitated by potassium chromothiocyanate ( $\text{Os}(\text{NH}_2 \cdot \text{CS} \cdot \text{NH}_2)_6 \cdot \text{Cr}(\text{SCN})_6$ ) and weighed with chemical yields of 30-60 percent. The isolated activities were determined by beta-counting of  $^{191}\text{Os}$  using an end-window G.M. counter.

In 1967, Crocket et al. (94) determined the concentration of Ru, Pd, Os, Ir, Pt and Au in chondrites using a combined distillation-anion exchange-solvent extraction-metal precipitation separation sequence. The 50-100 mg samples were irradiated for 20 hours at a nominal flux of  $2 \times 10^{13} \text{ n} \cdot \text{cm}^{-2} \cdot \text{sec}^{-1}$ . The osmium was isolated by  $\text{H}_2\text{SO}_4$ - $\text{H}_2\text{O}_2$  distillation followed by ruthenium distillation with  $\text{NaBiO}_3$ . The reported osmium and ruthenium levels of 0.66 and 1.6 ppm respectively were obtained by beta counting of  $^{191}\text{Os}$  and gamma-ray counting

$^{103}\text{Ru}$  using a NaI(Tl) detector coupled to a 256-channel analyzer. Osmium chemical yields as the reduced metal were ca. 60 percent with some count rates of 4-10 cpm above a 1.5 cpm background. The uranium content of some samples produced sufficient fission product ruthenium to prevent its determination. None of the ruthenium determinations had reported chemical yields.

A subsequent work by Crocket et al. (95) expanded the above investigation to silicate rocks, meteorites and sulfide ores. The reported concentrations were apparently a factor of ten too low based on the erroneous comparison to previous work. The reported levels ranged down to  $0.74 \pm .02$  ppb for osmium and  $1.50 \pm .04$  ppm for ruthenium.

Morgan et al. (96) reported nonradiogenic osmium levels of 20 ppb down to one ppb which represented only upper detection limits since the osmium abundances were vanishingly small. Samples of ten to 100 mg were irradiated for one week at a flux of  $3 \times 10^{12} \text{ n} \cdot \text{cm}^{-2} \cdot \text{sec}^{-1}$ . The osmium activity was isolated and counted by the same method as previously reported (93) in which the comparator standards were prepared by spiking 20 to 30 mg of Specpure  $\text{SiO}_2$  with ca. 0.5  $\mu\text{g}$  of rhenium and 3.0  $\mu\text{g}$  of osmium.

Chung and Beamish (97) reported the determination of osmium and ruthenium by quantitative distillation from sulfide ores. Ore samples of 100-200 mg were irradiated four to five days at a flux of  $5 \times 10^{12} \text{ n} \cdot \text{cm}^{-2} \cdot \text{sec}^{-1}$ . The irradiated samples were fused with sodium peroxide using an iron(III) hydroxide precipitation to prevent loss of osmium due to volatilization occurring when trace solutions were evaporated. Tracer studies of spiked sulfide ores indicated quantitative recovery, hence carrier yields were not reported. The osmium and ruthenium were each isolated by a 40-minute distillation at  $105^{\circ}\text{C}$  with  $\text{H}_2\text{SO}_4\text{-H}_2\text{O}_2$  mixture to distill  $\text{OsO}_4$  followed by a one hour distillation at  $100^{\circ}\text{C}$  with  $\text{NaBrO}_3$  to distill  $\text{RuO}_4$ . The tetroxides were collected in 9M NaOH and counted with a NaI(Tl) detector coupled multichannel analyzer. Very small amounts of ruthenium, ca. 0.5-1.5 ng, were found to co-distill with the osmium. Some qualitative spectra were obtained using a  $22\text{-cm}^3 \text{ Ge(Li)}$  detector. Reported osmium levels of  $24 \pm 10$  ppb and ruthenium levels of  $290 \pm 200$  ppb were an order of magnitude higher for standard rocks, G-1 and W-1, than the values reported by Morgan (93).

Gijbels and Hoste (98) published another article in 1968 in their continuing investigation of platinum metals. Osmium,

ruthenium, iridium and gold were determined in 100 mg platinum samples irradiated for 11 days at a thermal neutron flux of  $4 \times 10^{11} \text{ n} \cdot \text{cm}^{-2} \cdot \text{sec}^{-1}$ . Osmium levels of 0.2-0.7 ppm and ruthenium levels of 0.3-0.7 ppm were reported. The lower limits of detection for the experimental conditions was reported as ca. 0.5 ppm for ruthenium and ca. 0.2 ppm for osmium. The platinum samples were dissolved with aqua regia in sealed silica tubes before irradiation. After irradiation the osmium and ruthenium were quantitatively distilled with  $\text{H}_2\text{SO}_4\text{-NaBiO}_3$  for two hours at ca.  $100^\circ\text{C}$  into iced 9M NaOH. The alkaline mixture was counted for ruthenium with a NaI(Tl) detector coupled to a 400 channel pulse-height analyzer using the 490 KeV  $^{103}\text{Ru}$  peak. The alkaline solution was then acidified with  $\text{HNO}_3$  to distill osmium into 9M NaOH which was then counted using the  $^{191}\text{Os}$  65 KeV or 129 KeV peak. Since it was previously reported (99) that osmium and ruthenium can be distilled almost quantitatively under the above conditions, no carrier yields were reported. The second distillation was assumed to be quantitative for osmium although the isolated  $^{191}\text{Os}$  activity was contaminated with some  $^{103}\text{Ru}$ . The extent of the contamination was not reported and no osmium or ruthenium gamma-ray spectra were shown.



Kiesl (100) reported osmium and ruthenium levels of 0.6 ppm and 1.6 ppm respectively along with 16 other elements in ordinary chondrites. Samples of 100-200 mg were irradiated 60-120 hours at a flux of  $3 \times 10^{13} \text{ n} \cdot \text{cm}^{-2} \cdot \text{sec}^{-1}$ . Carriers were added to the irradiated samples and dissolved in  $\text{H}_2\text{SO}_4$ . The osmium and ruthenium were reported to quantitatively distill with  $\text{NaBrO}_3$  into 2M  $\text{NaOH}$  following distillation of selenium, arsenic, antimony, tin, mercury and rhenium with a hydrogen halide mixture of concentrated  $\text{HCl}$  and 40 percent  $\text{HBr}$ . The osmium and ruthenium distillation method had been shown by radiochemical tracers to be respectively 97 and 94 percent quantitative.

Laul et al. (101) reported a group separation technique for the determination of 15 elements in rocks and chondrites. Three groups were isolated by extraction, distillation and ion exchange. For osmium, in the distillation group, levels down to ca.  $0.42 \pm 0.07$  ppm were reported which were upper limits only since the sensitivity limits did not permit its quantitative assessment in one g samples. Irradiations were for six days at a flux of  $8 \times 10^{12} \text{ n} \cdot \text{cm}^{-2} \cdot \text{sec}^{-1}$ . The irradiated samples were dissolved in a  $\text{HF-H}_2\text{SO}_4$  mixture which were extracted with 6N  $\text{HCl}-(\text{C}_2\text{H}_5)_2\text{O}$  after the excess  $\text{HF}$  had been destroyed with

$\text{H}_3\text{BO}_3$ . The  $(\text{C}_2\text{H}_5)_2\text{O}$  was removed by heating followed by distillation of As, Sb, Hg, Re, and Se as volatile bromides with  $\text{HBr-H}_2\text{SO}_4$ . The osmium was subsequently distilled with  $\text{H}_2\text{O}_2$  at  $110^\circ\text{C}$  as the volatile tetroxide with a carrier yield of nine percent. The carrier yield coupled with the reported detection limit of  $0.08\ \mu\text{g}$  meant that ca.  $0.9\ \mu\text{g}$  of osmium could be determined for a one gram sample.

Since ruthenium and osmium usually occur together, several of the neutron activation investigations for osmium also included a ruthenium determination (92,94,95,97,98,100). Although radiochemical methods for the determination of fission product radio-ruthenium were reported by 1949 (102), it was 1962 before Killick and Morris (103) used neutron activation for traces of ruthenium in platinum. The irradiation conditions were described earlier (90). The ruthenium activity was isolated by dissolving the sample in  $\text{HCl-HNO}_3$ , fuming with  $\text{H}_2\text{SO}_4$ , treating successively with potassium permanganate, iron(II) ammonium sulfate, nitric acid and then carbon tetrachloride to extract osmium holdback carrier. The ruthenium in the aqueous phase was oxidized by silver(II) oxide and the octavalent oxide was extracted with carbon tetrachloride to be back-extracted into sodium hydroxide and

dithionite solution. A gold salt was added as a scavenger and ruthenium was finally precipitated as the hydrated oxide by methanol. Ruthenium levels of 0.83 to 1.96 ppm were obtained after chemical yield determinations.

Gijbels and Hoste (104) determined ruthenium and iridium in osmium. The irradiation conditions have been described previously (91). Ruthenium contents ranged from  $11 \pm 7$  ppm for purified osmium samples up to  $106 \pm 9$  ppm in commercial osmium. The 10 mg irradiated samples were fused with sodium peroxide followed by  $\text{H}_2\text{SO}_4\text{-H}_2\text{O}_2$  distillation of osmium with an interim destruction of peroxide with potassium permanganate followed by a continuation of the  $\text{H}_2\text{SO}_4\text{-H}_2\text{O}_2$  distillation. The ruthenium was then removed by distillation from a  $\text{H}_2\text{SO}_4\text{-NaBrO}_3$  medium to leave the iridium in the residue. It was reported that some iridium was distilled along with ruthenium when  $\text{HClO}_4$  was used. Ruthenium levels down to 10 ppm in 10 mg samples ( $10^{-7}$  g) could be determined under the experimental conditions. The second-order  $^{190}\text{Os}(\text{n},\gamma)^{191}\text{Os} \xrightarrow{\beta^-} ^{191}\text{Ir}(\text{n},\gamma)^{192}\text{Ir}$  reaction was reported to produce 0.03 to 0.21 ppm spurious iridium impurity levels after irradiation periods of three to ten days.

Fourcy et al. (105) reported a radioecological study

using ammonium aquopentachlororuthenate(III) added to a closed aquatic ecosystem. Although the study is not germane to this investigation, the reported method of ruthenium analysis is of interest. The biological samples were dry ashed before irradiations of 120 hours with a thermal flux of  $2 \times 10^{13} \text{ n} \cdot \text{cm}^{-2} \cdot \text{sec}^{-1}$ . The irradiated sample was heated gently with concentrated  $\text{H}_2\text{SO}_4$  after the addition of ruthenium carrier. The ruthenium activity was then quantitatively distilled from a  $\text{HClO}_4\text{-H}_2\text{SO}_4$  at  $130^\circ\text{C}$  for an unspecified time into 6N NaOH. The reported sensitivity was  $3 \times 10^{-3} \text{ } \mu\text{g}$  i.e. 3 ppb in a one gram sample. The aquatic ecosystem has a theoretical initial concentration of 54 ppb, but after one hour elapsed time only six ppb were detected. This dropped to ca. 0.2 ppb aqueous concentration after nine days which then remained constant for three months. The reported NaI(Tl) gamma-ray spectrum of the distilled ruthenium contained two peaks not characteristic of  $^{103}\text{Ru}$ .

Abdel-Rassoul et al. (106) analyzed high purity palladium for Ru plus Co, Fe, Zn, Cd and Hg by neutron activation. Samples of 100 mg were irradiated for 48 hours with a mean activation neutron flux of  $1.3 \times 10^{13} \text{ n} \cdot \text{cm}^{-2} \cdot \text{sec}^{-1}$ . The irradiated sample was dissolved in  $\text{HNO}_3$ , carriers added, and silver car-

rier precipitated with HCl. The palladium matrix was then precipitated by boiling with formic acid after which the solution was loaded onto an anion exchange column in the chloride form. The elution sequence had ruthenium and the other non-absorbing chloro-complexes eluded first with 12M HCl which was followed in sequence by Co, Fe, Zn, Cd and Hg. The ruthenium fraction was precipitated with zinc powder giving carrier yields of 30-40 percent. Two separate sources, A.R. grade palladium chloride and palladium foil, yielded 24 and 11 ppm of ruthenium respectively via a comparator method using scintillation gamma-ray spectrometry.

This completed the review of thermal neutron activation investigations of osmium and ruthenium reported through early 1971. Beamish et al. (107) published a critical review of neutron activation and tracer methods for the noble metals reported through 1965. The bibliography by Lutz et al. (18) indexed reported activation analysis methods by matrix analyzed, element determined, technique used, and author.

Many other analytical methods have been applied to the noble metals. Beamish et al. (108) have published a critical review of atomic absorption, spectrochemical and X-ray fluorescence methods. In general, all three techniques require a

sample size of 1-20 g in order to achieve a sensitivity approaching sub-ppm levels. In the case of spectrochemical methods, 80 ppm osmium and five ppm ruthenium are the reported lower limits. Kohler and Lincoln (109) were able to extend emission spectrochemical limits down to 20 ppm osmium and two ppm ruthenium. Beamish also reviewed gravimetric methods (110), titrimetric methods (111), and colorimetric methods (112) for noble metals. A comprehensive summary of the analytical methods applied to the noble metals was published by Beamish (113) in addition to a summary by Walsh and Hausman (114). Gupta and Sen (115) utilized distillation plus cation exchange separation to apply spectrophotometric methods for all six platinum group metals in iron and stony meteorites. With sample sizes of 4-20 g, osmium and ruthenium levels down to 0.54 and 0.50 ppm respectively were obtained.

The predominate method used for the separation of osmium and ruthenium from the other platinum metals plus from each other is their distillation as volatile tetroxides. Nitric acid and hydrogen peroxide are the only reagents that have been cited as being useful for the selective isolation of osmium. Selective chloroform solvent extraction (116,117), chromatographic separation (118) and alkaline ethyl alcohol

precipitation (92) are the only other reported osmium-ruthenium separation methods. These are usually subject to interferences when a large excess of another noble metal is present. Consequently the selective distillation method seemed the most promising.

Chung and Beamish (119) studied osmium-ruthenium distillations utilizing radioactive tracers. They reported that a quantitative separation of osmium from ruthenium could be achieved by distillation from peroxide-sulfuric acid solution at  $110^{\circ}\text{C}$  for about 40 minutes. Slow or incomplete distillations were observed when osmium was present as either the chloro or bromo complex. Use of the nitric acid selective distillation method was avoided because it was reported to interfere in the subsequent removal of ruthenium while perchloric acid oxidized both osmium and ruthenium at  $150^{\circ}\text{C}$ . It was also reported that negligible amounts of active ruthenium ( $<0.2\text{ }\mu\text{g}$ ) distilled using the peroxide-sulfuric acid method recommended, although  $0.2\text{ }\mu\text{g}$  represented 0.4-4.0 percent of the added ruthenium.

## EXPERIMENTAL

The Ames Laboratory Research Reactor (ALRR) was used for all sample irradiations. This is a five megawatt (5 MW) tank-type reactor, fueled with fully enriched  $^{235}\text{U}$ , cooled and moderated with heavy water. The reactor core assembly consists primarily of the uranium fuel elements within the heavy water tank and surrounded by a stainless steel thermal shield within a light water tank. A total of 35 experimental facilities, including radiation ports, beam tubes, vertical thimbles, rabbit tubes and a thermal column, penetrate the concrete shielding to permit access to the reactor core for irradiations. One vertical thimble (V-5) was used throughout this work for sample irradiations. This thimble is about 14 inches from the center of the core. At this location, the thermal flux is approximately  $3 \times 10^{13} \text{ n} \cdot \text{cm}^{-2} \cdot \text{sec}^{-1}$  when the reactor is operating at 5 MW full power. The cadmium ratio at this point is approximately 20.

Beta radioactivity measurements were obtained using a model 196 scaler manufactured by Nuclear Chicago which was equipped with a timer supplied by the same company. The lead shielded Geiger-Mueller (GM) counting tube was a Nuclear Chicago type D-34 with a window thickness of  $1.4 \text{ mg} \cdot \text{cm}^{-2}$



and an operating voltage of 975 volts.

All the gamma-ray measurements were conducted using a 3" x 3" NaI(Tl) crystal optically coupled to a photomultiplier tube. The entire assembly was shielded by a 3' x 3' lead brick cave. The circular NaI(Tl) crystal had a 9.5 mm x 25 mm deep well. But except for the use of the well in some early qualitative investigations, all samples were counted in 20 ml vials setting on top of the crystal. The gamma-ray energy resolution  $\eta$  of the crystal, usually defined as

$$\eta = \frac{\Delta E, \text{ full width at half-height of } ^{137}\text{Cs peak}}{\bar{E}, \text{ average energy of } ^{137}\text{Cs peak (0.661 MeV)}} \quad (16)$$

was 9.7 percent. The NaI(Tl) crystal detector assembly was coupled to a multichannel pulse height analyzer. The analyzer was a Radiation Instrument Development Laboratory (RIDL) Model 34-12B transistorized 400-channel pulse height analyzer consisting basically of an amplifier, an analog-to-digital (ADC) converter, a computer with a ferrite memory core of  $10^6$  counts per channel capacity, a cathode ray tube (CRT) display, and control circuitry for automatic operation. Integrated with the analyzer was a timing system which permitted counting in either of two modes. The live time mode, in which the timer operated only during the time when the ADC was accept-

ing counts, which automatically compensated for analyzer dead time. The clock time mode, in which the timer indicated elapsed clock time for the counting period, had a provision for manual dead time compensation through an external dead time indicator. Data manipulation accessories included a RIDL Model 52-35 magnetic tape recorder, a Tally Model 420 paper tape punch, and Tally Model 429 paper tape reader. The data stored in the analyzer memory could also be read out with a Frieden printer which permitted manual integration of counts in desired regions of gamma-ray energy spectra. A spectrum in the analyzer memory could also be plotted in either log or linear display with a Mosely Co. Model 2D-2 X-Y Recorder.

All spectrophotometric measurements were conducted on a Cary Model 14 spectrophotometer equipped with a high intensity visible light source. This permitted scanning from 650-350 m $\mu$  with a precision of 0.005 absorption units when readings were taken from chart paper.

The spectra obtained were immediately stored on punch paper tape for subsequent analysis. The data were transferred to 7-track magnetic tape using the IBM paper-to-magnetic tape converter facilities of the ISU Cyclone Computer Laboratory. The 400-channel spectra on magnetic tape were then converted

to IBM card decks using PRESTO (120), a FORTRAN-IV computer program. The data could then be processed from cards with the option to transfer reference spectra from cards onto 9-track magnetic tape for subsequent retrieval. The single or multicomponent spectra were quantitatively analyzed using RESOLF, a computer program written by Korthoven (68) and modified by this author. RESOLF, based on a linear least squares procedure, consisted of a set of 13 subroutines, written in FORTRAN-IV for use on the IBM 360/50 computer.

#### Materials

The commercial platinum was purchased from J. Bishop Chemical Company as #12 (ca. 2.6 mm) diameter wire. The irradiation samples were prepared by cutting the wire into ca. 100 mg pieces, pickling with hot HCl, then hot HNO<sub>3</sub> plus a final washing with distilled water.

The high-purity platinum stock was the above commercial material which had been subjected to a chemical procedure developed in this laboratory specifically for the removal of iridium. The procedure was expected to also reduce possible trace levels of other platinum metals. An outline of the procedure is cited below:

1. Dissolve the metal in aqua regia.
2. Make solution basic (pH 10) and reduce with hydrazine to platinum black.
3. Coagulate and wash repeatedly with aliquots of water until neutral.
4. Repeatedly digest with HCl until the supernatant becomes only slightly colored (light yellow) after digestion.
5. Wash with water until obtaining negative chloride test, then repeat step four using only  $\text{HNO}_3$ .
6. Dissolve residue in a minimum amount of aqua regia.
7. Evaporate to near dryness, add concentrated HBr, heat to near dryness. Repeat at least three times.
8. Add excess KBr to hot  $\text{H}_2[\text{PtBr}_6]$  and allow to cool slowly.
9. Separate the precipitate and recrystallize from water three times.
10. Reduce  $\text{K}_2\text{PtBr}_6$  crystals to platinum black by repeating steps one through four.

### Reagents

The osmium used in the preparation of the irradiation standards and carrier solutions was purchased from K and K

Laboratories, Inc. in the form of  $(\text{NH}_4)_2\text{OsCl}_6$  crystalline powder and as  $\text{OsO}_4$  crystals. The iridium was purchased from the same company as  $\text{Na}_2\text{IrCl}_6$  powder as was ruthenium as  $(\text{NH}_4)_2\text{RuCl}_6$  crystalline powder. Some ruthenium metal powder was purchased from Baker Chemical Company. All other chemicals used in this study were of reagent analytical grade except for the irradiated aqua regia solutions. The  $\text{HCl}$  was distilled three times from a glass still as the constant boiling ( $110^\circ\text{C}$ ) mixture (20.24%). The  $\text{HNO}_3$  was also distilled two times at  $86^\circ\text{C}$  with the middle two-thirds fraction of each acid retained for the next distillation. Water used in the preparation of solutions was drawn from the distilled water tap and redistilled from alkaline permanganate.

### Preparation and Standardization of Carrier Solutions

#### Ruthenium

An accurately weighed amount of ruthenium powder was dissolved in an alkaline-hypochlorite solution to form a ruthenate-perruthenate mixture of ca. 1.7 mg of ruthenium per ml. The above solution was standardized by two separate methods. One was a photometric procedure reported by Larsen and Ross (121). An aliquot of the ruthenium solution was precipitated as  $\text{RuO}_2 \cdot x\text{H}_2\text{O}$  with ethanol from the alkaline solu-

tion. The precipitate was washed twice with water and then dissolved in concentrated HCl. The resulting dark red-orange solution was fumed with H<sub>2</sub>SO<sub>4</sub> before being quantitatively distilled from a sodium bismuthate-6N sulfuric acid mixture as ruthenium tetroxide into iced 1N sodium hydroxide-0.05M sodium hypochlorite. The catch solution was diluted to volume with 1N NaOH to give ca. 16  $\mu\text{g}\cdot\text{ml}^{-1}$ . The absorbance of the yellow perruthenate solution was measured at 385 m $\mu$  against a reagent blank also carried through the entire procedure. The 385 m $\mu$  peak to 365 m $\mu$  valley absorbance ratio of 1.10 was used for an interference check.

A second confirmatory ruthenium standardization was conducted using a gravimetric method involving reduction by magnesium (122). An aliquot was initially treated as above through the HCl dissolution step. The ruthenium was precipitated by reduction with powdered magnesium. The powdered ruthenium precipitate was filtered onto a tared fritted glass filter, washed with hot 2N HCl, water, acetone and then dried under vacuum. The two standardization methods had agreement within one percent and also indicated the ruthenium was 99+ percent pure.

The ammonium hexachlororuthenate solutions were prepared

by dissolving weighed portions of the salt in dilute aqua regia to give ca. one mg of ruthenium per ml. The resulting solution was then standardized by both of the above methods.

### Osmium

Weighed osmium tetroxide glass ampoules were broken into cold 6N NaOH and diluted to volume to give ca. 1.5 ml of osmium per ml. The recovered glass fragments were weighed to determine the amount of  $\text{OsO}_4$  as one standardization method. Aliquots of the osmium solution were also standardized by a gravimetric method similar to that used for ruthenium. Since osmium does not precipitate with ethanol, the osmium aliquots were iced during neutralization with HCl to prevent loss of osmium by volatilization. The orange color of the basic solution was discharged to colorless when slight acidity was reached. The osmium was then precipitated in the same manner as for ruthenium. A blank check was obtained by heating the osmium precipitate overnight at ca.  $200^\circ\text{C}$  on a hot plate in the hood to volatilize osmium metal as  $\text{OsO}_4$ . The blank correction was usually a negligible amount.

A second osmium standardization was conducted using a spectrophotometric method described by Sandell (123). An osmium aliquot was quantitatively distilled from a  $\text{H}_2\text{SO}_4\text{-H}_2\text{O}_2$

mixture into 1N  $\text{H}_2\text{SO}_4$ -three percent thiourea ( $\text{SC}(\text{NH}_2)_2$ ). The absorbance was measured at 480  $\text{m}\mu$  against a blank carried through the complete procedure. The 480  $\text{m}\mu$  peak to 505  $\text{m}\mu$  valley absorbance ratio of 1.41 was used as a check for possible interferences. The absorbance of the red thiourea complex was quite insensitive to excess reagents and time of color development. The triangular osmium standardization method had agreement within one percent. Another standardization method of thionalide precipitation (124), applicable to both osmium and ruthenium, was found unsuccessful due to incomplete precipitation which had been experienced by other investigators (125,126). The  $(\text{NH}_4)_2\text{OsCl}_6$  solution of ca. 1 ml of osmium per ml was similarly standardized by the gravimetric and spectrophotometric methods used above.

An internal standardization check was also obtained when samples were irradiated. This was achieved by quantitative comparison of the radioactivity induced in the standardized osmium and ruthenium solutions prepared from the two different chemical sources. This radioactivation check gave agreement within two percent precision.

### Iridium

Solutions of  $\text{Na}_2\text{IrCl}_6$  were prepared by dissolving the powder in dilute  $\text{HCl}$  to give ca. five ml of iridium per ml.



The spectrophotometric standardization procedure (127) used a 10:10:1  $\text{HClO}_4\text{-H}_3\text{PO}_4\text{-HNO}_3$  mixed acid solution to which the iridium aliquot was added. The solution was heated at  $110^\circ\text{C}$  for one hour to expel any volatile constituents. The temperature was then raised to  $150^\circ\text{C}$  and held at this temperature for seven minutes after the initial development of a deep purple color. The cooled solution was diluted to volume with one percent  $\text{HNO}_3$  to give a final concentration of 6-100 ppm of iridium. The absorbance at  $564\text{ m}\mu$  was measured against a blank taken through the entire procedure.

### Platinum

Platinum carrier solution was prepared from  $\text{K}_2\text{PtCl}_6$ , obtained from L. Hunter of this laboratory, by dissolving accurately weighed amounts to give 2.34 mg of platinum per ml. The platinum salt had been prepared by dissolving high-purity platinum in aqua regia, removing nitrate ion by repeated evaporation to near dryness with  $\text{HCl}$  aliquots, and then precipitating with excess  $\text{KCl}$ . The precipitate was washed with alcohol and then ether before air drying.

### Irradiation Procedure

The platinum samples analyzed in this investigation were of two types; the purified material as platinum black powder

and the commercial wire as solid chunks. All the platinum samples, in 100-200 mg amounts, were irradiated in sealed, evacuated eight mm ID quartz ampoules. Some early samples were irradiated as solids but the majority of the samples were irradiated as solutions. This was done because of the volatile nature of osmium and ruthenium which was evidenced by loss of sample during evaporations before and after irradiation. Furthermore, considerable difficulty was experienced in quantitatively dissolving the standards after irradiation.

The solution irradiations were prepared by adding cold (ca. 0°C) aqua regia, 150  $\mu$ l  $\text{HNO}_3$ -450  $\mu$ l  $\text{HCl}$ , to the platinum samples with enough water added to make 1 ml of solution. The cold aqua regia solution containing the solid platinum sample was frozen in liquid nitrogen and evacuated before sealing the quartz tube with a  $\text{H}_2$ - $\text{O}_2$  flame. The platinum samples were then dissolved by placing the sealed tubes in a 140°C oven for 24 hours.

The irradiation standards were prepared by micropipetting aliquots into cold quartz ampoules along with 150  $\mu$ l of  $\text{HNO}_3$  plus 450  $\mu$ l of  $\text{HCl}$ . The volumes were diluted to one ml with water before liquid nitrogen freezing, evacuation and sealing.

The sealed samples were also subjected to the 140°C oven treatment primarily to check for leaks and mechanical strength before irradiation. The samples were irradiated in 2.6 cm by 20 cm aluminum cans with  $\text{HAuCl}_4$  or  $\text{NH}_4\text{Br}$  used as flux monitors when two or more cans were irradiated. After irradiations of 150-1335 MWH, the samples were opened in a dry box by first freezing in liquid nitrogen and then breaking into water before thawing occurred. The appropriate amounts of carriers were then added before distillation or dilution to volume.

### Chemical Separations

Preliminary investigation of the separation of osmium from ruthenium indicated they would effectively be separated by using a  $\text{H}_2\text{SO}_4\text{-H}_2\text{O}_2$  mixture to first distill  $\text{OsO}_4$  and then adding  $\text{NaBiO}_3$  to distill  $\text{RuO}_4$ . The distillation apparatus is shown in Figure 7. The sample in flask A was electrically heated via a controlled voltage to carefully regulate the temperature. The heating apparatus was further controlled by a timer for automatic shutdown. Gaseous products formed in flask A were swept into flask B by sparging with air. This was accomplished by attaching the bubbler to an aspirator. Flask B was initially empty while traps C and D contained the appropriate catch solution. Flask B was heated in the same

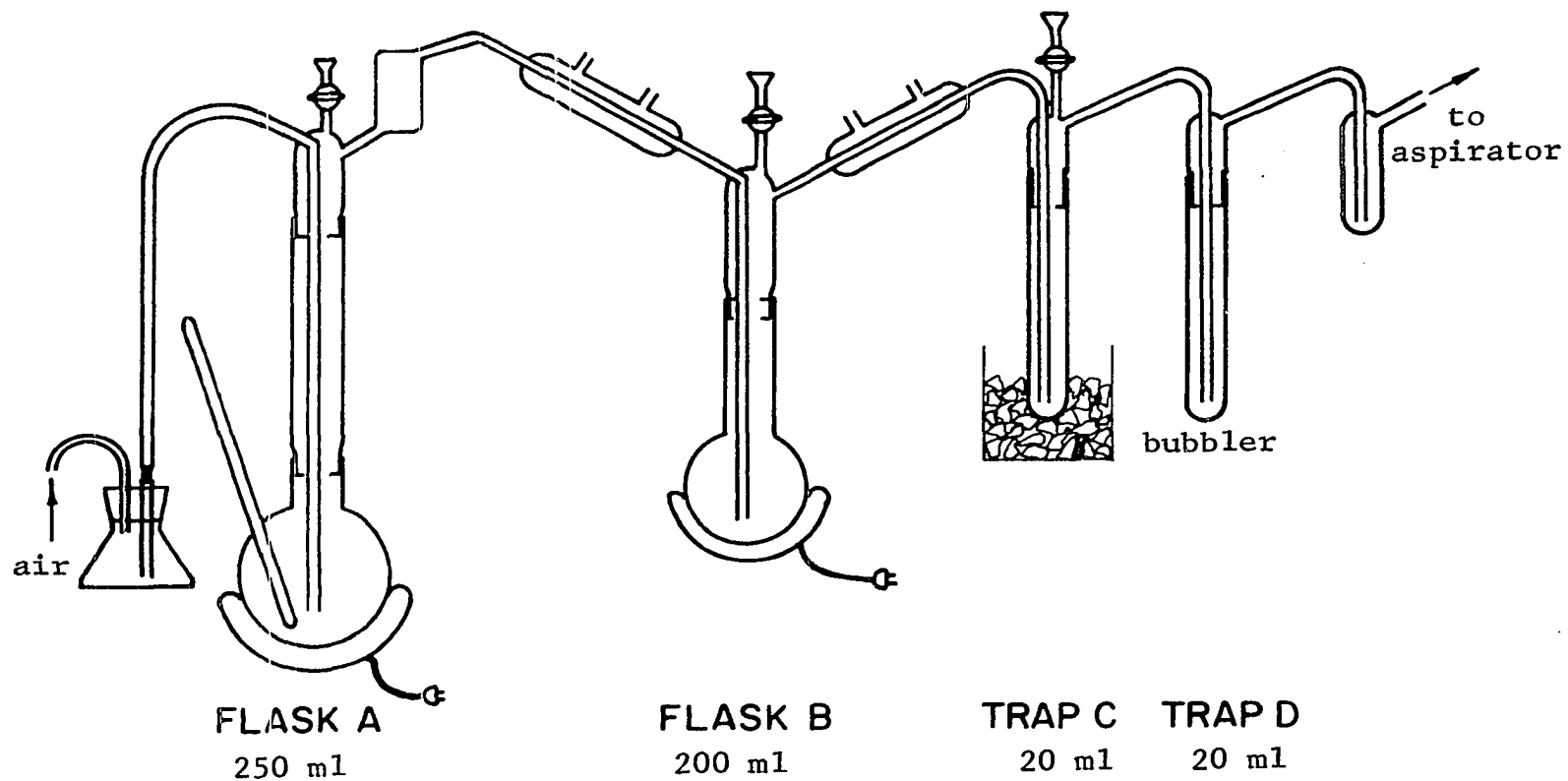


Figure 7. Distillation apparatus used in a fume hood with Flask A behind a Pb brick shield

manner as flask A to distill any desired condensation products into trap C. Ideally, all the desired products were retained in trap C while trap D and the bubbler served as safety catch solutions. Experimentally, 97-100 percent of the desired material remained in trap C. As mentioned above, the  $\text{H}_2\text{SO}_4$ - $\text{H}_2\text{O}_2$  mixture was found to separate effectively osmium from ruthenium, but in the presence of platinum, ruthenium partially co-distilled with osmium. This was not too surprising since Beamish (113) repeatedly cautioned against the possibility of a platinum group element behavior being modified by the presence of other elements. Other investigations (97,98) found some co-distillation with  $\text{H}_2\text{SO}_4$ - $\text{H}_2\text{O}_2$  or  $\text{HNO}_3$  as the oxidizing media. No other oxidizing agent has been reported to selectively oxidize osmium to  $\text{OsO}_4$  in the presence of ruthenium.

The use of sodium bromate-sulfuric acid, bromic acid, perchloric acid, sodium hypochlorite, ammonium peroxysulphate, ceric, permanganate and chromate have been reported for the simultaneous oxidation of both metals. The use of  $\text{HClO}_4$  was tested in this investigation to distill both elements from platinum into flask B where they could be trapped for subsequent separation. Although a  $\text{H}_2\text{SO}_4$ - $\text{H}_2\text{O}_2$  catch solution was

in flask B, a detectable amount of  $\text{OsO}_4$  was found to pass into trap C along with some  $\text{RuO}_4$ . It was noted that  $\text{RuO}_4$  apparently did not form below  $140^\circ\text{C}$  as evidenced by color changes. A careful investigation of distillation temperatures indicated a selective distillation could be accomplished by utilizing the increasing oxidizing power of  $\text{HClO}_4$  with increasing temperature. The distillation sequence developed is shown by schematic form in Figure 8. Step I distilled the osmium into both flask B and partially into flask C. Step II distilled the remaining condensed osmium from flask B into trap C. The collected osmium was removed from trap C which was then charged with the ruthenium catch solution. Step III oxidized ruthenium to  $\text{RuO}_4$  which distilled into flask B. Since the liquid contents of flask B reduced most of the  $\text{RuO}_4$  to some nonvolatile species, step IV was necessary to collect the ruthenium in trap C.

Table 5 summarizes the preliminary investigations conducted on the distillation of osmium. Each experiment represents two to five runs under the stated conditions. The distilled  $\text{OsO}_4$  was condensed into 15 ml of two percent thiourea-2N  $\text{H}_2\text{SO}_4$  in trap C. All distillation distribution calculations were obtained from spectrophotometric and or radioactive

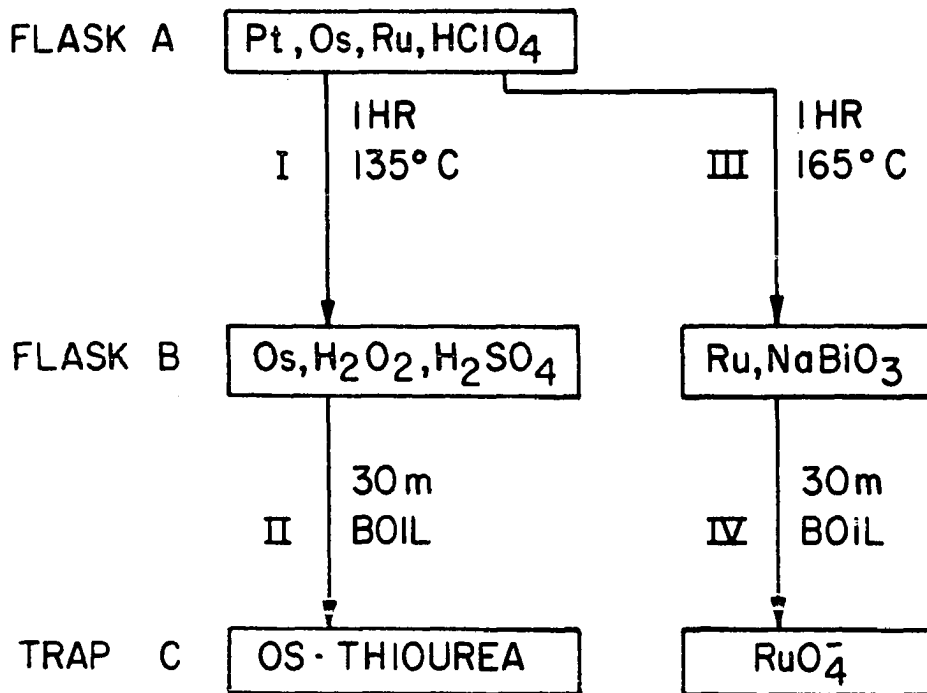


Figure 8. Radiochemical distillation procedure for the analysis of the platinum samples

Table 5. Distillation of osmium

Expt. no.	Sample	Element added, mg	Oxidant	Flask A Temp. °C	Time, min.
1	Os	3.178			
2	Os	3.178	72% HClO <sub>4</sub> , 10 ml conc H <sub>2</sub> SO <sub>4</sub> , 5 ml	140	15
3	Os + tracer	0.728	72% HClO <sub>4</sub> , 20 ml	140	10
4	Os + tracer	0.728	72% HClO <sub>4</sub> , 20 ml conc H <sub>2</sub> SO <sub>4</sub> , 5 ml	140	5
5	Os + tracer	0.728	72% HClO <sub>4</sub> , 15 ml	138	45

<sup>a</sup>The temperature in flask B was that of boiling-reflux conditions of ca. 100-105°C.



Oxidant	Flask B <sup>a</sup>		Residual A, %	Residual B, %	Recovery C, %
	Time,				
	min.				
conc. H <sub>2</sub> SO <sub>4</sub> , 3 ml 30% H <sub>2</sub> O <sub>2</sub> , 15 ml	30	-	0	100	
conc. H <sub>2</sub> SO <sub>4</sub> , 2 ml 30% H <sub>2</sub> O <sub>2</sub> , 5 ml	15	0	0	98.2	
none		4.1	94.6	1.3	
conc. H <sub>2</sub> SO <sub>4</sub> , 3 ml 30% H <sub>2</sub> O <sub>2</sub> , 5 ml	20	18.8	0.1	80.2	
conc H <sub>2</sub> SO <sub>4</sub> , 5 ml 30% H <sub>2</sub> O <sub>2</sub> , 3 ml	30	0.9	0.1	98.8	

tracer measurements. Although flask B was initially empty, the distilled liquid condensing into flask B resulted in the retention of most of the  $\text{OsO}_4$  as evidenced by experiment three. Furthermore, just boiling the distilled liquid in flask B was found not to force the distilled  $\text{OsO}_4$  on into trap C indicating some reduction to a lower oxidation state. Hence it was necessary to reoxidize to  $\text{OsO}_4$  with the  $\text{H}_2\text{SO}_4$ - $\text{H}_2\text{O}_2$  mixture. The 30 minute boiling of flask B plus using a minimal amount of  $\text{H}_2\text{O}_2$  reflected a subsequently found need to reduce most of the excess  $\text{H}_2\text{O}_2$  which could reduce the  $\text{NaBiO}_3$  added for the ruthenium distillation. Experiment 3 of Table 5 indicated that very little osmium distilled from flask A passed directly on into trap C. The osmium which was found in trap C probably passed through flask B during the early stages of the distillation when the detectable amount of pink color was formed in trap C. When the sparging rate was held to under 2.5-3.0 bubbles per second, less than one percent of the osmium passed into trap D.

The ruthenium distillation studies are summarized by Table 6. The obviously stronger oxidizing condition necessary for ruthenium is illustrated by comparing experiment 3 of Table 6 with experiment 4 of Table 5. Visually,  $\text{RuO}_4$  does

Table 6. Distillation of ruthenium

Expt. no.	Sample	Element added, mg	Oxidant	Flask A	
				Temp., °C	Time, min.
1	Ru	4.091			
2	Ru	4.091	72% HClO <sub>4</sub> , 15 ml	165	40
3	Ru + tracer	0.532	72% HClO <sub>4</sub> , 15 ml conc. H <sub>2</sub> SO <sub>4</sub> , 5 ml	165	5
4	Ru + tracer	0.532	72% HClO <sub>4</sub> , 15 ml	165	60

<sup>a</sup>The temperature in flask B was that of boiling-reflux condition of ca. 100-105°C.

Oxidant	Flask B <sup>a</sup>	Residual A, %	Residual B, %	Recovery C, %
	Time, min.			
conc. H <sub>2</sub> SO <sub>4</sub> , 5 ml NaBiO <sub>3</sub> , 1 gm	15	-	0	100
conc. H <sub>2</sub> SO <sub>4</sub> , 5 ml NaBiO <sub>3</sub> , 2 gm		0	0	99
conc H <sub>2</sub> SO <sub>4</sub> , 5 ml NaBiO <sub>3</sub> , 2 mg	15	85.5	0.1	14.3
conc. H <sub>2</sub> SO <sub>4</sub> , 5 ml NaBiO <sub>3</sub> , 2 gm	30	.2	0.1	99.6

not start to form until flask A reaches 145-148°C. From this temperature on the orange solution in flask A changes to yellow to yellow-green to essentially colorless at 160°C. Yet the tracer, irradiated aqua regia solutions of ammonium hexachlororuthenate(IV), was not significantly distilled at 165°C after five minutes as shown by experiment 3 of Table 5. Experiment 4 indicated that quantitative distillation could be obtained after one hour at 165°C. The formation of quite stable nitric oxide complexes of ruthenium (128) was probably the reason for the apparently different behavior between carrier and tracer. Consequently later carrier solutions were aged with aqua regia and the ruthenium distillation conditions were selected to be quantitative. Some distillations were taken up to 200°C where copious amounts of  $\text{HClO}_4$  fumes were produced. Even at this temperature, no distillation of iridium occurred when the sparging rate was maintained below the previously mentioned maximum. It was also necessary to keep the heating rate low enough to prevent spray from being forced over.

Table 7 summarizes the combined osmium-ruthenium distillation studies. Experiments 2 and 3 represent several tracer studies involving both  $\text{HClO}_4$  and  $\text{H}_2\text{SO}_4\text{-HClO}_4$  as the oxidizing

Table 7. Distillation of osmium-ruthenium mixture

Expt. no	Sample	Element added, mg	Oxidant	Flask A	
				Temp., °C	Time, min.
1	Os +	3.178			
	Ru	4.091			
2	Os +	0.728	72% HClO <sub>4</sub> , 15 ml conc. H <sub>2</sub> SO <sub>4</sub> , 5 ml	136	60
	Ru + Pt	0.532		165	60
3	Os +	0.728	72% HClO <sub>4</sub> , 15 ml	138	60
	Ru + Pt	0.532		165	60

<sup>a</sup>The temperature in flask B was that of boiling reflux conditions of ca. 100-105°C.

Flask B <sup>a</sup>		Residual A, %	Residual B, %	Recovery C, %
Oxidant	Time, min.			
conc. H <sub>2</sub> SO <sub>4</sub> , 3 ml 30% H <sub>2</sub> O <sub>2</sub> , 15 ml NaBiO <sub>3</sub> , 2 mg	15	-	0	97.9
conc. H <sub>2</sub> SO <sub>4</sub> , 5 ml 30% H <sub>2</sub> O <sub>2</sub> , 4 ml NaBiO <sub>3</sub> , 2 gm	15	-	0	100
conc. H <sub>2</sub> SO <sub>4</sub> , 5 ml 30% H <sub>2</sub> O <sub>2</sub> , 4 ml NaBiO <sub>3</sub> , 2 gm	30	0.6	0.2	98.2
conc. H <sub>2</sub> SO <sub>4</sub> , 5 ml 30% H <sub>2</sub> O <sub>2</sub> , 4 ml NaBiO <sub>3</sub> , 2 gm	30	0	0	100
conc. H <sub>2</sub> SO <sub>4</sub> , 5 ml 30% H <sub>2</sub> O <sub>2</sub> , 4 ml NaBiO <sub>3</sub> , 2 gm	30	.3	0.2	98.4
conc. H <sub>2</sub> SO <sub>4</sub> , 5 ml 30% H <sub>2</sub> O <sub>2</sub> , 4 ml NaBiO <sub>3</sub> , 2 gm	30	0	0	99.8

media in flask A. When the specified temperature and duration were maintained, essentially quantitative recovery was obtained for both elements. The amount of tracer activity used permitted the detection of 0.1-0.2 percent of the original activity added to flask A. No detectable ruthenium activity was found when aliquots were withdrawn from flask B after step II in Figure 8. The amount of undistilled osmium activity left in flask A after step II of Figure 8 was calculated from an activity balance of flask B, trap C, and trap D.

#### Irradiated platinum distillation

An irradiated platinum sample was placed in flask A along with osmium carrier (0.728 mg of osmium) and ruthenium carrier (0.532 of ruthenium). Both carriers were aqua regia solutions of the ammonium hexachlorides. After the 15 ml of 72 percent  $\text{HClO}_4$  was added, the combined liquid volume in flask A was 120-150 ml. Flask B remained empty while traps C and D each contained 15 ml of thiourea- $\text{H}_2\text{SO}_4$  catch solution with trap C cooled by an ice bath. The entire apparatus was in a fume hood with flask A surrounded by a lead brick shield.

Flask A was rapidly brought to ca.  $100^\circ\text{C}$  boiling temperature at which time the heating rate was reduced to maintain a distillation rate of 0.8-1.0 ml per minute. A sparging



rate of 1.5-2.0 bubbles per second was present during the entire distillation. When a boiling temperature of 135-138°C was reached, the heating rate was reduced to just maintain refluxing conditions. After one hour of refluxing, flask A was allowed to cool a few minutes before the  $\text{H}_2\text{SO}_4\text{-H}_2\text{O}_2$  reagent mixture was added to flask B. Flask B was then heated at boiling-refluxing conditions for 30 minutes. The distillation apparatus was allowed to cool to room temperature before the red osmium thiourea complex in trap C was diluted with water to 25 ml for a carrier yield determination prior to gamma-ray counting. Trap D contents were diluted with water to 20 ml in a screw-top polyethylene vial for subsequent gamma-ray counting.

The distillation apparatus was then prepared for the ruthenium distillation step by charging traps C and D with 15 ml each of 1N NaOH-0.5 percent NaOCl. Trap C was ice cooled. The distillation of liquid from flask A was resumed at the previously specified rate until a 165-170°C temperature was reached. The heating rate was then reduced to maintain refluxing conditions for one hour. After allowing flask A to cool, two gm of  $\text{NaBiO}_3$  was added to flask B which was then heated to maintain boiling-reflux conditions for 30

minutes. Visible amounts of yellow  $\text{RuO}_4$  carrier condensed on the still walls when boiling conditions in flask B were initially reached. At the end of the distillation, excess  $\text{NaBiO}_3$  was indicated by a brown tint in flask B instead of only white decomposition product. The apparatus was allowed to cool to room temperature before diluting the yellow perruthenate solution in trap C to 25 ml with 1N  $\text{NaOH}$ -0.5 percent  $\text{NaOCl}$ . Trap D contents were diluted with water to 20 ml in a screw-top polyethylene vial for subsequent gamma-ray counting.

The carrier yield measurements were obtained spectrophotometrically by carefully pipetting trap C aliquots into one cm cells. The reference cell sample contained trap C reagent solution which had been subjected to a "blank" distillation. A spectrum of the osmium-thiourea complex is illustrated by Figure 9. The 480  $\text{m}\mu$  peak (molar absorptivity of  $4190 \text{ M}^{-1} \text{ cm}^{-1}$ ) was used for carrier yield determinations while the 480  $\text{m}\mu$  peak to 503  $\text{m}\mu$  valley absorbance ratio was used as a monitor for possible interferences. The blank was found not to be essential since water or  $\text{H}_2\text{SO}_4$ -thiourea reagent as the reference for the thiourea complex yielded absorbance values identical to those obtained with the blank. The osmium sample solution was then removed from the one cm

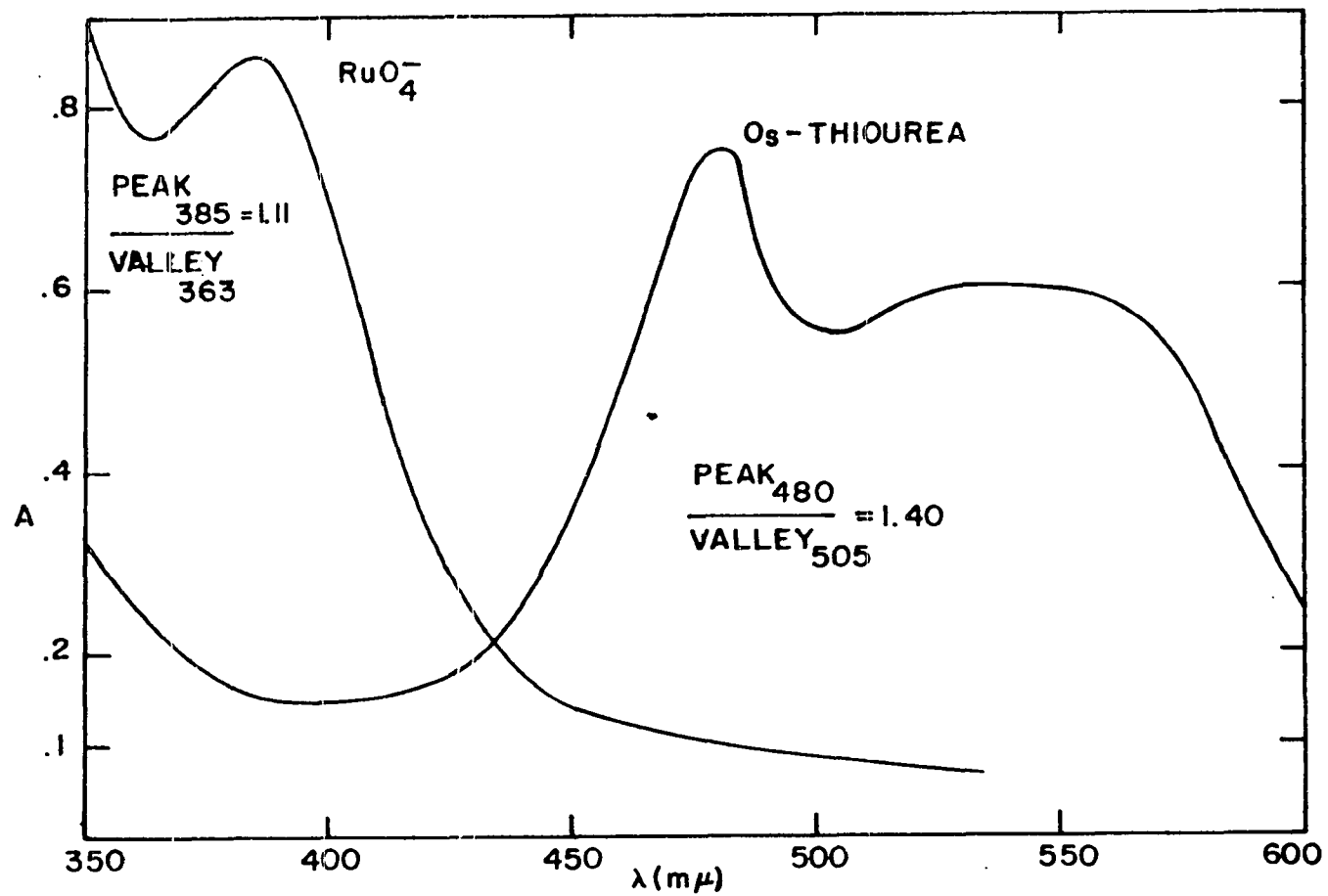


Figure 9. Visible absorption spectra of osmium and ruthenium species

cell by pipetting back into the 25 ml volumetric flask. A 20 ml portion of the 25 ml osmium-thiourea sample was placed in a 20 ml polyethylene vial for gamma-ray counting.

The ruthenium carrier yield was obtained in a manner similar to that used for osmium. The perruthenate spectrum is also illustrated by Figure 9. The 385 m $\mu$  peak (molar absorptivity of  $2,150 \text{ M}^{-1} \cdot \text{cm}^{-1}$ ) was used for carried yield determinations while the 385 m $\mu$  peak to 365 m $\mu$  valley ratio was used to monitor for possible interferences. The blank was quite critical for the perruthenate since the chlorine decomposition product of  $\text{HClO}_4$  was readily absorbed by the catch solution. This produced a significant absorption in the 385 m $\mu$  region which increased sharply but almost linearly in going from 400 to 350 m $\mu$ . The 385 m $\mu$  to 365 m $\mu$  absorbance ratio was very sensitive to this interference. Consequently the ruthenium carrier yield accuracy was questionable for some distillations because of the chlorine interference. For this reason the ruthenium oxidation conditions were made severe enough in flask A to insure quantitative oxidation of ruthenium to volatile  $\text{RuO}_4$ .

## Radiochemical Analyses of the Irradiation Standards

Osmium

The irradiated sample was opened in the manner described previously and osmium carrier (3.68 mg of osmium) as  $\text{OsCl}_6^{2-}$  in dilute aqua regia was added before dilution to a measured volume in a volumetric flask. An aliquot was then distilled from flask A in the usual manner to obtain a pure osmium counting sample. The presence of iridium activity in the osmium sample necessitated this purification step. The spectra of the undistilled osmium counting aliquots were treated as multicomponent spectra to calculate the osmium amount in the distilled sample. The distillation residue, with the iridium peaks greatly enhanced, was used for subsequent calculation of the iridium level in the osmium samples. All counting aliquots were contained in 20 ml polyethylene vials, diluted if necessary to make 20 ml total liquid volume.

Ruthenium

The irradiated sample was opened in the usual manner and ruthenium carrier (3.67 mg of ruthenium) as  $\text{RuCl}_6^{2-}$  in dilute aqua regia was added before dilution to a measured volume in a volumetric flask. The presence of iridium activity necessitated a distillation treatment analogous to that used for the

osmium standards.

### Iridium

The irradiated sample was opened in the usual manner and iridium carrier (6.17 mg of iridium) as  $\text{IrCl}_6^{3-}$  was added before dilution to a measured volume in a volumetric flask. Counting aliquots were taken without any further chemical manipulation.

### Gamma-ray Spectra

All radioactivities for quantitative work were measured by NaI(Tl) scintillation gamma-ray spectrometry. The counts were accumulated in a 400-channel RIDL pulse height analyzer for later storage on punch paper tape. All spectra were recorded with a two KeV per channel gain for a zero to 800 KeV full 400 channel display. Day to day gain drifts were corrected by positioning the 661 KeV peak of  $^{137}\text{Cs}$  in channel number 330. All activity measurements were performed using the live time mode of the analyzer which automatically corrected the count rate for dead time losses. The activity of all counting samples was selected to maintain an instrument dead time under 20 percent since a quantitative reduction of up to five percent in indicated activity was found to occur for dead time levels of 30 percent or over. Activities pro-

ducing dead time levels of 90 percent or over resulted in a visible reduction of peak resolution by drastically broadening the peaks.

All samples were counted in solution form. The counting geometry was normalized by all samples having a 20 ml liquid volume in the 20 ml polyethylene counting vials. The counting vials were accurately positioned in a disposable polystyrene sample holder which was taped to the top of the NaI(Tl) crystal.

The osmium activity was measured as 15d  $^{191}\text{Os}$  by using the 64 and 129 KeV peaks from channel 17 to 86. The ruthenium activity was measured as 40d  $^{103}\text{Ru}$  by using the 498 KeV peak from channel 215 to 285 while the iridium activity was measured as 74d  $^{192}\text{Ir}$  by using the 310 KeV peak from channel 125 to 190. Samples containing platinum activity were measured as 3.15d  $^{199}\text{Au}$  by using the 158 KeV peak and 4.1d  $^{195\text{m}}\text{Pt}$  by using the 70 KeV peak. At least one background spectrum of 100 to 200 minutes was taken daily, usually at the end of day, which allowed a check on possible contamination. The normal background spectrum rose to a broad peak at ca. 200 KeV and dropped nearly linearly to a factor 1/7th of the peak value by 800 KeV.

The quantitative analysis of a gamma-ray spectrum was obtained using RESOLF (68), a computer program which employed a linear least squares method. A complex spectrum was analyzed by assuming it to be a linear combination of pure components, all known and measured under identical experimental conditions. The general equation relating the sample spectrum to a linear sum of  $N$  components was:

$$A_j = \sum_{i=1}^N X_i S_{ij} + R_j \quad (17)$$

$A_j$  = count rate in channel  $j$  of the sample spectrum

$S_{ij}$  = count rate of component  $i$  in channel  $j$

$X_i$  = contribution factor of component  $i$  in the mixture

$R_j$  = difference between calculated and observed counts.

Least squares analysis requires that the sum  $R$  of the weighted squares of the residuals,  $R_j$ , be minimized to obtain the "best" estimates of the unknown  $X_i$ 's, that is:

$$F = \sum_{j=n_1}^{n_2} W_j R_j^2 = \sum_{j=n_1}^{n_2} W_j \left( A_j - \sum_{i=1}^N X_i S_{ij} \right)^2 \quad (18)$$

$W_j$  = weight factor

$n_1$  = first channel in the fit

$n_2$  = last channel in the fit



In order to find the minimum, partial derivatives of  $F$  with respect to  $X_1, X_2, \dots, X_N$ , yields a set of  $N$  normal equations which is solved for the  $N$  unknown quantities,  $X_i$ 's. To test the quality of the fit, the quantity, called FIT, was calculated:

$$FIT = \frac{R'}{N_f} \quad R' = \sum_{n_1}^{n_2} \frac{A_j - \sum_{i=1}^N X_i S_j^2}{\sigma_j} \quad (19)$$

$N_f$  = number of degrees of freedom

$\sigma_j$  = standard deviation of observation  $j$ .

Since instrumental gain shifts as small as a few hundredths to a few tenths of a percent could cause appreciable errors in the results, a subprogram consisting of an iterative procedure based on a direct search method was employed to shift the component spectra individually to obtain the best fit. The channel limits between which the sample spectrum was analyzed included the major peaks present which were listed earlier for each element. A subtraction procedure for spectrum stripping purposes was used which allowed a quick visual check of how good the fit was. The subtraction was performed on the entire spectrum, independent of the channel limits between which the fit was made. A computer print-out of the residual spectrum illustrated how good the calculated

contribution factors were in addition to revealing hidden peaks of unsuspected components.

The RESOLF program as written by Korthoven (68) was pared by reducing the maximum number of components in a sample spectrum which could be analyzed for from ten to five. The maximum number of component spectra which could be stored in the program was reduced from 15 to seven. This was necessary to keep the computer storage requirements below 128K after a subprogram DECOR was added to conduct radioactive decay corrections on the calculated contribution factors. The 128K size limit also necessitated removing the WTAPE subprogram which initiated and updated a tape library of component spectra.

## RESULTS AND DISCUSSION

### Irradiation Conditions

The conditions used for the irradiation of the samples analyzed are listed in Tables 8 and 9. The selection methods used for the platinum samples have been described previously. Table 9 represents initial irradiations conducted on evaporated samples. Because of volatility and solubility difficulties, these irradiations were essentially qualitative and were used for distillation tracer studies.

### Analysis for Osmium in Platinum

The data and results for the determination of osmium in purified platinum are shown in Table 10. Each irradiation involved two platinum samples except XI in which three samples were irradiated. A representative gamma-ray energy spectrum of an osmium counting sample distilled from irradiated platinum is illustrated in Figure 10. Gamma-ray spectra of undistilled and distilled osmium aliquots are also illustrated. All spectra have been background corrected. The undistilled spectrum indicates the presence of 310 KeV  $^{192}\text{Ir}$  peak which is removed by distillation. A low energy component activity adding to the 42 KeV photon peak was also indicated in the undistilled osmium gamma-ray spectrum. This was also absent

Table 8. Irradiation conditions used in the thermal neutron activation of Pt samples<sup>a</sup>

Irradiation	VI	VII	VIII	IX	X	XI
Time out of ALRR (date, hour)	1/8/70 1755	4/25/70 2255	6/8/70 0830	9/24/70 1000	11/25/70 2400	2/5/71 1115
Total dose (MW hours)	151	300	180	352	857	1335
Wt. of Pt black samples (mg)	12.41 12.11	101.72 102.51			215.84 206.32	207.60 214.79 197.67
Wt. of Pt wire samples (mg)			123.37 130.37	178.46 190.55	101.89 94.14	87.24 109.18 96.99
Wt. of irradi- ation stds: Os (mg)	0.1819	0.9097 0.3971	0.09097 0.1587	0.09097 0.1587	0.09097 0.1587	0.09097 0.1587
Ru (mg)	0.1331	0.06657	0.09171 0.06657	0.09171 0.06657	0.09171 0.06657	0.09171 0.06657
Ir (mg)	0.6171	0.06171	0.06171	0.03086	0.03086	0.03086

<sup>a</sup>All irradiations were in V-5 position of the ALRR at 5 MW power.

Table 9. Addition irradiation conditions used in the thermal neutron activation of Os and Ru standards

Irradiation	I	II	III	IV	V
Time out of ALRR (date, hour)	2/5/69 2305	3/14/69 0800	6/9/69 0825	6/20/69 0915	8/7/69 2330
Total dose (MW hours)	153	153	120	151	162
Wt. of Ru samples (mg)	0.2037	0.1629 0.2037	0.1834 0.2293	0.06657 0.2293	0.06657 0.2293
Wt. of Os samples (mg)	0.1587		0.1587	0.09097 0.1587	0.09097 0.3971
Wt. of Ir samples (mg)			0.6171	0.3086	0.6171

Table 10. Neutron activation analysis for osmium in purified platinum

Irradiation	VI	VII	X	XI
Wt. of $^{191}\text{Os}$ counting aliquot ( $10^{-3}$ mg)	3.081	3.728	0.4438	0.3290
Contrib. of $^{191}\text{Os}$ activity in Pt	.00873 .01707	~0 .00103	.218 1.004	.188 .264 .181
Counting time factor	1.6,4,2 8,4	10 10	20 80	10 10 10
Relative abundance of $^{191}\text{Os}$ activity in Pt	.00577 .00467	- .000103	.0109 .0126	.0188 .0264 .0181
Chemical yield factor (%)	100 100	- 100	94.7 96.7	96.6 93.0 91.6
Wt. of Pt irradiation sample (mg)	12.41 12.11	101.72 102.51	215.84 206.32	207.60 214.79 197.67
Os content of Pt samples (ppb)	1,430 1,190	- 3.8	24 28	31 44 33

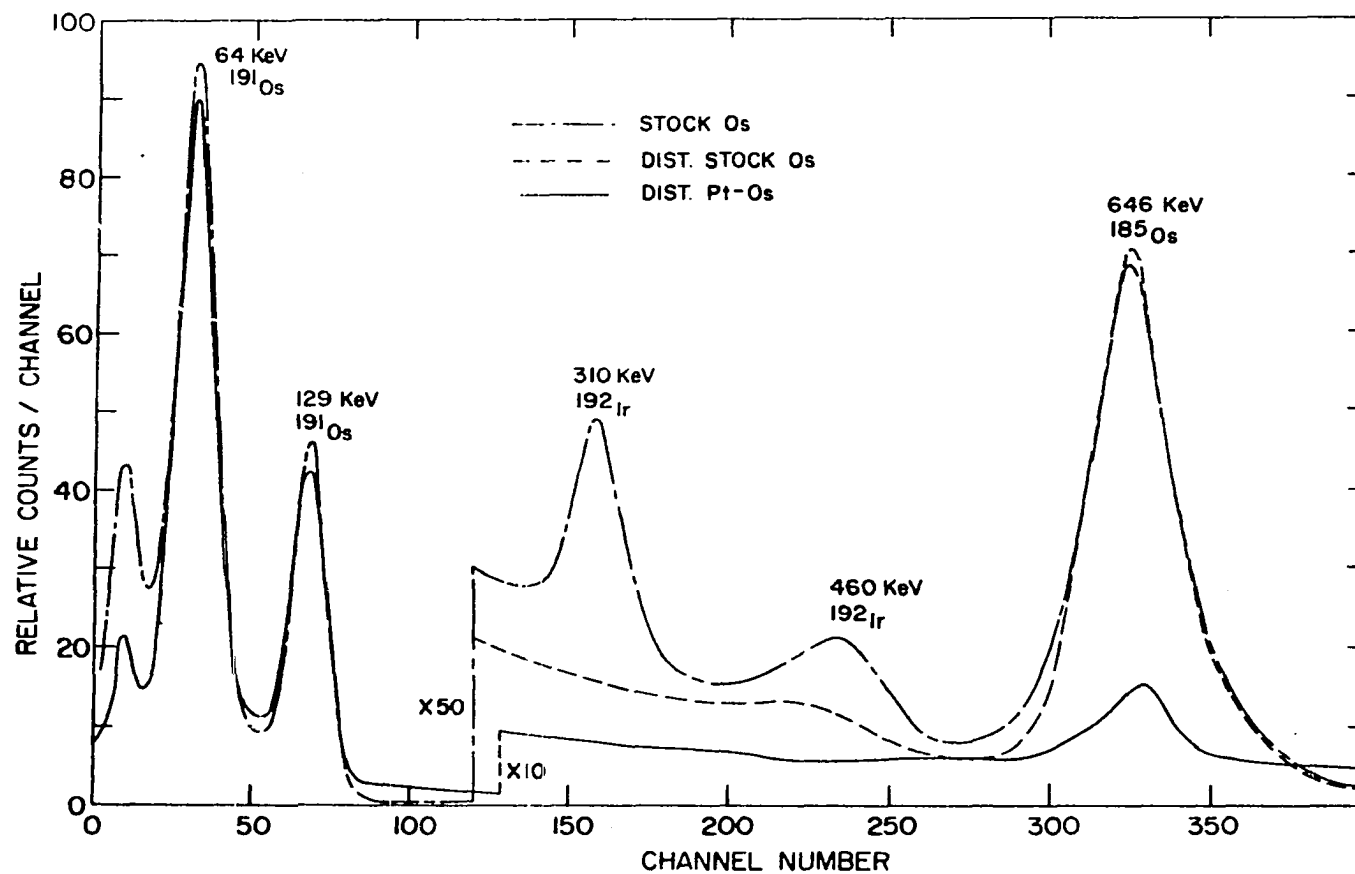


Figure 10. Gamma-ray energy spectra of activities present for osmium determination

from the distilled osmium spectrum. The osmium spectrum obtained from the distillation of platinum was essentially superimposeable on the distilled osmium spectrum with no platinum radionuclide contamination. The activity of 31 hour  $^{193}\text{Os}$  was allowed to decay by counting at least ten days after irradiation. A calculated half-life of 15.2 days for osmium was close to the literature value of 14.6 days for  $^{191}\text{Os}$ . The contribution from the 94-day  $^{185}\text{Os}$  compton background probably made the calculated value slightly too large.

The osmium irradiation standard counting aliquot values in Table 10 represent an aliquot of distilled osmium activity. A sample of the osmium irradiation standard was distilled after the platinum distillations were completed. Three equal counting aliquots of undistilled osmium, having activities differing by less than one percent, were treated as multicomponent spectra in their use to calculate the amount of osmium in the distilled counting aliquot.

The contribution factors in Table 10 represent the RESOLF calculated value for the decay corrected fraction of the osmium gamma-ray spectrum in trap C of the platinum sample as compared to the gamma-ray spectrum of osmium counting aliquots. The counting time factor represented how much longer



the sample was counted than the reference aliquot. The relative abundance values were calculated from a division of the contribution factor by the time factor. Irradiation VI had the possible osmium activity in two or three counting vials, hence the contribution factors and relative abundances are sum values. The gamma-ray spectra obtained from irradiations VI and VII appeared to be essentially background with no detectable osmium peaks. The resulting RESOLF calculations were obviously in error and illustrated two limitations. First, the sample size plus length of irradiation were not sufficient to produce an accurately measureable amount of activity. Second, for sample contributions less than one or two percent of the standard spectrum, spurious values were calculated. This was confirmed when normal background counts were analyzed as four component spectra. Contribution values of less than  $\pm 0.01$  were randomly calculated for each component as various RESOLF options were selected.

Because the amount of osmium activity produced in irradiation VI platinum samples was not detectable, four times larger samples and a two times longer irradiation were used for irradiation VII. Again the distilled activity from the platinum sample had no visible osmium peaks in the spectra

which was confirmed by the low or negative contribution factors calculated. To check on the determinable osmium impurity limits, comparative counts of successively smaller aliquots of a distilled osmium standard were counted from irradiation VII. The results indicated that ca.  $4 \times 10^{-9}$  gm of  $^{191}\text{Os}$  could be accurately determined for a 150 MWH (30 hours at 5 MW) irradiation. This represented a 40 ppb determination limit for 100 mg platinum samples, assuming 100 percent osmium recovery with no spectrum interference. This calculation was based on a 64 KeV  $^{191}\text{Os}$  peak twice the height of background. Since a 150 MWH irradiation was far from saturation (S.F. = 0.056) for 15 day  $^{191}\text{Os}$ , an extrapolation calculation for a five times longer irradiation and two times larger sample indicated that less than a five ppb level could be determined.

Irradiations X and XI calculations indicate the osmium level was below determination limits for irradiations VI and VII. Some 35 hour  $^{82}\text{Br}$  activity was found to distill from the irradiated platinum samples. Figure 11 illustrates the  $^{82}\text{Br}$  spectrum which seriously masked both low levels of distilled osmium and ruthenium activity. The  $^{82}\text{Br}$  activity was allowed to decay before the quantitative 15 day  $^{191}\text{Os}$  spectra were counted. The source of the bromine activity was ini-

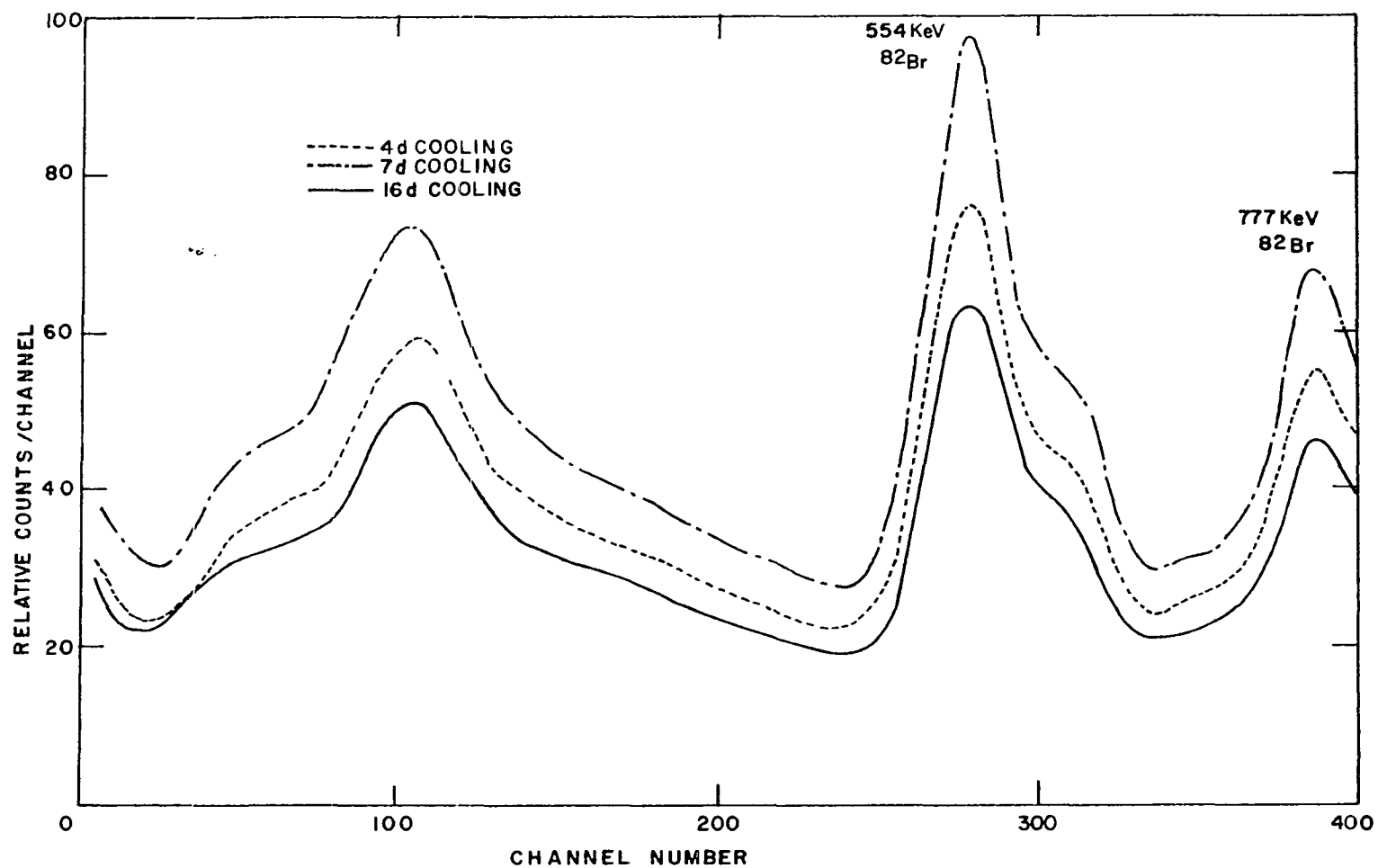


Figure 11. Gamma-ray spectra of bromine activity

tially suspected as an impurity in the HCl used since the bromine activity was also found in the platinum wire samples. An irradiation of HCl did reveal some bromine activity present which was removed by the triple distillation of HCl. But the continued presence of bromine activity indicated its removal was not complete after the reduction of the  $K_2PtBr_6$ . The bromine activity was produced even after the purified platinum was again subjected to the HCl and  $HNO_3$  digestion steps using purified acids. A  $NH_4Br$  standard was included in irradiation XI. The calculated bromine level was found to be ca. 40 ppm. Some of the  $K_2PtBr_6$  in the platinum reduction step must have been trapped within platinum black particles which then remained impervious to the subsequent acid digestion since  $K_2PtBr_6$  is appreciably soluble in acid and water.

An average osmium content of 32 ppb was obtained in the analysis of five purified platinum samples with a standard deviation of 7 ppb or 22 percent.

Platinum wire analysis was investigated after the inconclusive results of irradiations VI and VII in Table 10. The data and results of the platinum wire analyses are listed in Table 11. The one obviously erratic 0.39 ppm value of irradiation VIII was discarded to yield an average osmium content of

Table 11. Neutron activation analysis for osmium in platinum wire

Irradiation	VIII	IX	X	XI
Wt. of $^{191}\text{Os}$ counting aliquot ( $10^{-3}$ mg)	2.08	.329	0.444	0.329
Contrib. of $^{191}\text{Os}$ activity in Pt	.177 .245	.250 .470	.268, .020	.759 1.822 .754
Counting time factor	20 10	3 6	12,40	20 40 20
Relative abundance of $^{191}\text{Os}$ activity in Pt	.00884 .0245	.0683 .0686	.0223, .0005	0.0380 0.0455 0.0377
Chemical yield factor (%)	100 100	94.6 96.7	99.8	99.4 99.4 100
Wt. of Pt irradiation sample (mg)	123.37 130.37	178.46 190.55	94.14	87.24 109.18 96.99
Os content of Pt samples (ppm)	.149 .391	133 122	.121	.144 .138 .128

0.134 ppm calculated from the analysis of seven platinum wire samples with a standard deviation of .010 ppm or 7.4 percent. The osmium distribution in the platinum wire samples was quite uniform with an easily detected level. Thus the osmium level in purified platinum was again investigated using the conditions of irradiations of X and XI yielding the results described earlier.

Previously reported investigations of platinum analyzed commercial samples. Morris (90) reported 0.080 to 1.00 ppm of osmium while Gijbels and Hoste (98) reported 0.20 to 0.70 ppm levels of osmium. These levels are similar to the 0.134 ppm found in the investigation. Since their platinum sources were different, no significant comparison could be made to this investigation. Although NBS has standard platinum reference samples available, they are not certified for either osmium or ruthenium.

#### Analysis for Ruthenium in Platinum

The data and results of the determination of ruthenium in purified platinum are listed in Table 12.

Irradiation VI samples were not large enough or irradiated long enough to produce accurately measureable amounts of ruthenium activity. The chlorine decomposition product of

Table 12. Neutron activation analysis for ruthenium in purified platinum

Irradiation	VI	VII	X	XI
Wt. of $^{103}\text{Ru}$ counting aliquot ( $10^{-3}$ mg)	4.482	0.7583	3.153	1.416
Contrib. of $^{103}\text{Ru}$ activity in Pt	.00335 .00573	.0503 .0671	.0646 .0765	.565 .232 .122
Counting time factor	5,10 10,20	10 10	20 24	20 40 20
Relative abundance of $^{103}\text{Ru}$ activity in Pt	.000728 .000670	.00503 .00671	.00323 .00318	.0282 .00579 .00611
Wt. of Pt irradiation sample (mg)	12.41 12.11	101.72 102.51	215.84 206.32	207.60 214.79 197.67
Ru content of Pt samples (ppb)	263 248	38 50	47 49	192 38 42

$\text{HClO}_4$  introduced a considerable uncertainty in the carrier yield measurements. Therefore the distillation conditions were selected to be quantitative as previously described by tracer studies. Figure 12 illustrates the gamma-ray spectra obtained for the distilled platinum samples after  $^{82}\text{Br}$  decay. The stock ruthenium spectrum had a visible  $^{192}\text{Ir}$  peak which was removed by distillation. The low energy peak at ca. 20 KeV present in both the stock ruthenium and distilled platinum did not introduce any appreciable interference in calculations using the 498 KeV  $^{103}\text{Ru}$  peak. The reference counting aliquot was obtained in a like manner to that used for osmium. The distillation of stock ruthenium was conducted after the platinum distillations since only one distillation apparatus was used. The distillation sequence for each irradiation was purified platinum samples first, then platinum wire, followed by osmium standards with ruthenium standards last. A blank distillation was conducted when switching to a new element. An inefficient blank distillation after the completion of irradiation X distillations was the reason attributed for the high ruthenium level in the first platinum sample of irradiation XI in Table 12.

A lower determination limit for ruthenium was calculated



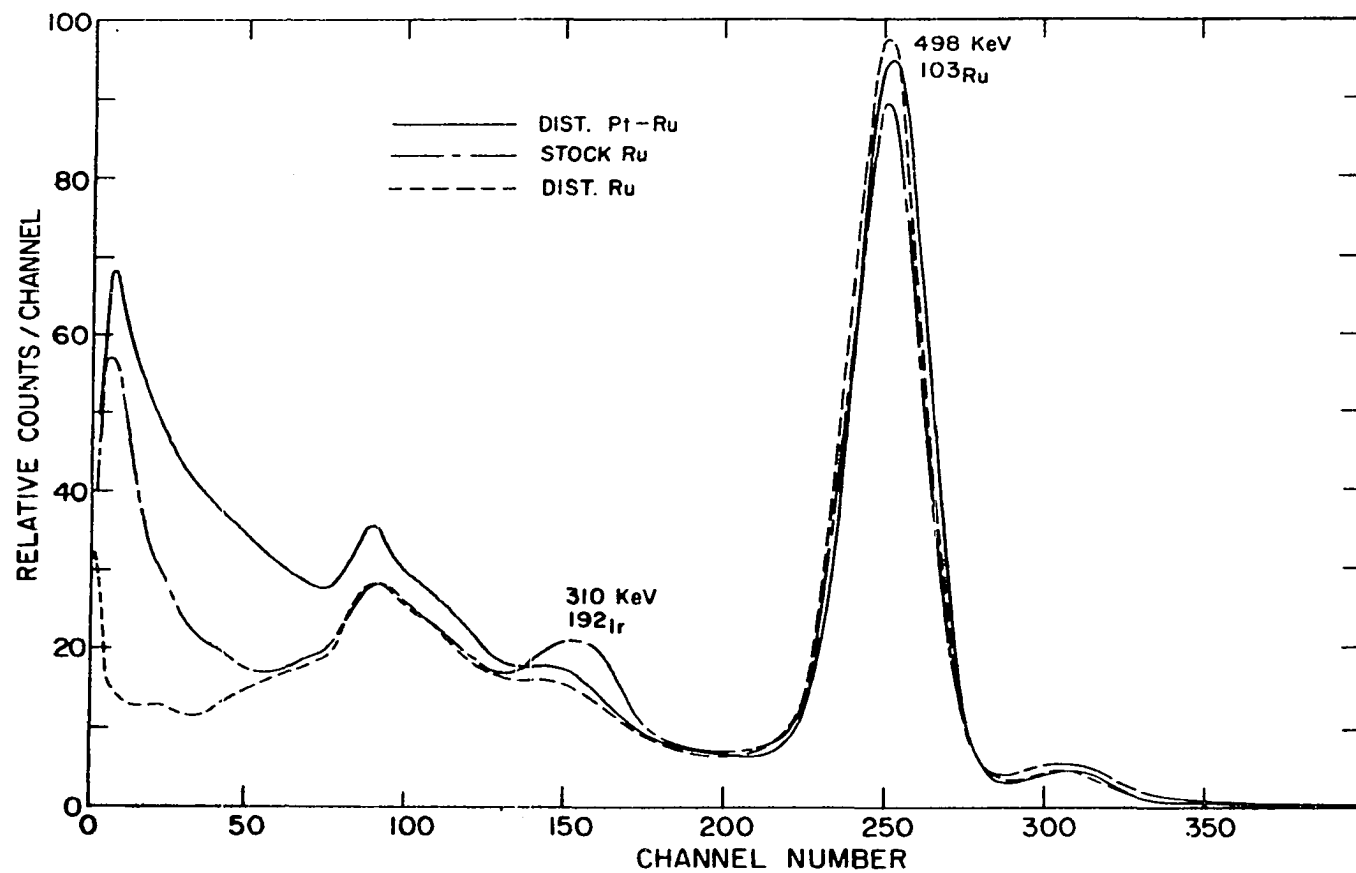


Figure 12. Gamma-ray energy spectra of activities present for ruthenium determination

by successive dilution of an aliquot from irradiation VII. For a 498 KeV  $^{103}\text{Ru}$  peak height twice that of background, ca.  $3 \times 10^{-9}$  gm could be determined for the 300 MWH irradiation. This corresponds to ca. 30 ppb for a 100 mg sample of platinum. Since the saturation factor was only 0.043 for irradiation VII, the determination level could be lowered to under 10 ppb by a longer irradiation and/or larger sample. Extrapolation of the above calculation to irradiations X and XI conditions yielded ca. six and four ppb determination limits respectively.

An average ruthenium content of 44 ppb was obtained in the analysis of six purified platinum samples with a standard deviation of 5 ppb or 11 percent.

The data and results of the determination of ruthenium in platinum wire are listed in Table 13. The precision was quite good for all samples analyzed. Spectra of the distilled samples were free from significant interfering activities although the previously mentioned low energy component of ca. 20 KeV was present. An average ruthenium content of 1.04 ppm was obtained in the analysis of seven platinum wire samples with a standard deviation of .04 ppm or 4 percent.

The previous investigations reported 0.83-1.96 ppm (103) and 0.30-0.70 ppm (98) levels of ruthenium in commercial

Table 13. Neutron activation analyses for ruthenium in platinum wire

Irradiation	VIII	IX	X	XI
Wt. of $^{103}\text{Ru}$ counting aliquot ( $10^{-3}$ mg)	4.217	3.008	3.153	1.416
Contrib. of $^{103}\text{Ru}$ activity in Pt	.152	.371 .694	.320	.616 1.610 1.469
Counting time factor	5	6 10	10	10 20 20
Relative abundance of $^{103}\text{Ru}$ activity in Pt	.0304	.0618 .0694	.0320	.0616 .0805 .0735
Wt. of Pt irradiation sample (mg)	130.27	178.46	94.14	87.24 109.18 96.99
Ru content of Pt sample (ppm)	0.98	1.04 1.10	1.07	1.00 1.04 1.07

platinum. As in the case for osmium, these values are close to the 1.04 ppm value for ruthenium found in this investigation, but no real significance can be placed on the similar results because of the different sources of platinum.

#### Analysis for Iridium in Osmium

The presence of the 310 KeV  $^{192}\text{Ir}$  peak in the osmium irradiation standards necessitated the distillation purification of osmium. Examination of the flask A residue revealed iridium as  $^{192}\text{Ir}$  would be an easily determined impurity with activation analysis by virtue of its large cross-section (700 barns) and a relatively long half-life (74 days). Iridium did not distill under the oxidizing conditions used for both the osmium and ruthenium distillations. Thus gamma-ray counting of the flask A distillation residue measured the quantitatively recovered iridium activity. Figure 13 illustrates the gamma-ray spectrum obtained from the flask A residue. The Res. Stock Os spectrum indicated essentially pure  $^{192}\text{Ir}$  activity from the 310 KeV peak to higher energies. The previously mentioned ca. 20 KeV component was the major source of activity since a 50X magnification was necessary to make the  $^{192}\text{Ir}$  peaks visible on the linear display. Although 64 and 129 KeV peaks of traces of  $^{191}\text{Os}$  residual activity could

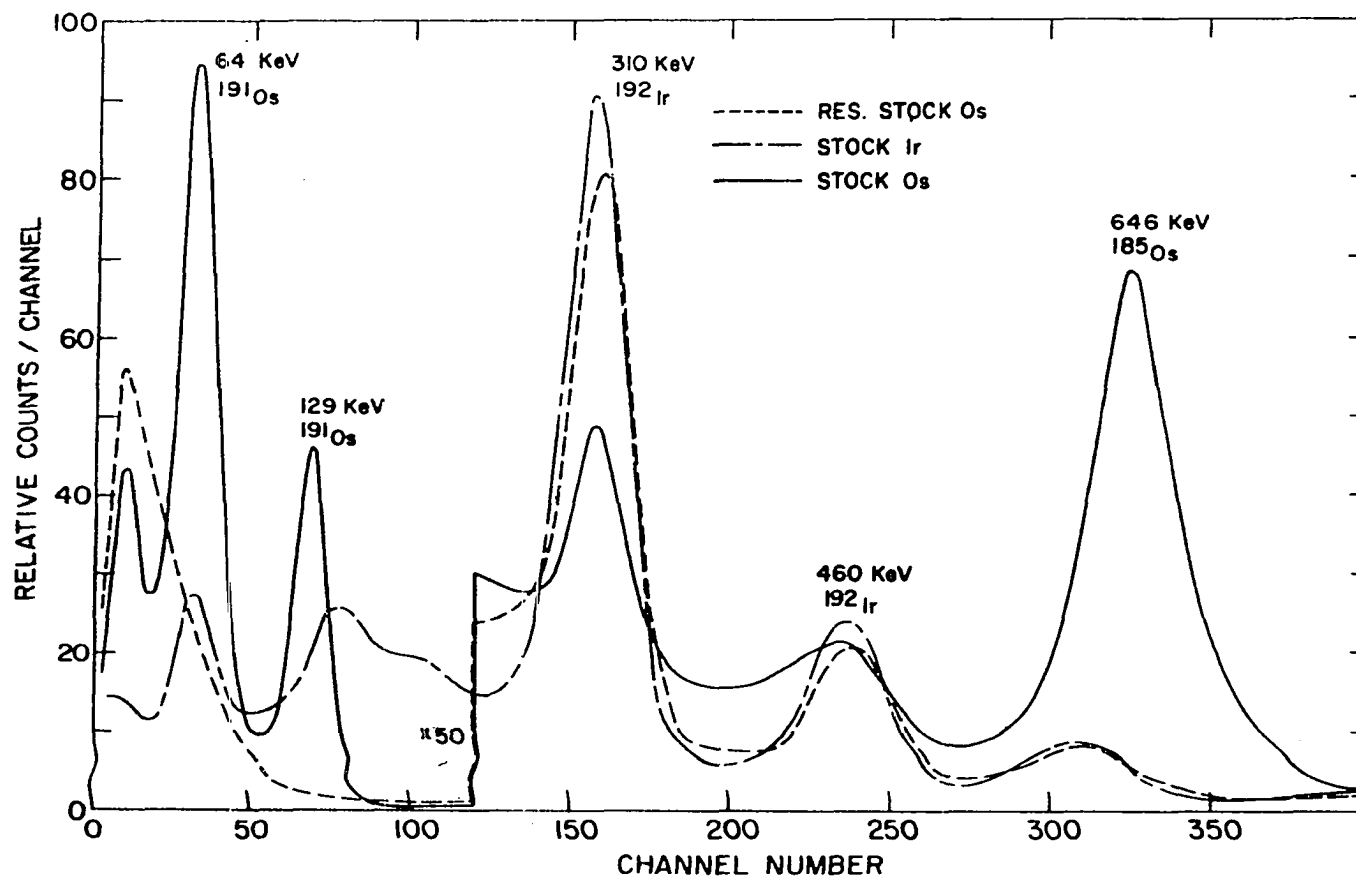


Figure 13. Gamma-ray energy spectra of activities present for determination of iridium in osmium

have been masked by the unidentified low energy component, the absence of the 646 KeV  $^{185}\text{Os}$  peak indicated complete distillation of osmium. The unknown low energy component was also found in the ruthenium samples indicating a common source. The activity was initially believed to be from the  $^{35}\text{Cl}(n,\gamma)^{36}\text{Cl}$  reaction originating from irradiation of both the HCl and chloride salts. The decay of  $^{36}\text{Cl}$  is by 0.716 MeV negatrons only which could penetrate the aluminum housing of the NaI(Tl) crystal. Counting of 2.62 hour  $^{31}\text{Si}$  (1.48 MeV  $\beta^-$ ) and 14.3 day  $^{32}\text{P}$  (1.71 MeV  $\beta^-$ ) indicated the unidentified activity spectrum was characteristic of a pure beta emitter. Irradiation of HCl samples, both commercial and three times distilled, revealed HCl as the activity source which would indicate a distillable impurity in HCl. The gamma-ray spectrum of irradiated 3X distilled HCl is illustrated in Figure 14. All the counts were on samples cooled for over 10 days. The activity dropped to essentially zero by ca. 140 KeV with no visible peaks out to 800 KeV. Additional measurements with higher gain settings revealed no gamma-ray peaks out to 3.4 MeV. A half-life determination indicated a value of  $90 \pm 10$  days.

Some radiochemical treatment was conducted on the irradi-

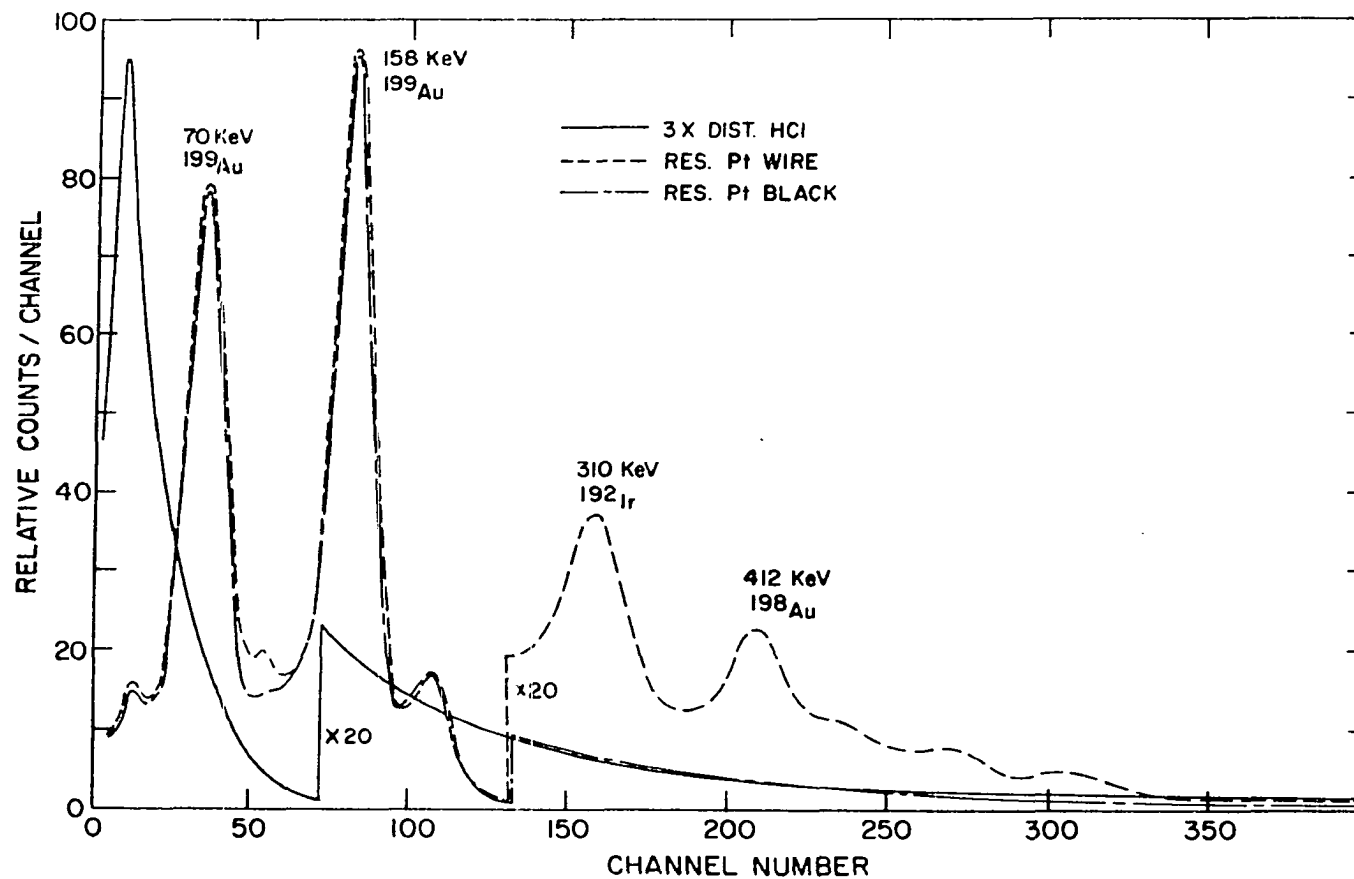


Figure 14. Gamma-ray energy spectra of HCl and residues from the distillation of platinum

ated 3X distilled HCl sample. A carrier of  $\text{H}_2\text{SO}_4$  was added and followed by oxidation with  $\text{H}_2\text{O}_2$ . A precipitation of chloride was effected by adding  $\text{AgNO}_3$  until the chloride was all removed. The excess silver was then precipitated with excess HCl which was then removed by boiling for 15 minutes. The sulfate remaining in solution was precipitated with  $\text{BaSO}_4$ . Samples of the two precipitates were mounted on aluminum planchets, covered with scotch tape, and counted on top of the NaI(Tl) crystal. The resulting gamma-ray spectra are illustrated in Figure 15. While both spectra are characteristic of beta decay, the AgCl precipitate activity consists of a significant amount of higher energy activity. If this higher energy was the  $^{36}\text{Cl}$  activity, then the  $\text{BaSO}_4$  precipitated activity had an energy considerably less than the 0.716 MeV negatron maximum for  $^{36}\text{Cl}$ .

Absorber studies with an end window G.M. tube refined the energy differences quite accurately as illustrated by Figures 16 and 17. The  $29 \text{ mg}\cdot\text{cm}^{-2}$  half thickness of the high energy component of the AgCl precipitate corresponded to a beta energy of 0.77 MeV (129), close to the 0.716 MeV  $^{36}\text{Cl}$  value. The lower energy component of Figure 16 had a half-thickness of ca.  $2.0 \text{ mg}\cdot\text{cm}^{-2}$ , corresponding to a beta energy



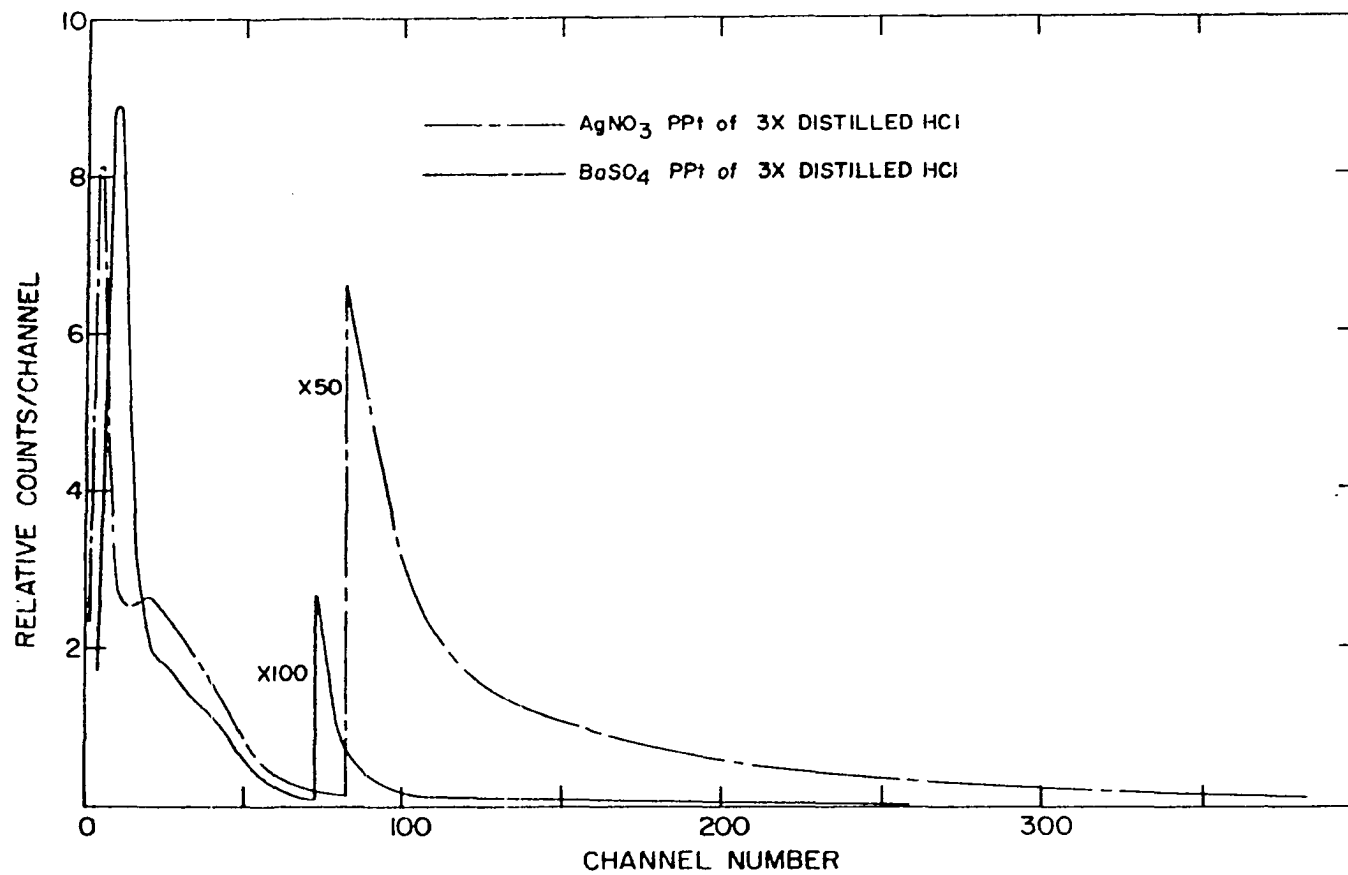


Figure 15. Gamma-ray energy spectra of AgCl and BaSO<sub>4</sub> precipitates

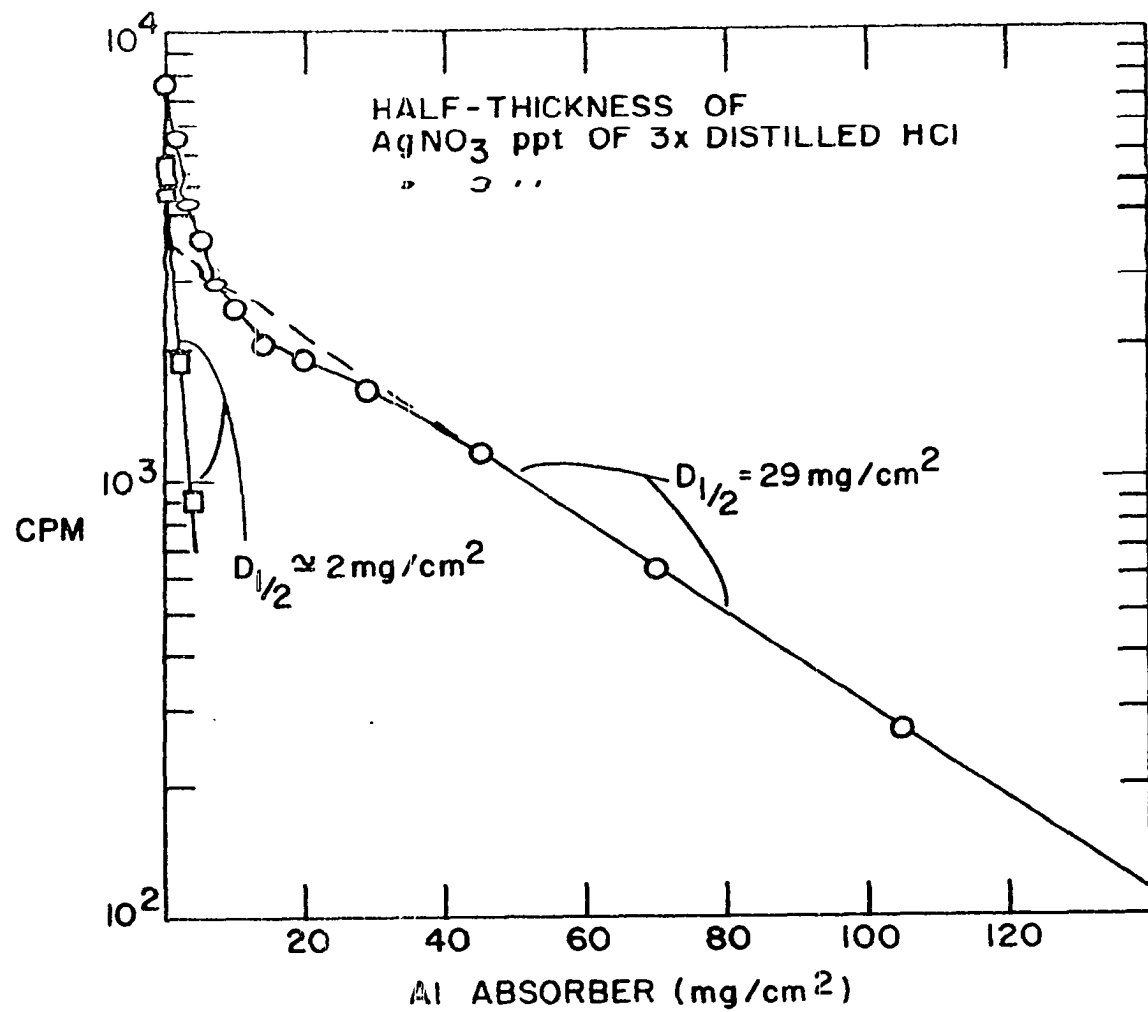


Figure 16. Aluminum absorption curve of AgCl precipitate

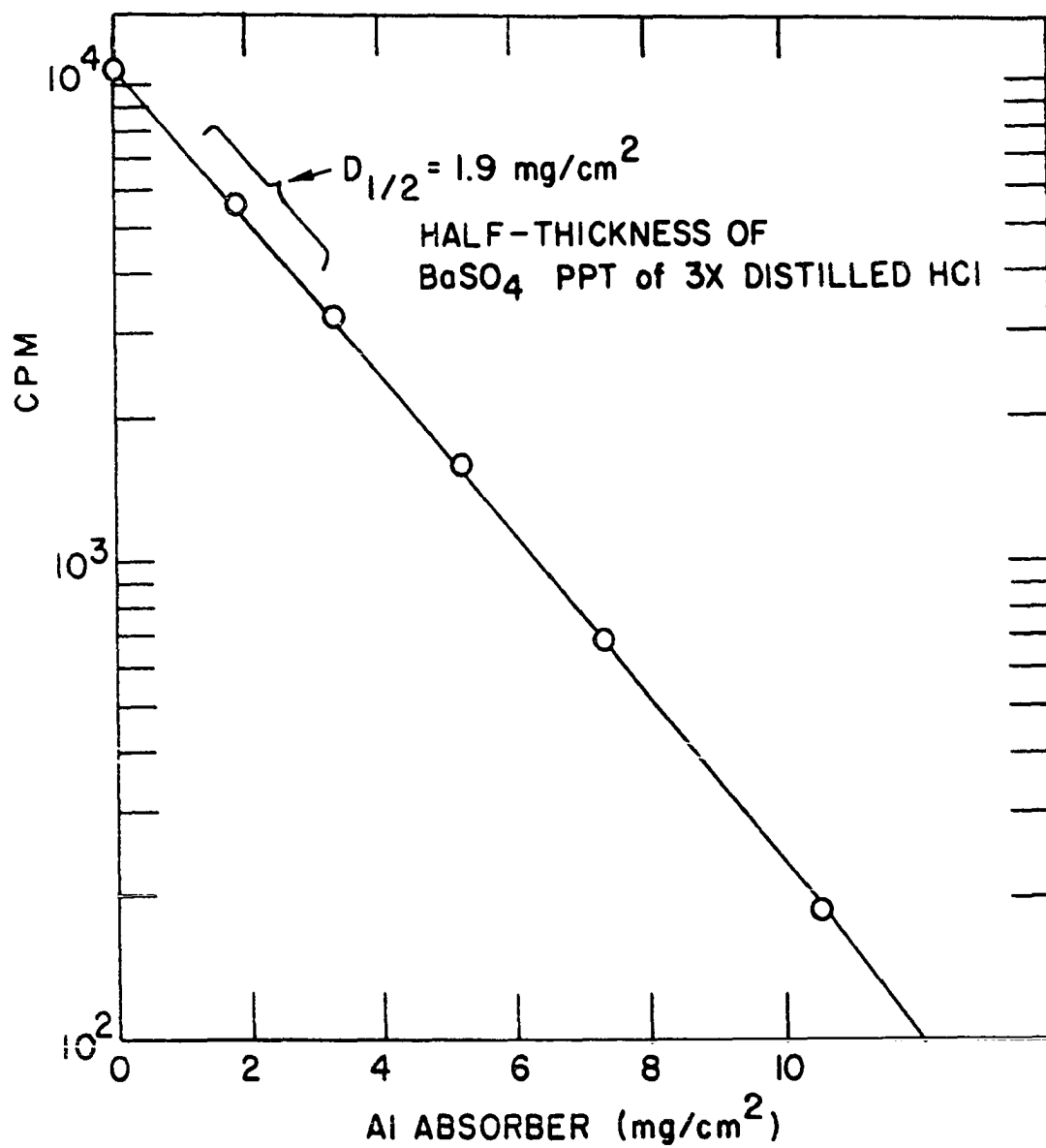


Figure 17. Aluminum absorption curve of  $\text{BaSO}_4$  precipitate

of ca. 0.17 MeV. Figure 17 half-thickness value of 1.9  $\text{mg}\cdot\text{cm}^{-2}$  indicated some coprecipitation had occurred with the AgCl. The 0.17 MeV energy coupled with the 90 day half-life suggested 87 day  $^{35}\text{S}$ , which decays by 0.167 MeV negatrons only, as the impurity activity in HCl. The  $^{34}\text{S}(\text{n},\gamma)^{35}\text{S}$  reaction could occur with the 4.22 percent naturally occurring isotope. This is the only reasonably expected radionuclide which fits the half-life and energy requirements. The  $^{35}\text{Cl}(\text{n},\text{p})^{35}\text{S}$  reaction could also occur and the presence of such activity in the irradiated  $\text{NH}_4\text{Cl}$  and  $\text{NaCl}$  samples did not eliminate this possibility. Irradiation of distilled  $\text{HNO}_3$  and distilled water eliminated these as sources of the activity while irradiation of empty  $\text{SiO}_2$  tubes eliminated the tubes as a source of leached impurities. The assay on the label of HCl acid bottles listed sulfate at the 0.00005 percent level and sulfite at the 0.0001 percent level.

If sulfate or sulfite was present in the triple distilled HCl, it indicated that a facil co-distillation occurred with the constant boiling ( $110^\circ\text{C}$ ) HCl which did not readily distill in  $\text{HClO}_4$  media below  $150^\circ\text{C}$ . Even at  $170^\circ\text{C}$  the major portion of the  $^{35}\text{S}$  activity remained in flask A. Since the boiling point of  $\text{H}_2\text{SO}_4$  is  $330^\circ\text{C}$  (98.3%) while  $\text{H}_2\text{SO}_4\cdot 4\text{H}_2\text{O}$  boils at

167°C the suggested anomalous distillation behavior with constant boiling HCl does not seem reasonable. Instead the  $^{35}\text{Cl}(\text{n},\text{p})^{35}\text{S}$  reaction, which is used for the commercial preparation of carrier-free  $^{35}\text{S}$ , must have produced the observed activity.

The data and results of the determination of iridium in both  $(\text{NH}_4)_2\text{OsCl}_6$  and  $\text{OsO}_4$  standard are listed in Tables 14 and 15. An average iridium content of 19.6 ppm was obtained in the analysis of five  $(\text{NH}_4)_2\text{OsCl}_6$  samples with a standard deviation of 2.8 ppm or 14 percent. An average iridium content of 2.2 ppm was obtained in the analysis of three  $\text{OsO}_4$  samples with a standard deviation of .3 ppm or 13 percent. The second-order  $^{190}\text{Os}(\text{n},\gamma)^{191}\text{Os} \xrightarrow{\beta^-} ^{191}\text{Ir}(\text{n},\gamma)^{192}\text{Ir}$  reaction was reported to produce 0.03-0.21 ppm spurious iridium levels in osmium (104). The results were based on an 11 day irradiation at a flux of  $10^{11} \text{ n}\cdot\text{cm}^{-2}\cdot\text{sec}^{-1}$ . This would be only one percent of the iridium level found for the  $(\text{NH}_4)_2\text{OsCl}_6$  but would be ca. 10 percent of the iridium level found for the  $\text{OsO}_4$ . Irradiation VIII was only for 1.5 days while irradiation XI was for 11 days. Since the second-order effect should increase with the length of irradiation, it appears not to be significant for the experimental conditions used.

Table 14. Neutron activation analysis for iridium in commercial  $(\text{NH}_4)_2\text{OsCl}_6$

Irradiation	VI	VIII	IX	XI
Wt. of $^{192}\text{Ir}$ counting aliquot ( $10^3$ mg)	0.0111	0.0123	.00772	.00617
Contribution of $^{192}\text{Ir}$ activity in Os	.332, .429	.300, .206	.349	.286 .259
Counting time factor	2, 5	10, 6	6	8 4
Relative abundance of $^{192}\text{Ir}$ activity in Os	.166, .086	.0300, .0343	.0580	.0357 .0649
Wt. of Os irradiation aliquot ( $10^{-3}$ mg)	146.6	45.49	18.19	11.37 22.74
Ir content of Os samples (ppm)	19	17	25	19 18

Table 15. Neutron activation analysis for iridium in commercial OsO<sub>4</sub>

Irradiation	VIII	IX	XI
Wt. of <sup>192</sup> Ir counting aliquot (10 <sup>-3</sup> mg)	.0123	.00772	.00617
Contribution of <sup>192</sup> Ir activity in Os	.0281, .0469	.0880	.635
Counting time factor	10, 10	12	4
Relative abundance of <sup>192</sup> Ir activity in Os	.00281, .00469	.00733	.0159
Wt. of Os irradiation aliquot (10 <sup>-3</sup> mg)	39.68 39.68	31.74 31.74	39.68 39.68
Ir content of Os samples (ppm)	2.3	1.8	2.5

### Analysis for Iridium in Ruthenium

The presence of iridium was indicated in the distilled ruthenium gamma-ray spectra and the spectrum illustrated in Figure 18 definitely shows  $^{192}\text{Ir}$  as a major component in the flask A residue from a distillation of ruthenium. The absence of the 498 KeV  $^{103}\text{Ru}$  peak in the residue stock Ru spectrum indicated complete ruthenium distillation. A significant portion of the low energy component of  $^{35}\text{S}$  also remained undistilled but did not alter the  $^{192}\text{Ir}$  spectrum from the 310 KeV peak on.

The data and results of the determination of iridium in both  $(\text{NH}_4)_2\text{RuCl}_6$  and Ru metal standards are listed in Tables 16 and 17. An average iridium content of 90.5 ppm was obtained in the analysis of four  $(\text{NH}_4)_2\text{RuCl}_6$  samples with a standard deviation of 3 ppm or 3 percent. An average iridium content of 122 ppm was obtained in the analysis of three ruthenium metal samples with a standard deviation of 8 ppm or 7 percent.

### Error Considerations

The chemical uncertainties introduced in the activation analysis should have been relatively small. The platinum samples were weighed to an accuracy of 0.02 mg, five signifi-



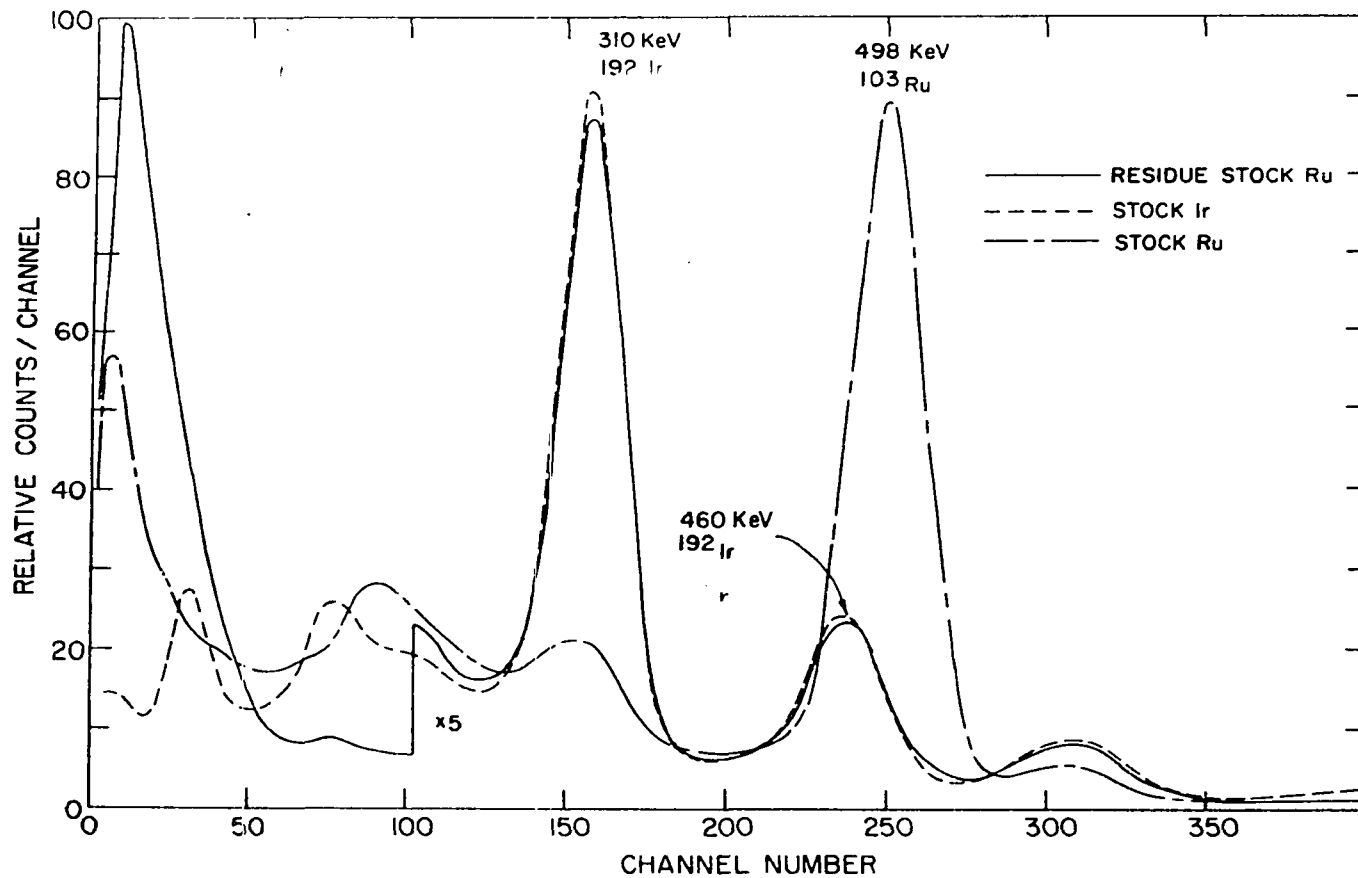


Figure 18. Gamma-ray energy spectra of the activities present for the determination of iridium in ruthenium

Table 16. Neutron activation analysis for iridium in commercial  $(\text{NH}_4)_2\text{RuCl}_6$ 

Irradiation	VI	VIII	IX	XI
Wt of $^{192}\text{Ir}$ counting aliquot ( $10^{-3}$ mg)	.0123	.0123	.00772	.00617
Contribution of $^{192}\text{Ir}$ activity in Ru	.757, .231, .0511	.503, .516	.605	.390
Counting time factor	1.5, 1.5, 5	4, 4	4	2
Relative abundance of $^{192}\text{Ir}$ in Ru	.505, .154, .010	.126, .129	.151	.195
Wt. of Ru irradiation aliquot ( $10^{-3}$ mg)	93.20	33.29	13.31	13.31
Ir content of Ru samples (ppm)	89	95	88	90

Table 17. Neutron activation analysis for iridium in commercial Ru metal

Irradiation	IX	XI
Wt. of $^{192}\text{Ir}$ counting aliquot ( $10^{-3}$ mg)	.00772	.00617
Contribution of $^{192}\text{Ir}$ activity in Ru	1.08	.387 .725
Counting time factor	4	1 2
Relative abundance of $^{192}\text{Ir}$ activity in Ru	.270	.387 .363
Wt. of Ru irradiation aliquot ( $10^{-3}$ mg)	18.34	18.34 18.34
Ir content of Ru samples (ppm)	114	130 122

cant figures for 100 mg samples, which introduced a negligible error compared to other considerations. The  $\mu\text{l}$  pipettes used in the preparation of the irradiation standards were calibrated to a tolerance of  $\pm 0.3$  percent. To avoid extraneous cross-contamination, a separate set of labeled pipettes was used for each element. Each pipetting of an irradiation standard had two additional rinses of distilled water from the pipet added to the quartz ampoule. The dilution provided by the aqueous media was expected to eliminate any serious self-shielding effects by spreading the sample homogeneously throughout the inert aqueous material. The water did not introduce any contamination except 15 hour  $^{24}\text{Na}$  which was allowed to decay before obtaining quantitative counts.

The uncertainty in the chemical yield factor of osmium was largely dependent on the accuracy of the spectrophotometric measurement for which an error of not more than one percent was expected. The chemical yield of ruthenium was assumed to be 100 percent within an error of two percent based on the preliminary studies.

The flux gradient effect due to different ampoule positions during irradiation was minimized by arranging the samples and standards in a 2.8 cm diameter bundle positioned vertically during irradiation. Comparison of flux monitors

from two different aluminum cans irradiated simultaneously yielded specific activities within  $\pm$  two percent. Since the flux monitors were separated by a minimum of seven cm, flux gradient effects within a single aluminum can were assumed to be less than  $\pm$  two percent.

Counting periods were all several times smaller than the activity half-lives. Therefore considerably less than one percent error was introduced by assuming the average count occurred at the mid-point of the count period (29). The counting statistics introduce an error due to the random nature of the radioactive decay process. The relative standard deviation,  $\sigma_R$ , for a given number of accumulated counts,  $C$ , is given by the equation

$$\sigma_R = \frac{\sqrt{C}}{C} . \quad (20)$$

Generally the counting period was long enough to accumulate at least  $10^4$  counts which would give a relative standard deviation of one percent. Since to obtain the true sample count involved the difference of two measurements, the source count and background count, the propagation of errors gives the true sample count standard deviation as the square root of the sum of the squares of the individual standard deviations (29). The magnitude of the true sample count standard

deviation can be reduced by lowering the background, increasing the counter efficiency (29) or obtained long counts. The background contribution to the standard deviation in this investigation was less than five percent by virtue of long background counts (100-200 minutes) and low background count rates. The counting geometry, quite important in the comparison method, was rigidly controlled in this investigation introducing an error of not more than one percent.

It was noted earlier that erroneous results were calculated when the component contribution factor in the sample was very small or nonexistent. Even in the more favorable examples of RESOLF applications (68) errors of up to five percent occurred. Errors up to seven percent were observed when RESOLF was tested on some "known" gamma-ray spectra by this investigator. A spectrum smoothing operation and an iterative gain shift search for the best FIT values were employed to improve the analysis of the samples with low count rates. Some activation analysts feel gamma-ray spectrometry gives intrinsic 5-15 percent error (29) which was probably the largest source of error in this investigation.

Sample inhomogeneity can produce a serious error due to the small sample size used in activation analysis. This

could indeed be the case for the wire samples in which the osmium and ruthenium could be heterogeneously distributed as grains in the platinum matrix. This could also be the case in the powder purified platinum samples since the reduced platinum black had flakes of metallic appearing precipitate which could have produced a selective concentration of impurities.

### Implications

This investigation demonstrated the application of the temperature dependence of  $\text{HClO}_4$  oxidizing power for a selective distillation of osmium and ruthenium. The distillation procedure achieved a very large decontamination factor from the high platinum matrix activities. The analysis was quite lengthy due to the separate distillations of the osmium and ruthenium irradiation standards although this step could be eliminated by purification before irradiations.

The high activity level of the matrix did not limit the performance of the necessary chemical manipulations since the matrix activities remained in the lead shielded flask A residue. The presence of the assumed  $^{35}\text{S}$  activity produced in the irradiated solutions provided some interference in the analysis but solution irradiations did eliminate some problems

associated with volatile and/or inert materials. The high sensitivity of the distillation method for the destructive activation analysis in this investigation could be extended to other systems in which volatile species with contrasting oxidation potentials could be analyzed. The presence of gold (2.7 day  $^{198}\text{Au}$ ) as an impurity in osmium and ruthenium standards was noted in the residue of preliminary irradiations but was not quantitatively measured due to the time required for the distillations employed for the platinum analyses.



## SUMMARY

Trace amounts of osmium and ruthenium in both commercial and purified platinum stock were simultaneously determined by destructive thermal neutron activation analysis utilizing gamma-ray spectrometry. One to two hundred milligram samples of platinum and irradiation standards consisting of submilligram amounts of the elements to be determined were irradiated for periods of up to 260 hours with a thermal flux of ca.  $3 \times 10^{13} \text{ n} \cdot \text{cm}^{-2} \cdot \text{sec}^{-1}$ . All samples were irradiated as aqua regia solutions sealed in eight mm ID silica ampoules using a liquid nitrogen freezing technique which was also employed for opening the irradiated samples.

A radiochemical separation scheme was developed which involved a selective distillation of the volatile tetroxides of osmium and ruthenium. The temperature dependent oxidative power of perchloric acid was utilized to first distill osmium tetroxide and then ruthenium tetroxide while qualitatively retaining the matrix activity in the undistilled residue. Osmium and ruthenium carriers were used with the distilled osmium collected in a thiourea catch solution for a spectrophotometric carrier yield. The ruthenium was distilled into 1N NaOH-.05M NaOCl solution for a spectrophotometric carrier

yield determination as the perruthenate anion. An iridium impurity in the irradiation standards was also determined by activation analysis.

The activities of 40-day  $^{103}\text{Ru}$ , 15-day  $^{191}\text{Os}$  and 74-day  $^{192}\text{Ir}$  were measured by accumulation of counts in a 400-channel pulse height analyzer using a NaI(Tl) crystal detector. The recorded gamma-ray spectra were analyzed using a computer technique. The computer calculated impurity levels were obtained by a comparison of the activities isolated from the platinum matrix with those of the corresponding irradiation standards.

Average impurity contents of  $32 \pm 7$  ppb of osmium in five analyses and  $44 \pm 5$  ppb of ruthenium in six analyses were obtained for the purified platinum stock investigated. The commercial platinum wire investigated yielded an average impurity content of  $0.134 \pm .010$  ppm of osmium in seven analyses and  $1.04 \pm .04$  ppm of ruthenium in seven analyses. The average iridium contents of the commercial irradiation standards were  $20 \pm 3$  ppm for osmium in five analyses and  $91 \pm 3$  ppm for ruthenium in four analyses. A minor interference activity was produced by the reaction,  $^{35}\text{Cl}(n,p)^{35}\text{S}$ , which partially distilled with ruthenium.

The over-all errors in the results appeared to be mostly due to uncertainties inherent in gamma-ray spectrometry and possible inhomogeneities in the platinum samples. The errors due to self-shielding during irradiation, and the interferences arising from secondary neutron reactions and threshold reactions, were deemed insignificant.

## BIBLIOGRAPHY

1. Cilindro, L. G. and Martin, D. S., J. Radioanal. Chem. 3, 195 (1969).
2. Lederer, C. M., Hollander, J. M., and Perlman, I. Table of Isotopes. 6th ed. John Wiley and Sons, Inc., New York, 1967.
3. Rich, R. L. and Taube, H., J. Am. Chem. Soc. 76, 2608 (1954).
4. Klason, P., Ber. deut. Chem. Ges. 37, 1360 (1904).
5. Johnson, R. C. and Basolo, F., J. Inorg. Nuc. Chem. 13, 36 (1960).
6. Ellison, H., Basolo, F. and Pearson, R. G., J. Am. Chem. Soc. 83, 3943 (1961).
7. Basolo, F., Messing, A. F., Wilks, P. H., Wilkins, R. G., and Pearson, R. G., J. Inorg. Nuc. Chem. 8, 203 (1958).
8. Pearson, R. G., J. Phys. Chem. 63, 321 (1959).
9. McCarley, R. E., Martin, D. S., and Cox, L. T., J. Inorg. Nuc. Chem. 7, 113 (1958).
10. Mason, R. W., Inorg. Chem. 9, 1528 (1970).
11. Syamal, A. and Johnson, R. C., Inorg. Chem. 9, 265 (1970).
12. von Hevesy, G. and Levi, H., Kgl. Danske. Videnskab. Selskab. Mat.-fys. Medd. 14, 5 (1936).
13. Curie, I. and Joliet, F., Compt. rend. 198, 254, 559, 2089 (1934).
14. Fermi, E., Amalde, E., and D'Agostino, O., Proc. Roy. Soc. A146, 483 (1934).
15. Seaborg, G. T. and Livingood, J. J., J. Am. Chem. Soc. 60, 1784 (1938).

16. Smythe, H. D., ed. Atomic Energy for Military Purposes: The Official Report on the Development of the Atomic Bomb under the Auspices of the United States Government 1940-45. U.S. Govt. Printing Office, Washington, D.C. 1945.
17. Boyd, G. E., Anal. Chem. 21, 335 (1949).
18. Lutz, G. J., Boreni, R. J., Maddock, R. S., and Meinke, W. W., eds. NBS Technical Note 467, 2 vols., U.S. Govt. Printing Office, Washington, D.C., 1969.
19. DeVoe, J. R., ed. Modern Trends in Activation Analysis 1968 International Conference. NBS Spec. Bull. 312, 2 vols., U.S. Govt. Printing Office, Washington, D.C., 1969.
20. Lutz, G. J., Anal. Chem. 43, 93 (1971).
21. Ricci, E. and Handley, T. H., Anal. Chem. 42, 378 (1970).
22. Gilat, J. and Gurfinkel, Y., Nucleonics 21, No. 8, 143 (1963).
23. Plumb, R. C. and Lewis, J. E., Nucleonics 13, No. 8, 42 (1955).
24. Hogdahl, O. T., Radiochemical Methods of Analysis, International Atomic Energy Agency, Vienna, Vol. 1, 1965, p. 23.
25. Hughes, D. J. and Harvey, J. A. Neutron Cross Sections, Rept. No. BNL 325, U.S. Govt. Printing Office, Washington, D.C., 1955.
26. Dabell, M. J. and Smales, A. A., Analyst 82, 390 (1957).
27. DeSoete, D. and Koste, J., International Atomic Energy Agency Symposium on Radiochemical Methods of Analysis, Salzburg, 1969, Paper SM-55/4, 1965, Vol. 1, p. 91.
28. Shutz, D. F., Tupekian, K. D. and Bolter, E., Society for Applied Spectroscopy, San Diego, California, 1964, Proceedings 2, Paper 35. 1964.
29. Leinihan, J. M. A. and Thomson, S. J., Activation Analysis, Academic Press, New York, 1965.

30. Kamenoto, Y., Int. J. Appl. Radiat. Isotopes 15, 447 (1964).
31. Girardi, F., Guzzi, G. and Pauly, J., Anal. Chem. 36, 1588 (1964).
32. Girardi, F., Guzzi, G. and Pauly, J., Anal. Chem. 37, 1085 (1965).
33. Speecke, A. and Maes, J. International Atomic Energy Agency Symposium on Radiochemical Methods of Analyses, Salzburg, 1964, Paper SM-55/5, 1965, Vol. 1, p. 51.
34. Adams, F. and Hoste, J., Atomic Energy Review 4, 113 (1966).
35. Kosta, L. and Cook, G. B., Talanta 12, 977 (1965).
36. Green, T. E., Law, S. L. and Campbell, W. J., Anal. Chem. 42, 1749 (1970).
37. Park, K. S., Gijbels, R. and Hoste, J., J. Radioanal. Chem. 5, 31 (1970).
38. Lukens, H. F., Yule, H. P. and Guinn, V. P., Nucl. Instrum. Meth. 33, 277 (1965).
39. Lukens, H. R., J. Radioanal. Chem. 1, 349 (1968).
40. Maenhaut, W. and Op De Beeck, J. P., J. Radioanal. Chem. 5, 115 (1970).
41. Roy, J. C. and Hawton, J. J., Table of Estimated Cross Sections for (n,p), (n, $\alpha$ ), and (n,2n) Reactions in a Fission Neutron Spectrum, AECL-1181, Atomic Energy of Canada Limited, Chalk River, Ontario, December, 1960.
42. Hughes, D. J., Neutron Cross Sections (Intern. Series Monographs on Nuclear Energy, Div. II, Vol. I) Pergamon Press, London, 1957.
43. Hughes, D. J. and Schwartz, R. B., Neutron Cross Sections, U.S. Atomic Energy Commission, Rept. BNL-325, 2nd ed., 1958.

44. Durham, R. W., Navalkar, M. P., and Recci, E., International Conferences on Modern Trends in Activation Analysis, Texas, Proceedings 1961, 1962, p. 67.
45. Maslov, I. A., International Atomic Energy Agency Symposium on Radiochemical Methods of Analysis, Salzburg, 1964, Paper SM-55/119, 1965, Vol. 1, p. 41.
46. Yule, H. P., Lukens, H. R. and Guinn, V. P., U.S. Atomic Energy Commission Report GA-5073 [General Atomic Division, General Dynamics Corp., San Diego, Calif.] 1964.
47. De Soete, D., Gijbels, R. and Hoste, J., in Modern Trends in Activation Analysis, DeVoe, J. R., Ed., NBS Special Publication 312, U.S. Govt. Printing Office, Washington, D.C., 1969, Vol. 2, p. 699.
48. Rudelli, M. C., Rocca, H. C., and Baro, G. B., in Modern Trends in Activation Analysis, DeVoe, J. R., Ed., NBS Special Publication 312, U.S. Govt. Printing Office, Washington, D.C., 1969, Vol. 1, p. 544.
49. Kahn, B. and Lyon, W. S., Nucleonics 11, #11, 61 (1953).
50. Lyon, W. S. and Reynolds, S. A., Nucleonics 13, #10, 60 (1955).
51. Crouthamel, C. E., Editor, Applied Gamma-ray Spectroscopy, Pergamon Press, Oxford, 1960.
52. Heath, R. L. U.S. Atomic Energy Commission Report, IDO-16880, 1964.
53. Girardi, F., Guzzi, G. and Pauly, J. Euratom Report, EUR 1898e, 1965.
54. Aude, G. and Laverlochere, J., Spectres Gamma de Radioelements Formes par Irradiation sous Neutrons de 14 MeV, Presses Universitaires de France, 1963.
55. Girardi, F., Guzzi, G. and Pauly, J., Radiochem. Acta 4, 109 (1965).
56. Prussian, S. G., Harris, J. A., and Hollander, J. R., Anal. Chem. 37, 1127 (1965).

57. Neirinckx, R., Adams, F., and Hoste, J., *Anal. Chim. Acta* 46, 165 (1969).
58. Lunar Sample Preliminary Examination Team, *Science* 165, 1211 (1969).
59. Covell, D. F., *Anal. Chem.* 31, 1785 (1959).
60. Sterlincki, S., *Anal. Chem.* 40, 1995 (1968).
61. Sterlincki, S., *Anal. Chem.* 42, 151 (1970).
62. Salmon, L., *Nucl. Instr. Methods* 14, 193 (1961).
63. Anders, O. U. and Beamer, W. H., *Anal. Chem.* 33, 226 (1961).
64. Breen, W. M., Fite, L. E., Gibbons, D., and Wainerdi, R. E., *Trans. Am. Nucl. Soc.* 4, 244 (1961).
65. Blackburn, J., *Anal. Chem.* 37, 1000 (1965).
66. Schonfeld, E., *Nucl. Instr. Methods* 52, 177 (1967).
67. Helmer, R. G., Metcalf, D. D., Heath, R. L., and Cazier, G. A., A Linear Least Squares Fitting Program for the Analysis of Gamma-Ray Spectra Including a Gain Shift Routine, Phillips Petroleum Co., IDO-17015 (1964).
68. Korthoven, P. J. M., Resolf, a Computer Program for the Analysis of Gamma-Ray Spectra, USAEC Report IS-1811, 1968.
69. Kowalski, B. R. and Isenhour, T. L., *Anal. Chem.* 40, 1186 (1968).
70. O'Kelley, G. D., Ed., *Applications of Computers to Nuclear and Radiochemistry*, NAS-NS-3107, p. 165 (1963).
71. Munzel, H., *Symposium of Radiochemical Methods of Analysis*, Salzburg, Austria, Vol. II, 141, 1964.
72. Yule, H. P., *Nucl. Phys.* A94, 442 (1967).



73. Yule, H. P., Nucl. Instrum. Methods 54, 61 (1967).
74. Yule, H. P., in Modern Trends in Activation Analysis, DeVoe, J. R., Ed., NBS Special Publ. 312, U.S. Govt. Printing Office, Washington, D.C., 1969, Vol. 2, p. 1155.
75. Girardi, F., in Modern Trends in Activation Analysis, DeVoe, J. R., Ed., NBS Special Publ. 312, U.S. Govt. Printing Office, Washington, D.C., 1969, Vol. 1, p. 577.
76. Wainerdi, R. E., Menon, M. P. and Fite, L. E. USAEC Report TEES-2671-4, 1965.
77. DeSoete, D. and Hoste, J., Radiochim. Acta 4, 35 (1965).
78. Adams, J. and Hoste, J., Nucleonics 22, No. 3, 55 (1964).
79. Lukens, H. R., J. Chem. Ed. 44, 671 (1967).
80. Routti, J. T., Anal. Chem. 40, 593 (1968).
81. Leddicotte, G. W., Anal. Chem. 36, 419R (1964).
82. Yule, H. P., Anal. Chem. 38, 818 (1966).
83. Girardi, F., Guizzi, G. and Pauly, J. European Atomic Energy Commission Report EUR-1898e, 1965.
84. Lutz, G. J., Anal. Chem. 43, 93 (1971).
85. Miller, C. E. U.S. Atomic Energy Commission Report ORNL-2715, 1959.
86. Jowanovitz, L. S., McNatt, F. B., McCarley, R. E. and Martin, D. S., Anal. Chem. 32, 1270 (1960).
87. Leddicotte, G. W., Mullins, W. T., Bate, L. C., Emery, J. F., Druschel, R. E. and Brooksband, W. A. Progress in Nuclear Energy Series IX 1, 123 (1959).
88. Merz, E. and Herr, W., Progress in Nuclear Energy Series IX 1, 137 (1959).

89. Herr, W., Hoffmeister, W. and Langhoff, J., Z. Naturforsch. 15a, 99 (1960).
90. Morris, D. F. C. and Killick, R. A., Talanta 8, 129 (1961).
91. Gijbels, R. and Hoste, J., Anal. Chim. Acta 29, 289 (1963).
92. Bate, G. L. and Huizenga, J. R., Geochim. Cosmochim. Acta 27, 345 (1963).
93. Morgan, J. W., Anal. Chim. Acta 32, 8 (1965).
94. Crocket, J. H., Keays, R. R. and Hsieh, S., Geochim. Cosmochim. Acta 31, 1615 (1967).
95. Crocket, J. H., Keays, R. R. and Hsieh, S., J. Radioanal. Chem. 1, 487 (1968).
96. Morgan, J. W., Lovering, J. F. and Ford, R. J., J. Geol. Soc. Aust. 15, 189 (1968).
97. Chung, K. S. and Beamish, F. E., Anal. Chim. Acta 43, 357 (1968).
98. Gijbels, R. and Hoste, J., Anal. Chim. Acta 41, 419 (1968).
99. Gijbels, R. and Hoste, J., Anal. Chim. Acta 39, 132 (1967).
100. Kiesel, W., in Modern Trends in Activation Analysis, DeVoe, J. R., Ed., NBS Special Publication 312, 1969, Vol. 1, p. 302.
101. Laul, J. C., Case, D. R., Wechter, M., Schmidt-Bleek, F. and Lipschutz, M. E., J. Radioanal. Chem., 4, 241 (1970).
102. Newton, A. S., Phys. Rev. 75, 17 (1949).
103. Killick, R. A. and Morris, D. J. C., Talanta 9, 349 (1963).

104. Gijbels, R. and Hoste, J., *Anal. Chim. Acta* 32, 17 (1965).
105. Fourcy, A., Neuburger, M., Garrec, C., Fer, A. and Barrec, J. P., in *Modern Trends in Activation Analysis*, DeVoe, J. R., Ed., NBS Special Publ. 312, 1969, Vol. 1, pp. 160.
106. Abdel-Rassoul, A. A., Aly, H. F. and Madbouly, R., *J. Radioanal. Chem.* 5, 193 (1970).
107. Beamish, F. E., Chung, K. S. and Chow, A., *Talanta* 14, 1 (1967).
108. Beamish, F. E., Lewis, C. L. and Van Loon, J. C., *Talanta* 16, 1 (1969).
109. Kohler, J. C. and Lincoln, A. J., *Engelhard Ind. Tech. Bull.* 10, 92 (1969).
110. Beamish, F. E., *Talanta* 13, 773 (1966).
111. Beamish, F. E., *Talanta* 13, 1053 (1966).
112. Beamish, F. E., *Talanta* 12, 789 (1965).
113. Beamish, F. E. *The Analytical Chemistry of the Noble Metals*. Pergamon Press, Oxford, London (1966).
114. Walsh, T. J. and Hausman, E. A., *The Platinum Metals*, in *Treatise on analytical chemistry*. Pt. 2. Analytical chemistry of the elements, Kolthoff, E., Ed. Interscience Publishers, Inc., New York, 1963, Vol. 8, pp. 379-522.
115. Gupta, J. and Sen, G., *Anal. Chim. Acta* 42, 481 (1968).
116. Sauerbrunn, R. D. and Sandell, E. B., *Anal. Chim. Acta* 9, 86 (1953).
117. Geilmann, W. and Neeb, R., *Z. Analyt. Chem.* 156, 420 (1957).

118. Blasius, D. and Fischer, M., Z. Analyt. Chem. 177, 412 (1960).
119. Chung, K. S. and Beamish, F. E., Talanta 15, 823 (1968).
120. Haustein, P. Ames Laboratory, Iowa State University, private communication (1970).
121. Larsen, R. P. and Ross, L. E., Anal. Chem. 31, 176 (1959).
122. Shannon, D. W., U.S. Atomic Energy Commission HW-48736, 1957.
123. Sandell, E. B., Colorimetric Determination of Traces of Metals, 3rd ed., Interscience Publishers, Inc., New York, 1959.
124. Hoffman, I., Schweitzer, J. E., Ryan, D. E. and Beamish, F. E., Anal. Chem. 25, 1091 (1953).
125. Theirs, R., Grayson, W. and Beamish, F. E., Anal. Chem. 20, 831 (1948).
126. Ayres, G. H. and Young, F., Anal. Chem. 22, 1277 (1950).
127. Ayres, G. H. and Quick, Q., Anal. Chem. 22, 1403 (1950).
128. Cotton, F. A. and Wilkinson, G., Advanced Inorganic Chemistry, 2nd ed., Interscience, New York, 1966, p. 995.
129. Radiological Health Handbook, U.S. Dept. of HEW, Washington, D.C., 1960, p. 135.

## ACKNOWLEDGMENTS

The author wishes to express his sincere gratitude to Dr. Don S. Martin, Jr., for the constructive guidance provided and abundant patience manifested throughout the author's graduate studies.

Appreciation is expressed to the Ames Laboratory for the funds plus facilities provided and to the members of Radio-chemistry Group II who have aided in many aspects of this investigation. Gratitude is extended to Verna Thompson for her very able assistance in transforming the manuscript into its final form.

A special gratitude is extended to my family; Sharon, Jennifer and Kathrina, who endured the trials and tribulations experienced in carrying this investigation to completion.